Dissertation

MOLECULAR RECOGNITION OF HUMAN CBP BY RETROVIRAL TRANSCRIPTIONAL ACTIVATORS

Submitted by
Andrew C. Vendel
Department of Biochemistry and Molecular Biology

In partial fulfillment of the requirements for the
Degree of Doctorate of Philosophy
Colorado State University
Fort Collins, Colorado
Fall, 2003

COLORADO STATE UNIVERSITY

Aug 19, 2003

WE HEREBY RECOMMEND THAT THE THESIS PREPARED UNDER OUR SUPERVISION BY ANDREW C. VENDEL ENTITLED

MOLECULAR RECOGNITION OF HUMAN CBP BY RETROVIRAL TRANSCRIPTIONAL ACTIVATORS

BE ACCEPTED AS FULFILLING IN PART REQUIREMENTS FOR THE DEGREE OF

Doctorate of Philosophy.

Committee on Graduate Work

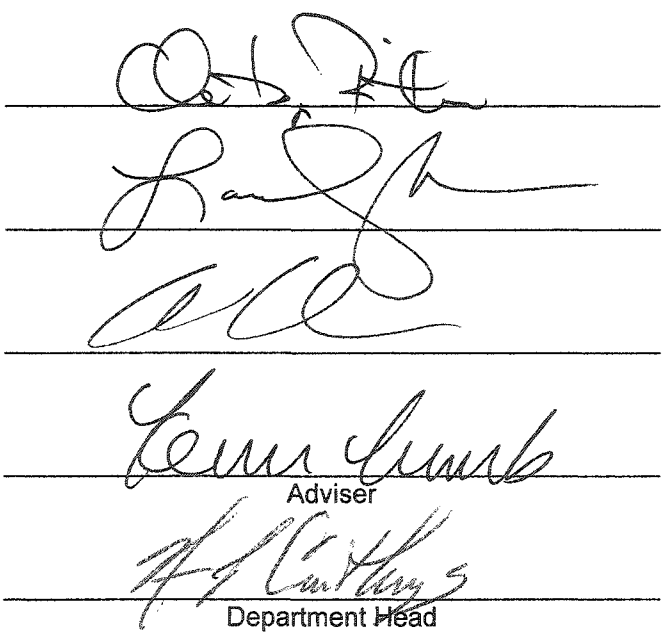

Adviser

Department Head

Abstract of Thesis

Molecular Recognition of Human CBP by Retroviral Transcriptional Activators

HIV-1 Tat is required for the expression of the viral genome. The coactivator and acetyltransferase CREB binding protein (CBP), and the paralog p300, are recruited to the HIV-1 promoter by Tat to aid viral expression. Here we identify the interacting domains of Tat and CBP. Circular dichroism and pulldown assays show that full-length Tat binds to the KIX domain of CBP, but not to the C/H1 or CR2 domains of CBP. Circular dichroism and NMR studies of Tat deletion mutants localize the KIX-binding domain of Tat to the N-terminal 24 residues of Tat. Transient cotransfections demonstrate that exogenous KIX behaves as a dominant negative to Tat-mediated transcription in human T-cells, suggesting that Tat and KIX interact *in vivo*. These findings indicate that Tat targets the KIX domain of CBP and provide insight into the molecular interactions involved in regulating HIV-1 gene expression. Chemical-shift perturbation mapping with heteronuclear nuclear magnetic resonance spectroscopy was used to identify the surface of human KIX that interacts with Tat. It was found that that Tat binds to

the c-Jun/MLL binding surface of KIX, as opposed to the CREB binding site. The results provide new insight into the molecular basis of the assembly of protein complexes involving p300/CBP and Tat during HIV gene expression.

The HTLV-1 transcription activator Tax is required for viral replication and pathogenesis. In concert with human CREB, Tax recruits the human transcriptional coactivator and histone acetyltransferase p300/CBP to the HTLV-1 promoter. Here we investigate the structural features of the interaction between Tax and the KIX domain of human p300/CBP. Circular dichroism spectroscopy, nuclear magnetic resonance chemical-shift perturbation mapping and sedimentation equilibrium show that a subdomain of Tax (residues 59-98) binds KIX. Chemical-shift perturbation mapping reveals that the Tax-binding surface of KIX is distinct from that utilized by CREB, and corresponds to the site of KIX that interacts with MLL, c-Jun, and HIV-1 Tat. Sedimentation equilibrium shows that Tax and the phosphorylated KID domain of CREB can simultaneously bind KIX to form a ternary 1:1:1 complex. The results provide a molecular description of the concerted recruitment of p300/CBP via the KIX domain by Tax and phosphorylated CREB during Tax-mediated gene expression.

Andrew C. Vendel
Department of Biochemistry and Molecular Biology
Colorado State University
Fort Collins, Colorado 80523
Fall 2003

Acknowledgements

I would like to thank Dr. Kevin Lumb for being an outstanding advisor and never giving up on me. During all the difficult times that accompany a doctoral degree, I have never regretted my choice of working for Kevin. He has inspired me to ask critical questions and to be a logical problem solver. More than anything, Kevin has been a good friend and is someone I trust greatly.

I also thank my committee members; Dr. Alan Kennan, Dr. Chris Rithner, and Dr. Laurie Stargell. Without a thoughtful and critical committee, one would not succeed in graduate school. My committee has always been there to help me with my projects and any problems that I have had.

I appreciate the use of CD instruments and help with them from Dr. A-Young Woody and Dr. Robert Woody, and Dr. Alan Kennan. I also thank Holli Giebler and Kirsten Scoggin for experimental help and training. I owe a deep gratitude to Dr. Chris Rithner for all the help and advice with my NMR experiments.

I would like to thank former members of the Lumb laboratory. Katie Campbell has been a great friend and mentor to me. Katie taught me the various techniques we use in the lab, especially NMR and without her I would not have succeeded. I would also like to thank Josh Adkins for being a great lab partner and friend; Ewa Bienkiewicz for being a source of entertainment; Yu Wei for being a good friend, collaborator, cooking me dinner, and teaching me Chinese;

and Shannon Flaugh for being a good friend and putting up with me in the lab. Finally, I want to thank Steve McBryant for being one of my closest friends in the department, helping me through all aspects of my degree, and being a collaborator.

I also thank the friends that have been an inspiration and helped through out the years. Brent Egeland has been a friend since we were in strollers and has always pushed me to succeed under any circumstances. Kirk Hagberg is another life-long friend who has always been there for me and helped me keep a sense of humor even through hard times. Mike and Robbin Dzubay have always been there for me and have done more for me than I could ever imagine. Aaron Swanson and Jenny Benson have been great friends throughout the years and I am glad they are a part of my life. Holli "Mama", Mike, and Mitchel Giebler have been great friends and I could not imagine not knowing them. Andy Stevens for crashing on our couch and always making me laugh. I finally thank David "Billy" Goldstrohm for allowing me to pick on him and teach him the ropes, and others that have been a part of my life I have not mentioned.

I would not be here, obviously, if it were not for my parents. They have given me every opportunity to succeed and taught me to never give up on anything or anyone. They always encouraged me to do what I want and accepted my decisions. I thank my parents for helping me become the person I am today. I

also thank my extended family and the Dickinson family for being great supporters and always interested in my work.

Finally, to whom I owe more than anyone is Natalie. If it were not for her I would not have accomplished this degree. She is my best friend, a greatest confidant, compassionate, and patient. She has supported me emotionally and financially throughout this adventure. I thank her for always being there and never giving up on me.

"Two things are infinite; the universe and human stupidity; and I'm not sure about the first one." A. Einstein

Table of Contents

Abbreviations

1D	One dimensional
$[\theta]_{222}$	molar ellipticity at 222 nm
AIDS	acquired immune deficiency syndrome
C/H1	Cys/His-rich region 1 of CBP
CBP	CREB-binding protein
CD	circular dichroism
CR2	conserved region 2 of CBP
CRE	cyclic-AMP response element
CREB	cyclic-AMP response element binding protein
DIEA	diisopropyl ethanolamine
DMF	dimethyl formamide
DNA	deoxy-ribonucleic acid
DSS	sodium 2,2-dimethyl-2-silapentane-5-sulfonate
DTT	dithiothreitol
EDTA	ethylenediamine tetraacetic acid
GST	glutathione-S-transferase
HBTU	2-(1H-benzotriazole-1-yl)-1,1,3,3-tetramethyluronium hexafluorophosphate
HIF-1	hypoxia inducible factor-1
HIV-1	human immunodeficiency virus type 1
HPLC	high performance liquid chromatography

HSQC	heteronuclear single quantum coherence
HTLV-1	human T cell leukemia virus type 1
IPTG	isopropyl-β-D-thiogalactoside
KID	kinase inducible domain of CREB
K_d	dissociation constant
KIX	KID interacting domain of CBP
LTR	long terminal repeat
MBHA	4-methylbenzhydrylamine hydrochloride salt
NMR	nuclear magnetic resonance
PAGE	polyacrylamide gel electrophoresis
P/CAF	p300 and CBP associated factor
ppm	parts per million
SDS	sodium dodecyl sulfate
TAR	transactivation region
Tat	transactivator of transcription
TFA	trifluoroacetic acid
TOCSY	total correlation spectroscopy

Chapter 1

Molecular Recognition of Transcriptional Activators

1.1 Molecular Recognition

Proteins are the fundamental units that regulate life in cells. Proteins are involved in processes that mediate cell structure and organelle organization, energy production, detoxification, signaling, cell cycle control, DNA replication and repair, DNA organization, and gene expression. A cornerstone of protein function is how they interact with other biomolecules and the mode of recognition that leads to a binding event.

The range of protein interactions that mediate cell function are vast. Molecular recognition of protein-protein and protein-ligand binding events are dynamic and defined by forces such as hydrophobic packing, hydrogen bonds salt bridges, and charge recognition. Examples of some well-studied protein interactions are those involved in immunological response pathways. The immune system is able to recognize and respond to millions of different antigens with only a limited number of protein receptors (Lydyard *et al.*, 2000). This is possible because the receptors have variable regions in the ligand-binding domain that allow for promiscuous recognition of very different sequences and structural conformations presented by invading antigens (Lydyard *et al.*, 2000).

The interacting regions of proteins usually fold into a unique conformation enabling them to interact specifically with ligands. A ligand is able to recognize exposed sites on a protein usually through a core determining region flanked by residues aiding in selectivity and contact surface. This is exemplified with the Fc

region of human immunoglobulin G (IgG) association with four different proteins (DeLano *et al.*, 2000). In this model the B1 domain of Protein A, the C2 domain of Protein G, rheumatoid factor, and neonatal Fc-receptor, all bind a hydrophobic consensus surface and flanking charged residues of the IgG-Fc subunit in structurally distinct modes (DeLano *et al.*, 2000). Binding domains such as this are versatile in their ability to interact with a number of divergent ligands that recognize a core region.

It was long assumed that molecular recognition required individual interacting domains to be folded into well-ordered structures. Recently, evidence has described unfolded, or intrinsically disordered, proteins that possess protein-binding domains (Frankel and Smith, 1998; Plaxco and Gross, 1997; Wright and Dyson, 1999). Many transcriptional activators are intrinsically disordered yet maintain the ability to specifically bind to target molecules (Campbell and Lumb, 2002; Campbell *et al.*, 2000; Goto *et al.*, 2002; Radhakrishnan *et al.*, 1997; Vendel and Lumb, 2003a; Wright and Dyson, 1999). The binding of transactivators to their partners is often accompanied with folding of the activation domain. For example, the kinase inducible domain (KID) of cyclic-AMP response element binding protein (CREB) is an unfolded activation domain that becomes folded when it binds the KIX domain of the coactivator CREB binding protein (CBP) (Mestas and Lumb, 1999; Radhakrishnan *et al.*, 1997).

1.2 Gene Expression

Regulation of gene expression occurs by recruitment and nucleation of DNA-dependant RNA polymerase and general transcription factors (termed the general transcription machinery) at a specific gene promoter (Orphanides and Reinberg, 2002; Roeder, 1996). Nucleation of the general transcription machinery onto the start site of a gene is aided by transcriptional activator and coactivator proteins (Naar *et al.*, 2001; Orphanides and Reinberg, 2002).

Initiation and expression of genes above basal levels or from histone bound promoters requires protein transcriptional activators that bind regulatory DNA elements and recruit the general transcription machinery (Orphanides and Reinberg, 2002; Ptashne and Gann, 1997; Tjian and Maniatis, 1994). Regulation of recruitment by transcriptional activators can occur upon chromatin remodeling, removal of repressors, and directly interacting with the general transcription machinery (Orphanides and Reinberg, 2002; Ptashne and Gann, 1997; Tjian and Maniatis, 1994). Recruitment of the general transcription machinery to gene promoters by transcriptional activators may impart a level of regulation for all cell processes.

Transcriptional activators generally possess at least two functionally independent domains (Triezenberg, 1995). One domain recognizes and binds a specific promoter element and the second activates transcription through protein-protein interactions with other transcription factors (Ptashne, 1988). Activators can also

contain dimerization domains, ligand binding domains, and regulatory domains that alter the activating potential of these proteins. These distinct domains are often modular and can function independently of the other domains (Ptashne, 1988). Therefore, an activation domain can function properly when linked to a different DNA binding domain as long as DNA binding is maintained (Ptashne, 1988).

There are three general types of activation domains called glutamine rich, proline rich, and acidic (Triezenberg, 1995). Acidic activation domains are unique in that they appear to function universally in all eukaryotic organisms from yeast to humans (Struhl, 1988). Examples of acidic activators that regulate many biological processes and implicated in human diseases include the proto-oncogene p53, which is mutated in over half of all cancers, the cellular oncogene products c-Fos and c-Jun, and the viral equivalents v-Fos and v-Jun (Chen *et al.*, 1996; Ko and Prives, 1996; Shaulian and Karin, 2001).

Although much is known about the structural and physical properties of the DNA binding domains of activators, very little is known structurally about activation domains. This is due, in part, to the unstructured nature of many isolated activation domains. Though activation domains are disordered in solution they still retain specificity for interactions with coactivators and the general transcription machinery. This unique property of activation domains has recently made them the focus of intense research.

Coactivators hold unique functions in that they do not make specific DNA contacts and regulate transcription by bridging activators and the general transcription machinery or by altering nucleosomal DNA (Figure 1) (Lemon and Tjian, 2000; Naar *et al.*, 2001; Orphanides and Reinberg, 2002; Ptashne and Gann, 1997). A growing number of coactivators have been described and many possess histone acetyltransferase activity (Lemon and Tjian, 2000). Thus, transcriptional activators may impart some of its activity by recruiting coactivators to remodel chromatin and allowing polymerase access to the promoter.

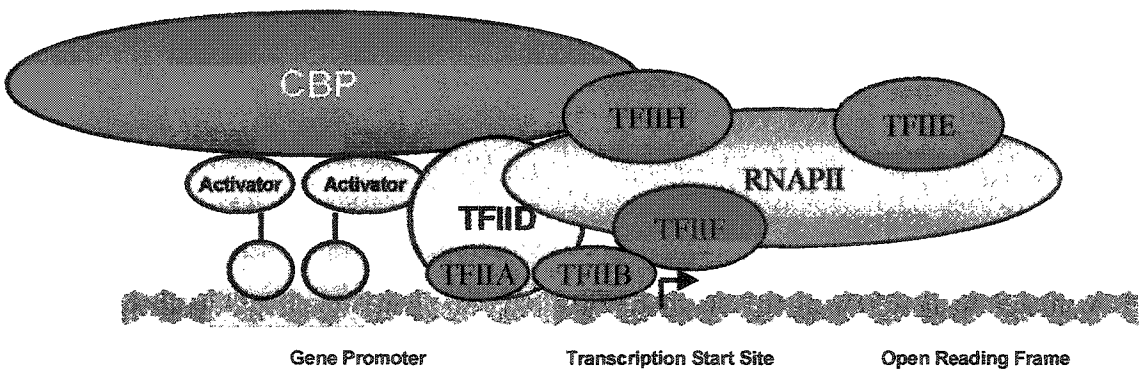

Figure 1. A model of transcription activation from a gene promoter mediated through recruitment of the transcriptional coactivator CBP by an activator at a gene promoter. The general transcription machinery includes RNA polymerase II (RNAPII) and the TATA box binding protein (TBP) containing general transcription factor TFIID, TFIIA, TFIIB, TFIIH, TFIIF, and TFIIE.

CREB-binding protein (CBP) is a large, multi-domain transcriptional coactivator that interacts with a multitude of mammalian and viral transcription activators, coactivators, corepressors and the general transcription machinery (Figure 2)

(Goodman and Smolik, 2000; Swope *et al.*, 1996). CBP has an intrinsic acetyltransferase activity (Chan and La Thangue, 2001) and interacts with other acetyltransferases such as P/CAF (Yang *et al.*, 1996). CBP and P/CAF can acetylate nucleosome histones to overcome the repressive effects nucleosomes impart on gene transcription (Brockmann *et al.*, 2001; Martinez-Balbas *et al.*, 1998).

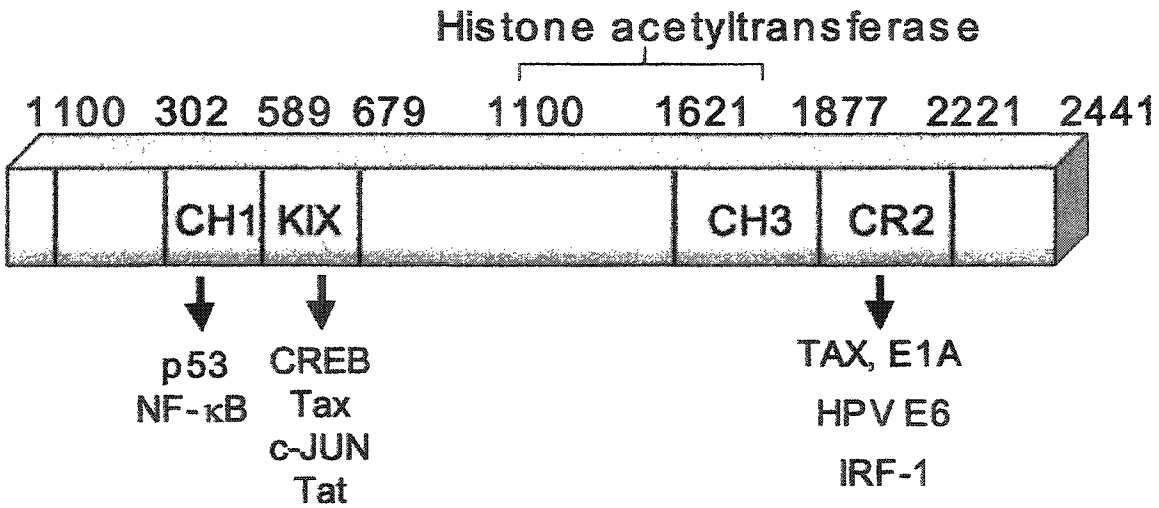

Figure 2. Schematic representation of the domain structures of CBP and Tat. Above, CBP possesses multiple, independently-folded protein-interacting domains (Goodman and Smolik, 2000). The minimal C/H1 domain (residues 300-450) binds a number of transcriptional activators in a Zinc-dependant manor (Dames *et al.*, 2002; Freedman *et al.*, 2002; Goodman and Smolik, 2000; Newton *et al.*, 2000). The KIX domain (residues 589-679) is an autonomously folded, globular protein [Radhakrishnan, 1997 #51; Campbell, 2002 #111; Vendel, 2003 #115; Vendel, 2003 #139; (Wei *et al.*, 2003). The minimal CR2 domain (residues 2055-2150) binds cellular and viral transcriptional regulators (Demarest *et al.*, 2002; Goodman and Smolik, 2000; Lin *et al.*, 2001).

CBP is recruited to a promoter through specific protein-protein interactions mediated by its numerous domains (Chan and La Thangue, 2001; Goodman and Smolik, 2000). The KIX (residues 589-679) domain is of interest because it has been shown to bind to numerous cellular proteins along with viral transcription activators (Figures 2 & 3) via two modes that employ structurally distinct surfaces of KIX (Campbell and Lumb, 2002; Goto *et al.*, 2002; Radhakrishnan *et al.*, 1997; Vendel and Lumb, 2003b). One mode is the binding of CREB to KIX, which is dependent on phosphorylation of Ser 133 of its KID domain (Radhakrishnan *et al.*, 1997). The phosphate on Ser 133 is involved in a specific intermolecular electrostatic interaction with Lys 662 and Tyr 658 of KIX (Mestas and Lumb, 1999; Radhakrishnan *et al.*, 1997). The second mode, which is distinct from the binding surface of KIX that recognizes phosphorylated CREB, is observed with the binding of MLL, c-Jun, and HIV-1 Tat to KIX (Campbell and Lumb, 2002; Goto *et al.*, 2002; Vendel and Lumb, 2003b).

Recently, it has been suggested that the HIV-1 transcription activator Tat associates with amino acids 1-670 of CBP which houses the cysteine/histidine rich domain 1 (C/H1 residues 300-450) and the KIX domain (Figure 2) (Benkirane *et al.*, 1998). The KIX domain of CBP is also involved in Tax-mediated activation of human T-cell leukemia virus-1 (HTLV-1) gene expression, another member of the retrovirus family (Giebler *et al.*, 1997; Yan *et al.*, 1998).

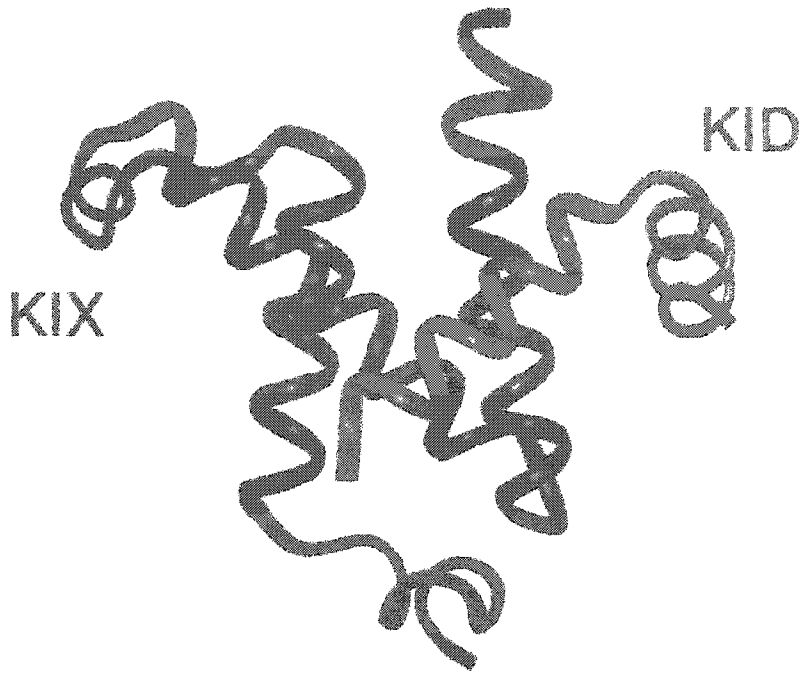

Figure 3. Structure of the KIX domain (blue) of CBP bound to the KID region (red) of CREB (Radhakrishnan *et al.*, 1997). KIX is made up of three α and two 3_{10} helices, which fold into a globular protein with a well packed hydrophobic core. The KID domain is intrinsically disordered but folds into two a helices when it binds KIX. Ser 133 in the KID region of CREB is phosphorylated and aids in the binding free energy to KIX by creating a favorable electrostatic interaction with Lys and Tyr residues on KIX (Mestas and Lumb, 1999).

1.3 HIV-1

The human immunodeficiency virus (HIV) has been under intense study for 20 years and is the known cause of Acquired Immune Deficiency Syndrome (AIDS). AIDS is characterized by the loss of $CD4^+$ T-lymphocytes, which leads to opportunistic infections that inevitably kills the infected individual. The World Health Organization reports that over 42 million people worldwide are thought to be infected, including close to 1 million Americans and over 29 million sub-Saharan Africans (Figure 4) (WHO, 2002). Of the people currently infected with

HIV-1, 3.2 million are children under the age of fifteen. By the end of 2002, over 23 million deaths were reported by the World Health Organization due to complications to AIDS, with 3.1 million in 2002 alone (WHO, http://www.unaids.org/worldaidsday/2002/press/Epiupdate.html).

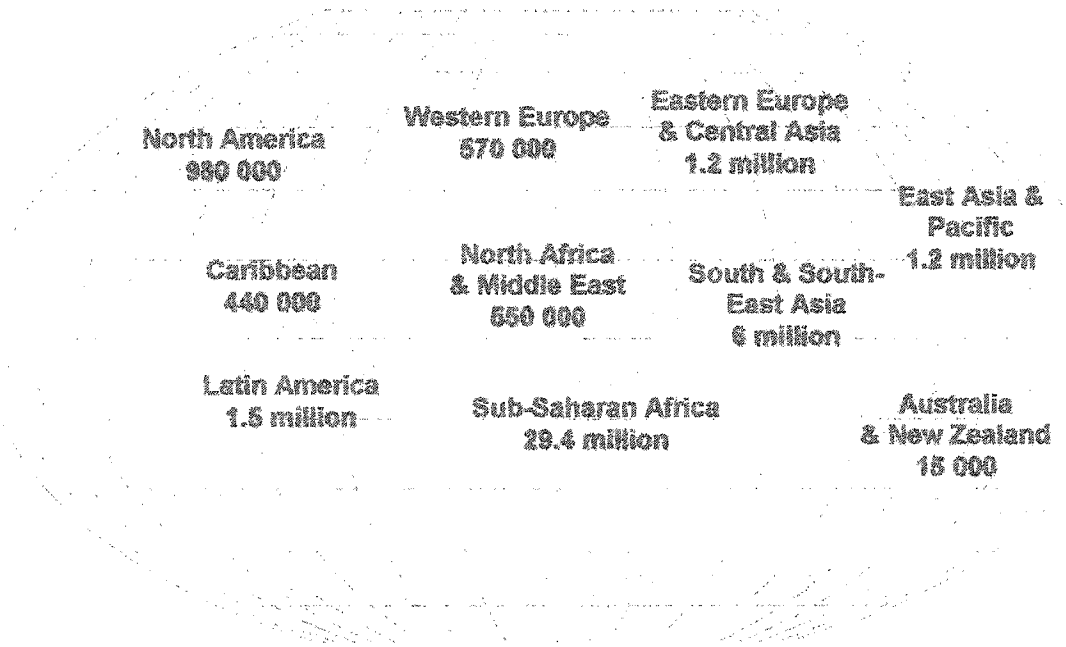

Figure 4. Map of the HIV-1/AIDS epidemic around the world. Data current as of January, 2003 from the World Health Organization (WHO, http://www.unaids.org/worldaidsday/2002/press/Epiupdate.html).

The HIV-1 virus is made up of fifteen different proteins and two copies of unspliced genomic viral RNA (Frankel and Young, 1998; Garcia *et al.*, 1988). The genome is a ~9.8 kb RNA that is reverse transcribed and recombined into the host DNA by virally encoded reverse transcriptase and integrase proteins (Frankel and Young, 1998; Garcia *et al.*, 1988). The proteins and RNA needed

for virus replication are encoded by the HIV-1 genome and are generated by alternative splicing (Figure 5).

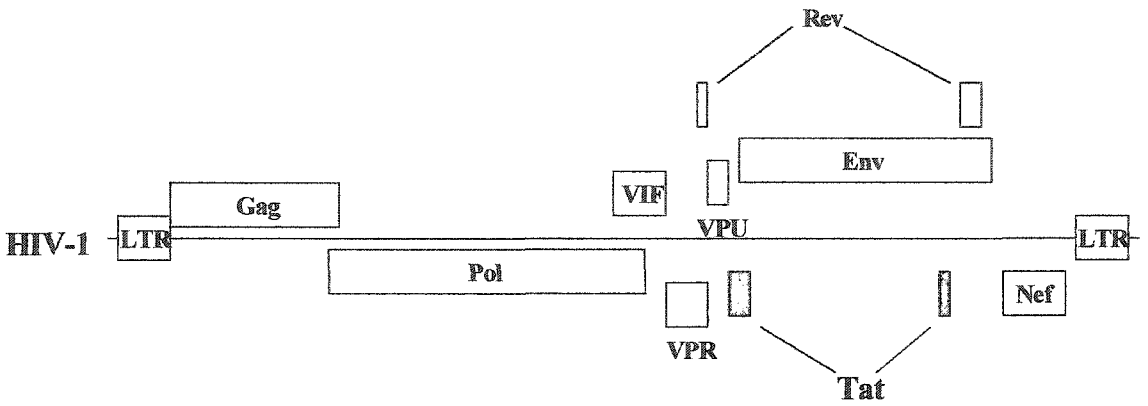

Figure 5. Structure of the HIV-1 genome flanked at both ends with long terminal repeats (LTR). The virally encoded proteins are listed. The HIV-1 transcriptional activator Tat is shaded yellow. Tat is a splice variant, with the single splice product encoding residues 1 through 86 and the unspliced product encoding residues 1 through 101. The single splice variant of Tat represents the minimal Tat needed to activate transcription of the HIV-1 genome.

The replication cycle of HIV-1 is unique to the retroviral family. It can be divided into an early and a late phase (Frankel and Young, 1998; Turner and Summers, 1999). The early phase involves docking of an HIV-1 virion to $CD4^+$ T-lymphocytes through the CD4 and chemokine receptors, import of the viral genome and proteins, reverse transcription of the HIV-1 RNA genome, and integration of the proviral DNA into the host genome (Figure 6). The late phase of viral infection involves expression of viral proteins needed for production of new virion, expression of the full-length viral genome, packaging two copies of the viral RNA into a proteinaceous matrix at the cell wall, budding of a new virus

particle, and maturation of the newly replicated virus enabling it to infect a new cell (Figure 6) (Frankel and Young, 1998; Turner and Summers, 1999).

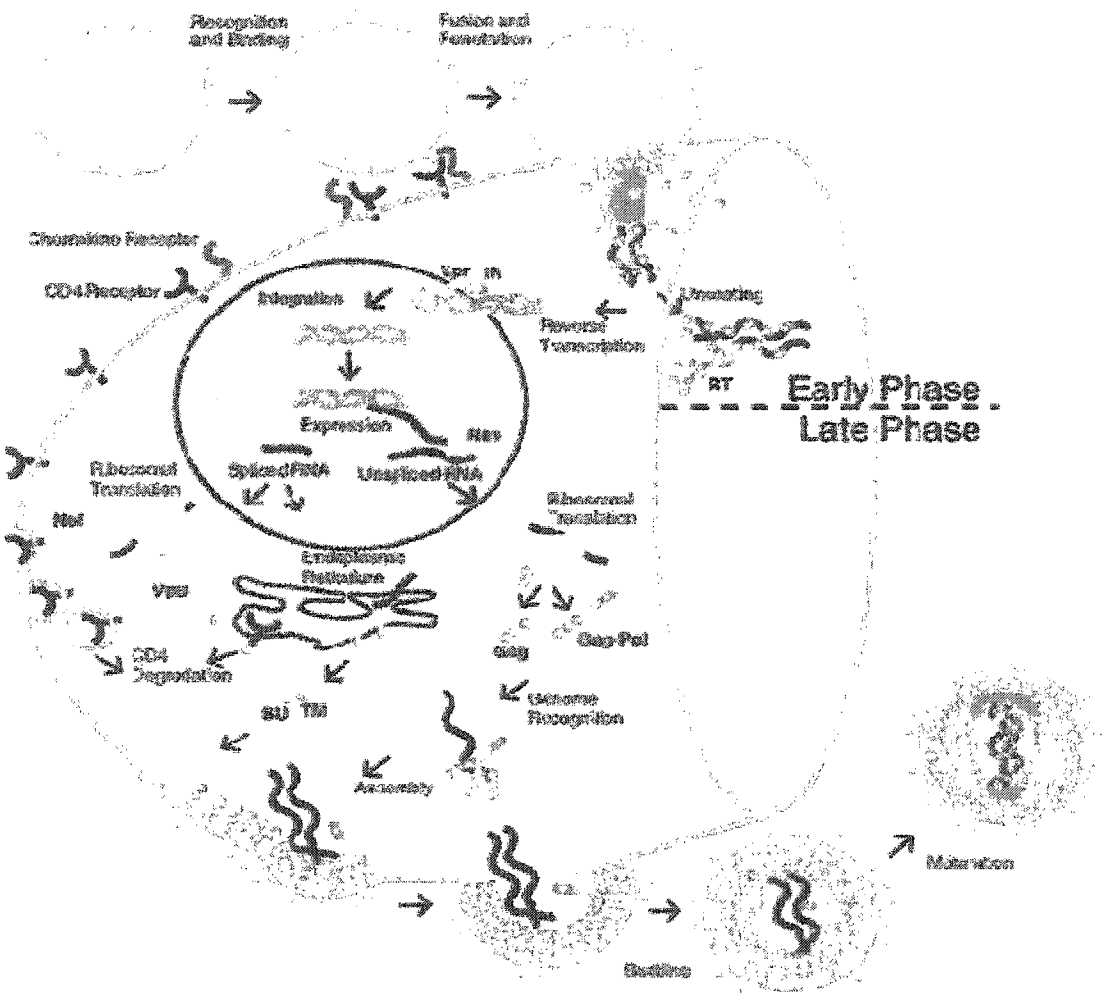

Figure 6. The HIV-1 infection and replication cycle. Notable features of infection include viral recognition and docking of the CD4 receptor on a T-lymphocyte, integration of the proviral genome into the host cell, usurping normal cell function to produce vast amounts of new virion, and budding and maturation of new virus particles (Figure from Turner and Summers, 1999).

Expression of the HIV-1 genome requires both human and viral transcription factors (Jones and Peterlin, 1994). The HIV-1 5' LTR promoter is reminiscent of human protein-coding counterparts, and viral expression requires the human transcription machinery, including RNA polymerase II, general transcription factors, activators and coactivators (Jones and Peterlin, 1994). The human activators NF-κB and SP1 are required for retroviral activation and assembly of the general transcription machinery at the HIV-1 promoter (Jones and Peterlin, 1994). After initiation, the HIV-1 transactivator Tat is required for viral RNA synthesis (Figure 7).

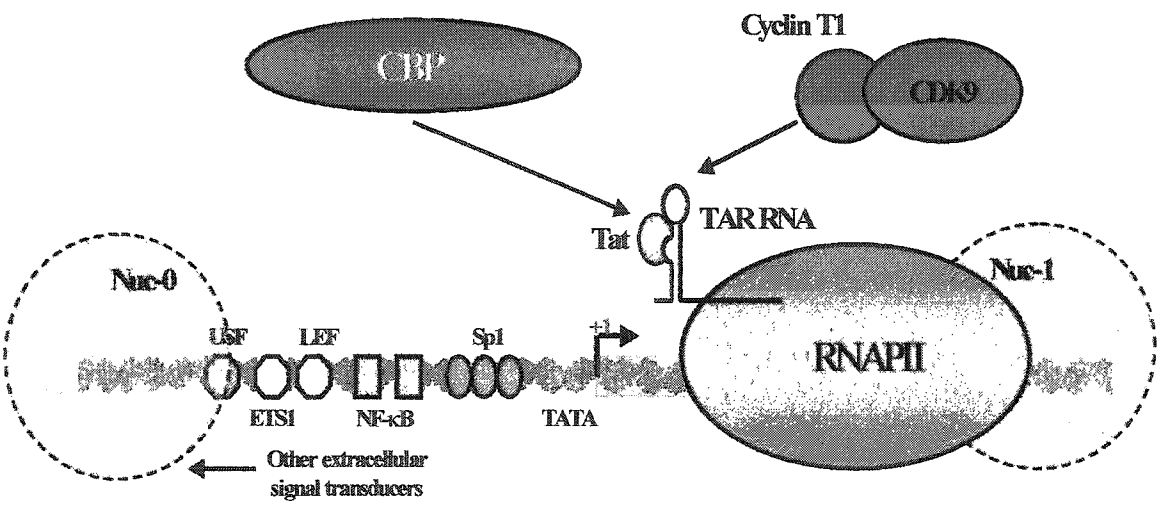

Figure 7. The HIV-1, 5' LTR promoter region and recruitment of the coactivators cyclin T1/CDK9 (p-TEFb) and CBP by Tat bound to the TAR RNA stem-loop. The nucleosomal archetecture surrounding the HIV-1 promoter is also shown. Nucleosome 1 (Nuc-1) is disrupted during viral transcription (He and Margolis, 2002).

Tat is produced early in the viral life cycle and is essential for HIV-1 genome replication and viral propagation (Jones and Peterlin, 1994). Attenuated viruses with mutated Tat integrate the HIV-1 genome into human cells, but are unable to propagate (Huq *et al.*, 1999b; Sadaie *et al.*, 1988).

Unlike human transcriptional activators, which bind DNA, Tat binds RNA at the stemloop of TAR through a basic arginine-rich motif (ARM, Figure 8) (Jones and Peterlin, 1994). TAR is transcribed within the first 60 nucleotides of the HIV-1 genome (Huq *et al.*, 1999b). Once bound, Tat recruits endogenous cellular factors that assist in transcription elongation and enhancement of HIV-1 genome expression (Benkirane *et al.*, 1998; Isel and Karn, 1999; Jones and Peterlin, 1994; Marzio *et al.*, 1998; Roebuck and Saifuddin, 1999).

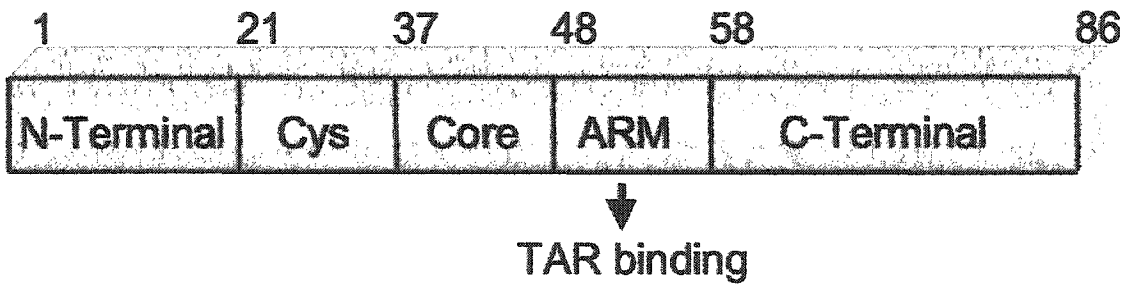

Figure 8. An N-terminal, Cys-rich, Core, and arginine rich motif (ARM) make up the four known Tat domains (Jones and Peterlin, 1994). The ARM domain of Tat is involved in binding the stem loop of TAR RNA during Tat-mediated activation of the HIV-1 genome (Jones and Peterlin, 1994).

After incorporation into the host DNA, the HIV-1 genome is packaged into nucleosomes (Figure 7) (Marzio and Giacca, 1999; Roebuck and Saifuddin, 1999). Due to the nucleosomes surrounding the 5′ LTR, the incorporated viral DNA may fall under similar architectural regulation to endogenous cellular genes. In fact, a nucleosome positioned near the transcription start site (Nuc-1; Figure 7), on the 5′ LTR is disrupted during transcriptional activation (Marzio and Giacca, 1999; Roebuck and Saifuddin, 1999). Furthermore, acetylation of the histone tails that make up Nuc-1 is coupled with transcriptional activation in a Tat-dependant manor (He and Margolis, 2002). It is likely that Tat, in part, recruits proteins involved in nucleosome remodeling to allow viral transcription.

Tat has previously been shown to recruit the cellular coactivator and acetyltransferase CBP/p300 to the HIV-1 LTR (Benkirane *et al.*, 1998; Marzio *et al.*, 1998). Recruitment of CBP/p300 is needed for efficient viral transcription (Benkirane *et al.*, 1998). Recruitment of human CBP and p300, and other coactivator complexes may result in the modification of the nucleosomal architecture downstream of the HIV-1 start site and facilitate viral replication (He and Margolis, 2002; Marzio and Giacca, 1999; Van Lint *et al.*, 1996).

1.4 HTLV-1

The lentivirus human T-cell leukemia virus type 1 (HTLV-1) was identified near the time of the HIV-1 outbreak in the United States (Poiesz *et al.*, 1980). HTLV-1 predominantly infects CD4+ T-cells and is the etiological agent of adult T-cell

leukemia and of the neurological disorder tropical spastic paraparesis/HTLV-1-associated myelopathy (Barmak *et al.*, 2003).

HTLV-1 posses two copies of a single-stranded genomic viral RNA that encode thirteen proteins. The genome is a ~9 kb RNA that is reverse transcribed and recombined into the host DNA by virally encoded reverse transcriptase and integrase proteins (Figure 9) (Chen *et al.*, 1983). After reverse transcription, the viral genome is randomly inserted into the host genome and possess two LTR regions at the 5 and 3 prime ends of the proviral genome (Chen *et al.*, 1983). These LTR regions are involved in the recombination event and house the promoter element that drives transcription of the viral genome.

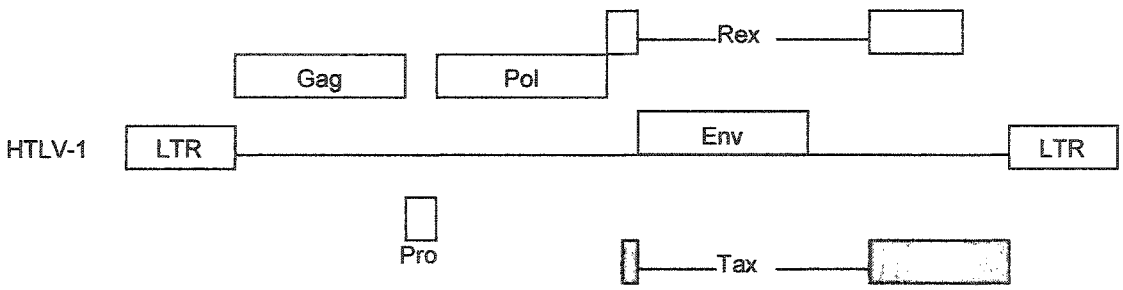

Figure 9. Schematic of the 9 kb HTLV-1 genome flanked at the 5' and 3' ends with LTR regions. HTLV-1 encoded proteins are listed. The HTLV-1 transcriptional activator Tax is shaded yellow.

HTLV-1 replication and pathogenesis is dependant on the virally encoded transcriptional activator Tax (Reviewed by Bex and Gaynor, 1998; Jeang, 2001; Yoshida, 2001). In addition to activating viral gene expression, Tax alters the expression of numerous cellular genes involved in cell cycle regulation and apoptosis (Bex and Gaynor, 1998; Jeang, 2001; Yoshida, 2001). The interference of Tax with normal cellular processes likely contributes to the extensive modulation of the transcriptional profile of HTLV-1 infected lymphocytes (Pise-Masison *et al.*, 2002) and to HTLV-1-associated pathogenesis (Bex and Gaynor, 1998; Jeang, 2001; Yoshida, 2001).

Tax is recruited to the HTLV-1 LTR promoter by directly associating with the basic leucine zipper domain (bZip) of CREB/ATF-1 (Bex and Gaynor, 1998; Kwok *et al.*, 1996). The bZip domain of CREB contacts cyclic AMP-responsive elements (CRE) in three 21-bp repeats found in the U3 region of the LTR (Bex and Gaynor, 1998; Kwok *et al.*, 1996). Tax also binds DNA by making contacts with G/C-rich regions flanking the CRE (Kimzey and Dynan, 1998; Lenzmeier *et al.*, 1998). Tax and CREB form a stable complex on the DNA and activate transcription from the viral promoter (Bex and Gaynor, 1998; Kwok *et al.*, 1996). Tax and CREB accomplish this, in part, by recruiting the cellular coactivator CBP, and the paralog p300, to the HTLV-1 promoter (Bex and Gaynor, 1998; Kwok *et al.*, 1996).

CBP acetylates the histone tails of chromatin occupied on the HTLV-1 LTR to dramatically up-regulate transcription (Georges *et al.*, 2003; Lu *et al.*, 2002). CBP is recruited to the HTLV-1 promoter through specific protein-protein interactions with the KIX domain (Yan *et al.*, 1998).

1.5 Dissertation Outline

Work by others have previously demonstrated the recruitment of CBP during transcription of both the HIV-1 and HTLV-1 viral genome. Although CBP plays an important role in HIV-1 an HTLV-1 viral transcription, the molecular basis of CBP recruitment by Tat and Tax, respectively, has not been rigorously studied in biophysical terms. The work detailed in this dissertation explores the basis for molecular recognition between the human coactivator CBP and the viral transcriptional activators HIV-1 Tat and HTLV-1 Tax.

In Chapter Two, we show through *in vivo* and numerous *in vitro* techniques that HIV-1 Tat directly binds the KIX domain of CBP. Tat is intrinsically disordered yet maintains the ability to activate transcription. The *in vivo* results demonstrate that Tat recruits CBP through the KIX domain to activate transcription. Circular dichroism studies suggest that Tat undergoes a folding event upon complex formation with KIX. This agrees with observations of other activation domains that become folded upon binding their partners. Furthermore, we show that binding to KIX is mediated through a short N-terminal region of Tat.

Chapter Three extends our study of molecular recognition between HIV-1 Tat and the KIX domain of CBP. We used NMR spectroscopy to map the residues on KIX that are involved in complex formation with the N-terminus of Tat. The results indicate that Tat binds to KIX in a similar mode to that used by the human transcriptional activators c-Jun and MLL and is distinct from the binding surface used by CREB and c-Myb. This work lays the foundation for future studies of the Tat-KIX interaction and has implications in Tat-associated pathogenesis.

Chapter Four concerns the interaction between the HTLV-1 transcriptional activator Tax and the KIX domain of CBP. Circular dichroism indicates that a 40 residue fragment of Tax binds to KIX and undergoes a folding event upon binding similar to that seen with HIV-1 Tat. NMR was used to map the Tax-binding surface on KIX. As seen for Tat, HTLV-1 Tax binds to the KIX surface used by c-Jun and MLL and not by CREB and c-Myb. Furthermore, Tax and CREB can together bind the KIX domain of CBP. This result suggests a molecular description of how Tax and CREB synergize to recruit CBP to the HTLV-1 promoter to activate transcription.

Chapter 2

Molecular Recognition of the Human Coactivator CBP by the HIV-1 Transcriptional Activator Tat

This chapter describes work published in *Biochemistry* (Vendel & Lumb, 2003). Experimental details and results have been expanded beyond those reported in *Biochemistry*.

2.1 Abstract

HIV-1 Tat is required for the expression of the viral genome. Tat binds to an RNA stem-loop and mediates the recruitment of human coactivators to facilitate HIV-1 transcription. The coactivator and acetyltransferase CBP, and the paralog p300, are recruited to the HIV-1 promoter by Tat. Here we identify the interacting domains of Tat and CBP. CD and pulldown assays show that full-length Tat binds to the KIX domain of CBP, but not to the C/H1 or CR2 domains. CD and NMR studies of Tat deletion mutants localize the KIX-binding domain of Tat to the N-terminal 24 residues of Tat. Transient cotransfections demonstrate that exogenous KIX behaves as a dominant negative to Tat-mediated transcription in human T-cells, suggesting that Tat and KIX interact *in vivo*. These findings indicate that Tat targets the KIX domain of CBP and provide insight into the molecular interactions involved in regulating HIV-1 gene expression.

2.2 Introduction

Expression of the HIV-1 genome requires both human and viral transcription factors (Frankel and Young, 1998; Jones and Peterlin, 1994). The HIV-1 LTR promoter is reminiscent of human protein-coding promoters, and viral expression employs the human general transcription machinery, including RNA polymerase II, general transcription factors, coactivators, and the activators NF–κB and SP1 (Frankel and Young, 1998; Jones and Peterlin, 1994). In addition to the host proteins, the HIV-1 transactivator Tat is needed for viral RNA synthesis and propagation (Frankel and Young, 1998; Jones and Peterlin, 1994). Attenuated viruses with mutated Tat integrate the HIV-1 genome into human cells, but are unable to propagate (Garcia *et al.*, 1988; Sadaie *et al.*, 1988). Unlike human transcriptional activators, which bind DNA, Tat binds RNA at the stem loop of TAR through a basic arginine rich motif (ARM, residues 49-57 of Tat) (Frankel and Young, 1998; Jones and Peterlin, 1994). Once bound to TAR, Tat recruits the endogenous cellular factors involved in elongation such as P-TEFb, which hyperphosphorylates the C-terminal domain of the large subunit of RNA polymerase II (Isel and Karn, 1999).

The human genome is packaged into nucleosomes that repress transcription until remodeled following histone acetylation (Orphanides and Reinberg, 2002). Since the incorporated HIV-1 genome is also packaged into nucleosomes, recruitment of proteins that regulate the modification of the nucleosomal architecture downstream of the HIV-1 start site is likely to be needed for viral

gene expression and replication. For example, nucleosome 1 near the transcription start site of the 5' LTR is disrupted during transcriptional activation (Marzio and Giacca, 1999; Roebuck and Saifuddin, 1999), and acetylation of the histone tails of nucleosome 1 is coupled with transcriptional activation in a Tat dependent manner (He and Margolis, 2002). It is likely that Tat, in part, recruits proteins involved in nucleosome remodeling, including acetyltransferases, to facilitate viral gene expression (Benkirane *et al.*, 1998; Marzio *et al.*, 1998).

CBP is large protein of 2441 amino acids comprised of several autonomously functional domains that contribute to different facets of CBP function (Figure 1) (Chan and La Thangue, 2001; Goodman and Smolik, 2000). CBP interacts with numerous mammalian and viral transcription activators, coactivators, corepressors and the general transcription machinery (Chan and La Thangue, 2001; Goodman and Smolik, 2000). For example, the C/H1 domain binds NF-κB, HIF-1 and HPV E6, the CR2 domain binds p53, SRC-1 and HTLV-1 Tax and the KIX domain contacts many cellular and viral transcriptional activators including CREB, HTLV-1 Tax, NAP-1, MLL and c-Jun (Chan and La Thangue, 2001; Goodman and Smolik, 2000). The combination of acetyltransferase activity and ability to interact with multiple transcription factors endows upon CBP a widespread role in transcription during basic cellular process such as cell growth, differentiation and tumor suppression (Chan and La Thangue, 2001; Goodman and Smolik, 2000).

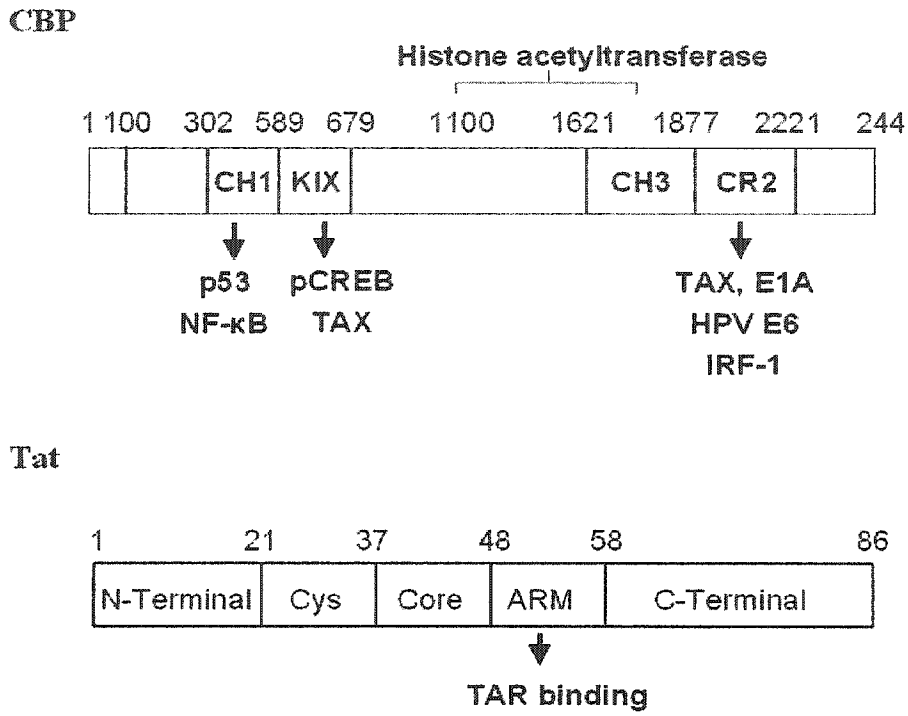

Figure 1. Schematic representation of the domain structures of CBP and Tat. CBP possesses multiple, functionally independent, protein-interacting domains, including C/H1 (residues 300-450), KIX (residues 589-679), and CR2 (residues 2055-2150) (Chan and La Thangue, 2001; Goodman and Smolik, 2000). Some transcriptional activators that bind C/H1, KIX and CR2 are listed. Tat comprises the N-terminal domain, Cys-rich domain, core domain and ARM (Jones and Peterlin, 1994).

Tat interacts with the histone acetyltransferase CBP, and with the highly related protein p300 (Benkirane *et al.*, 1998; Marzio *et al.*, 1998). Recruitment of CBP by Tat during HIV-1 gene expression may provide a mechanism for nucleosome remodeling and transcription regulation (Benkirane *et al.*, 1998; Marzio *et al.*, 1998). Beyond the protein-protein interactions involved in viral transcription, Tat also makes contacts with a number of cellular transcription factors, coactivators

and other cellular proteins that may disrupt normal cellular function and contribute to infection-associated pathogenesis (Col *et al.*, 2002; de la Fuente *et al.*, 2002; Ptak, 2002). For example, the C-terminus of a 101-amino acid version of Tat, which is deleted in the 86-residue Tat, globally represses the histone acetyltransferase activity of CBP and other HAT proteins, and decreases the expression of a number of cellular, but not viral, genes (Col *et al.*, 2002; de la Fuente *et al.*, 2002; Ptak, 2002).

Although CBP plays an essential role in Tat-dependent HIV-1 transcription (Benkirane *et al.*, 1998; Marzio *et al.*, 1998), the molecular basis of CBP recruitment by Tat during viral gene expression is unclear. Here we show that the N-terminus of Tat recognizes the KIX domain of CBP *in vitro*, and that the interaction modifies Tat behavior in human T-cells. Our results implicate KIX as the domain of CBP that is targeted by Tat during HIV-1 propagation.

2.3 Methods

2.3a Protein Preparation and Purification

The Tat used here corresponds to the 86-residue Tat from the HIV-1 isolate HXB2. The amino-acid sequence, derived by DNA sequencing of the expression plasmid, is:

GSH MEPVDPRLEP WKHPGSQPKT ACTNCYCKKC CFHCQVCFIT
KALGISYGRK KRRQRRRPPQ GSQTHQVSLS KQPTSQSRGD PTGPKE

The N-terminal residues GSH are derived from the pET-15b expression plasmid.

Tat was expressed as an N-terminal His-tagged fusion protein with a pET-15b plasmid (pET-15b:Tat) harboring a PCR product encoding Tat amplified from the plasmid GST-Tat (86R) obtained from the NIH AIDS Research and Reference Reagent Program (Rhim *et al.*, 1994). The coding sequence for Tat was confirmed with dRhodamine sequencing. Tat was expressed in *Escherichia coli* strain Rosetta BL21 (DE3) pLysS (Novagen). Cells were grown at 37 °C to an optical density at 600 nm of 0.8 and induced with 0.5 mM IPTG for 2 hours. Cells were harvested with centrifugation and lysed by sonication. Tat was purified from the insoluble cell-lysate fraction resuspended in 6 M urea, 20 mM Tris-base, 500 mM NaCl, and 50 mM imidazole, pH 7.8, with His-bind resin (Novagen). Tat was eluted with 20 mM Tris-base, 500 mM NaCl, and 400 mM imidazole, pH 7.8. The His-tag was than cleaved with thrombin (Novagen) in elute buffer, pH 8.4, overnight at room temperature. Tat was treated with 50 mM EDTA and 0.1 M DTT, pH 8.4, prior to final purification with reversed phase C_{18} HPLC using a linear water/acetonitrile gradient containing 0.1% TFA. The identity of Tat was confirmed with electrospray mass spectrometry, and the observed and expected masses agreed to within 1 Da. The final yield of Tat was 2 mg/L.

^{15}N-labeled Tat was prepared in the same way as unlabeled Tat except cells were grown in M9 minimal media supplemented with thiamine (McIntosh and Dahlquist, 1990) containing 0.8 g/L $^{15}NH_4Cl$ as the sole nitrogen source. The final yield of ^{15}N-Tat was 1 mg/L.

The C-terminal, RNA-binding domain of HIV-1 Tat (ARM) was expressed as an N-terminal His-tagged fusion protein with a pET-15b plasmid (pET-15b:ARM) harboring a PCR product encoding residues 48-86 of Tat amplified from pET-15b:Tat. The coding sequence of ARM was confirmed with dRhodamine sequencing. ARM was expressed in *E. coli* strain Rosetta BL21 (DE3) pLysS (Novagen). Cells were grown at 37 °C to an optical density at 600 nm of 0.8 and induced with 0.5 mM IPTG for 2 hours. Cells were harvested with centrifugation and lysed by sonication. ARM was purified from the insoluble cell-lysate fraction resuspended in 6 M urea, 20 mM Tris-base, 500 mM NaCl, and 50 mM imidazole, pH 7.8, with His-bind resin (Novagen). ARM was eluted with 20 mM Tris-base, 500 mM NaCl, and 400 mM imidazole, pH 7.8. The His-tag was cleaved with thrombin (Novagen) in elute buffer, pH 8.4, overnight at room temperature. ARM was treated with 50 mM EDTA and 0.1 M DTT, pH 8.4, prior to final purification with reversed phase C_{18} HPLC using a linear water/acetonitrile gradient containing 0.1% TFA. The identity of ARM was confirmed with electrospray mass spectrometry, and the observed and expected masses agreed to within 1 Da. The final yield of ARM was 3 mg/L.

KIX (residues 589-679 of human CBP with an additional N-terminal Met) was expressed in *E. coli* strain BL21 (DE3) pLysS and purified as described previously (Campbell and Lumb, 2002; Mestas and Lumb, 1999). Cells were grown at 37 °C to an optical density at 600 nm of 0.8 and induced with 0.5 mM IPTG for 3 hours. Cells were harvested with centrifugation and lysed by sonivation. KIX was purified from the soluble fraction by ion exchange chromatography with SP sepharose Fast Flow cation exchange column (Amersham Pharmacia Biotech). Final purification was by reversed phase C_{18} HPLC using a linear water/acetonitrile gradient containing 0.1% TFA. The identity of KIX was confirmed with electrospray mass spectrometry, and the observed and expected masses agreed to within 1 Da. The final yield was 6 mg/L.

C/H1 (residues 300-450 of murine CBP) was expressed as a GST-fusion protein in *E. coli* strain BL21 (DE3) pLysS using the plasmid pGST-C/H1 (Gift from J.K. Nyborg; Van Orden *et al.*, 1999a). Cells were grown at 37 °C to an optical density at 600 nm of 0.8 and induced with 1 mM IPTG for 3 hours. Cells were harvested with centrifugation and lysed by sonication. GST-C/H1 was purified from the soluble cell-lysate fraction with glutathione sepharose 4B (Amersham Pharmacia Biotech). GST-C/H1 was eluted with 20 mM Tris-base, 150 mM NaCl, and 5 mM glutathione, pH 7.8. The GST-tag was cleaved in elute buffer with thrombin (Novagen) at 25 °C overnight. Cleaved protein was dialyzed

against GST-bind buffer and C/H1 was separated from GST by further GST-affinity chromatography. Final purification was by reversed-phase C_{18} HPLC. The identity of C/H1 was confirmed with electrospray mass spectrometry, and the observed and expected masses agreed to within 1 Da. Final yields of GST-fusion proteins were roughly 0.5 mg/L.

HPLC-purified CR2 (conserved region 2, residues 2055-2150 of murine CBP) was a generous gift of S. J. McBryant.

All HPLC-purified proteins were stored as a lypholized powder and dialyzed against 10 mM sodium phosphate, 150 mM NaCl and 1 mM DTT, pH 7.0, overnight before use.

GST-fusion proteins of HIV-1 isolate HBX2 Tat (expressed with GST-Tat 1 86R, NIH AIDS Research & Reference Reagent Program) (Rhim *et al.*, 1994), C/H1 (residues 300-450 of murine CBP expressed with plasmid pGST-C/H1, gift of J. K. Nyborg) (Van Orden *et al.*, 1999a), KIX (residues 451-720 of murine CBP expressed with plasmid pGST-KIX, gift of J. K. Nyborg) (Giebler *et al.*, 1997) and CR2 (residues 2055-2150 of murine CBP expressed with plasmid pGST-$CR_{2055-2150}$, gift of J. K. Nyborg) (Scoggin *et al.*, 2001) were expressed in *E. coli* strain BL21 (DE3) pLysS. Cells were grown to an optical density at 600 nm of 0.8 at 37 °C and induced with 1 mM IPTG for 3 hours. Cells were harvested with centrifugation and lysed by sonication. GST-fusion proteins were purified from

the soluble fractions by cation-exchange chromatography on HiTrap SP (AP Biotech) followed by GST-affinity chromatography with glutathione sepharose 4B (Amersham Pharmacia Biotech). Proteins were dialyzed in 10 mM sodium phosphate, 150 mM NaCl, and 10% glycerol, pH 7.0 and stored at -70 ˚C.

2.3b Peptide Synthesis

Tat_{1-24}, corresponding to residues 1-24 of Tat from HIV-1 isolate HXB2, was synthesized on MBHA (4-methylbenzhydrylamine hydrochloride salt) resin (100-200 mesh) using manual Boc chemistry (Schnölzer *et al.*, 1992). The sequence of the peptide is MEPVDPRLEP WKHPGSQPKT ACTN-NH_2. The C-terminus was amidated. 0.373 g MBHA resin was swelled in 10 ml DMF for 30 min. 0.36 g HBTU and 0.413g (1 mmol) of the first C-terminal amino acid Boc-Asn(Xan) were mixed with 2.5 ml DMF and 0.25 ml DIEA in a glass tube and sonicated until clear. The amino acid was allowed to activate for two minutes prior to coupling to the resin. The first amino acid was coupled for 40 minutes while subsequent amino acids were coupled for 12 minutes. Each coupling reaction was confirmed with the Kaiser ninhydrin test (Kaiser *et al.*, 1970) or chloranil test for proline (Christensen, 1979). The Boc group and protecting groups were removed with two washes with 6 ml of TFA for two minutes. The side chains of Arg, Asn, Asp, Cys, Gln, Glu, His, Lys, Ser, Thr, and Trp were protected during Boc chemistry with Tos, Xan, Bzl, MeBzl, Xan, Bzl, DNP, ClZ, Bzl, Bzl, and CHO, respectively (Nova Biochem). The DNP protecting group of His was removed after final coupling with 5 ml of thiolphenol incubated overnight at room

temperature. The completed peptide was extensively rinsed with DMF, methylene chloride, diethyl ether, and methanol. The resin was dried overnight under vacuum to remove residual solvents.

The peptide was cleaved for two hours (1 hour extra for Tos groups) from the resin with HF cleavage using approximately 10 ml of HF per 1 g of dried resin and 1 ml anisol per 1 g of dried resin. The cleaved peptide and resin were resuspended and rinsed in 100 % ether. The peptide was eluted from the resin with 5 % acetic acid in water. The eluded peptide was then lyophilized.

Tat_{1-24} was purified by reversed phase C_{18} HPLC using a linear water/acetonitrile gradient containing 0.1% TFA. The identity of Tat_{1-24} was confirmed with electrospray mass spectrometry, and the observed and expected masses agreed to within 1 Da.

2.3c GST-Pulldown Binding Assays

GST-fusion proteins (25 pmol) were bound to a 30 μl slurry of glutathione sepharose 4B (AP Biotech) in 200 μl of GST binding buffer (50 mM Tris-base, 150 mM NaCl, 100 mM NaF, 200 μM sodium orthovanadate, 0.5% NP-40, and 10 mM DTT, pH 8.0) for 2 hours at 4 °C. Bound GST-fusion proteins were incubated in 200 μl of binding buffer with 25 pmol of target protein for 2 hours at 4 °C. Bound proteins were washed four times with wash buffer (50 mM Tris-base, 350 mM NaCl, 100 mM NaF, 200 μM sodium orthovanadate, 0.5% NP-40,

and 10 mM DTT, pH 8.0) and eluted by boiling in SDS-PAGE load buffer (50 mM Tris-base, 0.06% bromophenol blue, 2% SDS, 10% glycerol, and 1 mM 2-mercaptoethanol). Target proteins were resolved with 16% SDS-PAGE. Proteins were blotted onto nitrocellulose (BioRad). KIX was detected with SYPRO ruby blot stain (BioRad) per the manufacturer's protocol. Tat was detected with a Tat specific rabbit antibody (HIV-1 BH10 Tat antiserum) obtained from the NIH AIDS Research and Reagent Reference Program (Hauber *et al.*, 1987; Toth *et al.*, 1995) visualized by chemiluminescence (ECL Plus, AP Biotech) with a Molecular Dynamics STORM 860 fluorescence imaging instrument.

2.3d Protein Concentration Determination

Concentrations of protein stock solutions used to prepare CD and NMR samples were determined with absorbance in 6 M GuHCl and 10 mM sodium phosphate, 150 mM sodium chloride, pH 6.5 at 25 °C (Edelhoch, 1967). Extinction coefficients for Tat, KIX, C/H1 and Tat_{1-24} at 280 nm of 8730, 12090, 6170 and 5690 M^{-1} cm^{-1} were used, respectively. Extinction coefficients for ARM and CR2 at 276 of 1450 and 6970 M^{-1} cm^{-1} were used, respectively.

2.3e CD spectroscopy

CD spectra were acquired with a Jasco J720 spectrometer. Samples were prepared in 10 mM sodium phosphate and 50 mM sodium chloride, pH 7.0, and contained 10 μM of each protein. Spectra comprised 25 scans recorded at 10

°C. The normalized molar ellipticity [θ] was calculated from the measured ellipticity θ using [θ] = θ*100/(n*l*c), where n is the total number of residues of the protein or mix of proteins, c is the total protein concentration in mM and l is the pathlength in cm. Binding was detected by differences in observed spectra of the protein mixes from the spectra expected if the two proteins do not interact, calculated as the normalized sum of the spectra of the individual proteins. Two proteins do not bind if the observed and calculated spectra overlap. Two proteins do bind if the observed and calculated spectra do not overlap, which presumably reflects a change in the secondary structure upon complex formation.

2.3f Analytical Ultracentrifugation

Sedimentation equilibrium was performed with a Beckman XL-I analytical ultracentrifuge. Data were collected at 280 nm at the rotor speeds and protein concentrations listed in Table 1. Samples were dialyzed against the reference buffer (10 mM sodium phosphate, 100 mM NaCl, 1 mM DTT, and +/- 1 mM $ZnCl_2$, pH 7.0). Calculated partial specific volumes at 10 °C of 0.7118 ml g^{-1} was used for Tat (Laue *et al.*, 1992). The solvent density of 1.004 g ml^{-1} was measured directly. Data were fit to an ideal, single-species model with ORIGIN (Beckman).

2.3g NMR Spectroscopy

All NMR spectra were acquired with a Varian Unity Inova operating at 500.1 MHz for ^{1}H and referenced to internal DSS at zero ppm.

^{15}N-edited HSQC NMR spectra was collected using 110 μM full-length ^{15}N-Tat in 10 mM sodium phosphate and 50 mM NaCl, 1mM DTT, pH6.0 containing 10% D_2O and DSS. Data was collected using spectral widths of 6000 and 1850 Hz in the ^{1}H and ^{15}N dimensions. Spectra consisted of 256 complex increments defined by 96 transients and 1024 complex points. Data was processed with NMRPipe and analyzed with NMRView (Delaglio *et al.*, 1995; Johnson and Blevins, 1994).

The K_d for the Tat_{1-24}-KIX complex was determined with 1D ^{1}H NMR spectroscopy at 10 °C from changes of the His 13 C2H chemical shift as 50 μM Tat_{1-24} was titrated with 0-150 μM KIX. Samples were prepared in 10 mM sodium phosphate and 50 mM NaCl, pH 7.0, lyopholized, and resuspended in D_2O. pH was adjusted to 7.0, uncorrected for the isotope effect. Chemical shifts were measured from 1D spectra collected with a digital resolution of approximately 0.001 ppm/point. The K_d was obtained from changes in the ^{1}H chemical shift with KIX concentration using

$$\delta = \delta_f + \delta_b - \delta_f*(P + L + K_d - \{(P + L + K_d)^2-(4*P*L)\}^{0.5}/2*[P]$$

where δ is the chemical shift at KIX concentration L, δ_f and δ_b are the free and bound chemical shifts, respectively, and P is the concentration of Tat_{1-24}. The fit assumes a 1:1 stoichiometry. The resonances of the two aromatic side chains of Tat (Trp 11 and His 13) were assigned at 10 °C from a TOCSY spectrum collected with a 60 ms DIPSI sequence. The sample contained 0.5 mM Tat_{1-24} in 10 mM sodium phosphate and 50 mM NaCl, pH 7.0.

2.3h Transient Cotransfection Assay

Mammalian expression plasmids encoding HIV-1 Tat (pSV2Tat72) and an LTR promoter linked to a luciferase reporter gene (pBlue3'LTR-luc-A) were obtained from the NIH AIDS Research and Reference Reagent Program (Frankel and Pabo, 1988). Mammalian expression plasmids for KIX (pRSV-KIX, encoding residues 459-679 of murine CBP) and CR2 (pCMV-CR2, encoding residues 2003-2212 of murine CBP) were gifts of J. K. Nyborg (Giebler *et al.*, 1997; Scoggin *et al.*, 2001). Jurkat cells grown in Iscove's modified Delbecco's media (IMDM) supplemented with 10% fetal bovine serum, 2 mM L-glutamine, and penicillin-streptomycin were transfected with plasmids using lipofectamine (Invitrogen). The total DNA for each transfection was normalized to 2 μg with pUC-19. Cells were lysed 24 hours post-transfection and LTR luciferase activity was normalized against 10 ng/transfection pRL-TK Renilla luciferase (Promega). Luciferase activity was monitored with a Turner Designs model TD 20-e luminometer. Tat expression was confirmed with Western blot analysis of the whole-cell lysate using a Tat specific rabbit antibody (HIV-1 BH10 Tat antiserum)

(Hauber *et al.*, 1987) obtained from the NIH AIDS Research and Reagent Reference Program visualized by chemiluminescence (ECL Plus, AP Biotech) with a Molecular Dynamics STORM 860 fluorescence imaging instrument.

2.3i Tat Functional Assay

Purified, recombinant Tat was tested for biological activity on the basis of cellular uptake (Frankel and Pabo, 1988) by Jurkat cells transfected with the LTR-luciferase reporter plasmid (pBlue3'LTR-luc-A) obtained from the NIH AIDS Research and Reference Reagent Program (Jeeninga *et al.*, 2000; Klaver and Berkhout, 1994). Jurkat cells were transfected as described above with 400 ng of pBlue3'LTR-luc-A plasmid and 10 ng of pRL-TK Renilla luciferase plasmid (Promega) using lipofectamine (Invitrogen). The total DNA for each transfection was normalized to 2 μg with pUC-19. Cells were grown in the presence or absence of 3.33 μM Tat protein. Cells were lysed 24 hours post-transfection and LTR luciferase activity was normalized against 10 ng/transfection pRL-TK Renilla luciferase (Promega). Luciferase activity was monitored with a Turner Designs model TD 20-e luminometer.

2.4 Results

2.4a Intrinsic Structural Disorder of Tat

The CD spectrum of Tat is reminiscent of an unfolded protein, with a minimum near 199 nm and a lack of spectral characteristics above 210 nm indicative of helix or sheet formation (Figure 2A). The CD signal at 222 nm becomes slightly

more negative with increasing temperature (Figure 2A), which is the opposite behavior expected for a typical globular protein. The ^{15}N-edited, two-dimensional HSQC NMR spectrum of ^{15}N-Tat also suggests that Tat is largely unfolded at pH 6.0. The limited H^N chemical shift dispersion between 8.0 and 8.8 ppm suggests Tat is intrinsically disordered (Figure 3), as seen for other transcriptional activators (Campbell and Lumb, 2002; Campbell *et al.*, 2000; McEwan *et al.*, 1996; O'Hare and Williams, 1992; Schmitz *et al.*, 1994).

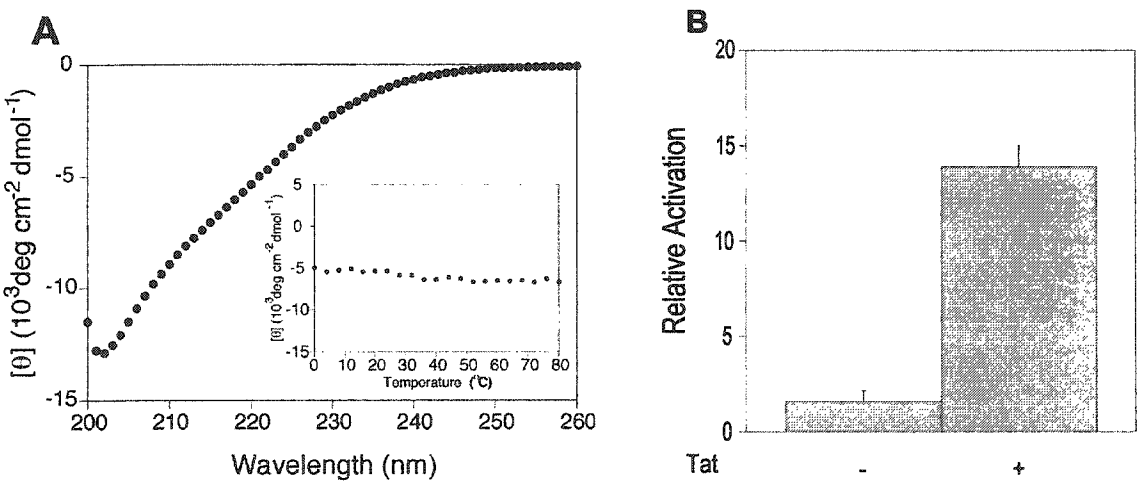

Figure 2. (A) CD spectroscopy indicates that full-length Tat is largely unfolded in isolation. Tat is devoid of signature CD signals that reflect significant helix or sheet formation, and has a minimum near 199 nm that is indicative of an unfolded protein. The CD signal at 222 nm becomes slightly more negative with increasing temperature (insert), which is the opposite behavior expected for a typical globular protein. (B) Tat is functional for cellular uptake and nuclear import. Recombinant Tat added to transfected human T cells activates luciferase expression from the HIV-1 LTR promoter above basal levels. Collectively, these results show that the Tat used here is an intrinsically disordered, biologically active protein.

A functional property of Tat is cellular uptake and nuclear import (Frankel and Pabo, 1988). This feature is maintained by the Tat used here (Figure 2B), demonstrating that the Tat is biologically active by its ability to activate transcription from the LTR promoter.

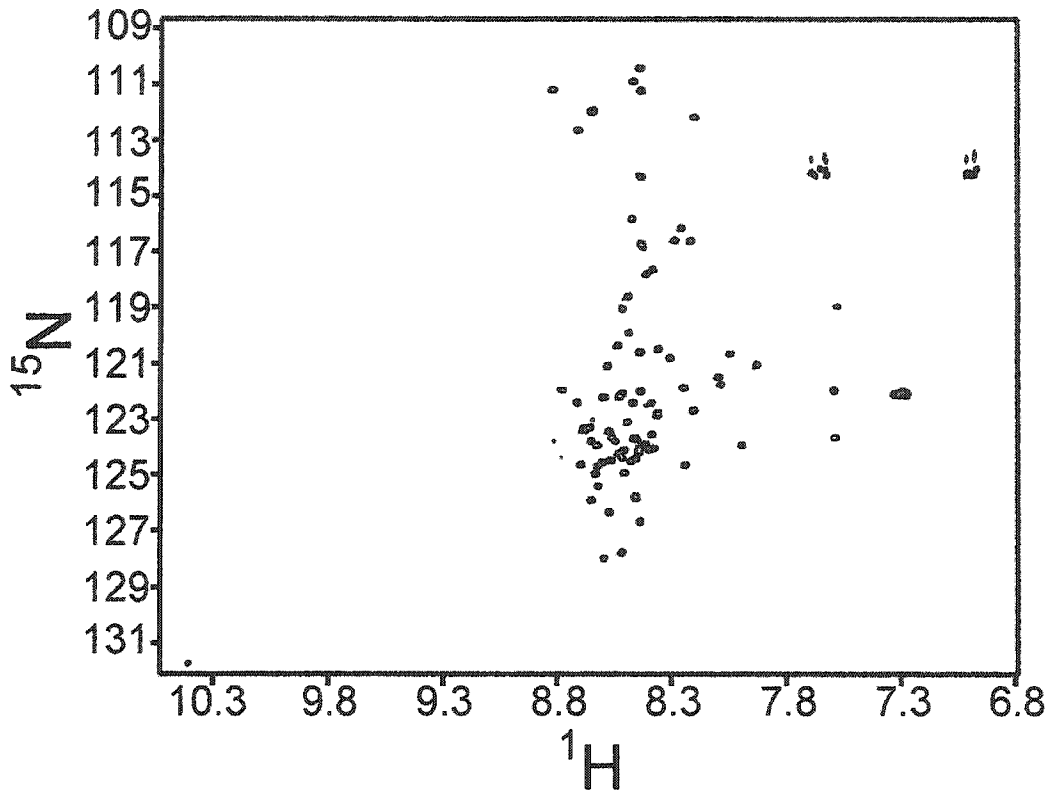

Figure 3. ^{15}N-edited HSQC NMR spectrum suggests that Tat is disordered in solution. Tat lacks significant H^N chemical shift dispersion in the proton dimension between 7.5 and 9.5 ppm.

The Cys-rich domain (Figure 1) of Tat may bind Zn^{2+} (Frankel *et al.*, 1989; Slice *et al.*, 1992). Addition of Zn^{2+} causes some changes in the CD spectrum, including a reduced intensity of the unfolded signature band at 190 nm (Figure

4). However, the changes are not indicative of a large-scale folding transition upon binding Zn^{2+}, as seen for bona fide Zn-binding proteins (Cox and McLendon, 2000).

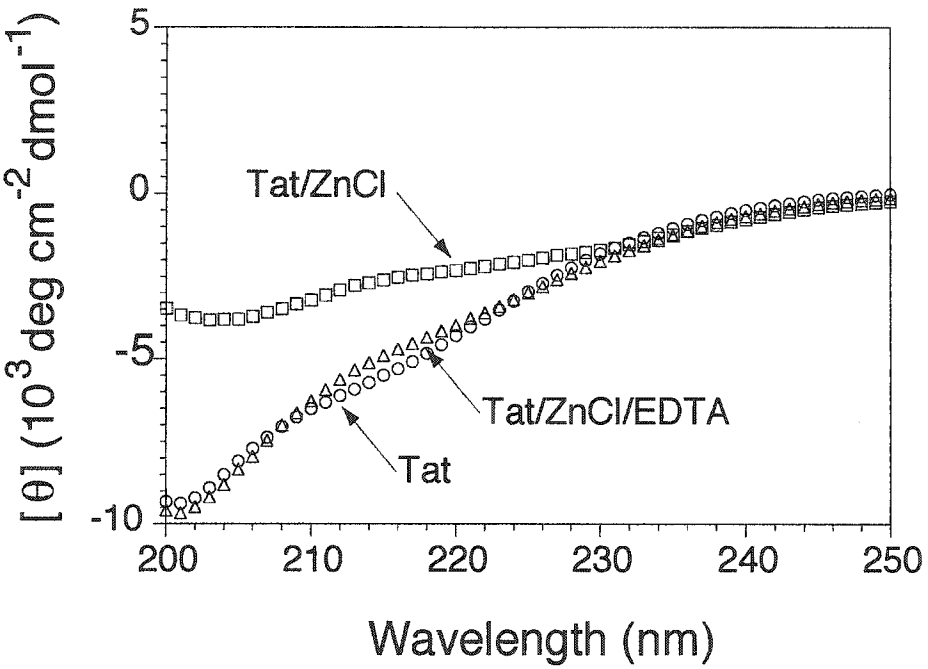

Figure 4. CD spectroscopy shows that Tat (o) undergoes a minor conformational change upon addition of 1 mM ZnCl ( ). This change is reversible with the addition of 1 mM EDTA (Δ). The observable changes in the CD signal are not indicative of a large-scale zinc-induced, global folding transition.

Sedimentation equilibrium indicates Tat forms a dimer upon the addition of Zn^{2+} (Figure 5A; Table 1). Characterization of Tat in the absence of Zn^{2+} indicates that Tat is a monomer with an observed mass of 11.5 kDa (Figure 5B; Table 1). Gel-filtration was also used to obtain the mass of Tat at 10 C in 10 mM sodium phosphate, 150 mM NaCl, 5 mM DTT, and pH 7.00. Tat had an observed mass for a monomer of 9 kDa and a mass for a high-ordered aggregate of 101.2 kDa.

These results indicate that Tat is predominantly a monomer, but may form high-ordered aggregates in the absence of Zn^{2+}. This is likely due to the propensities of the seven Cys residues to form intermolecular disulfide binds with other Tat molecules.

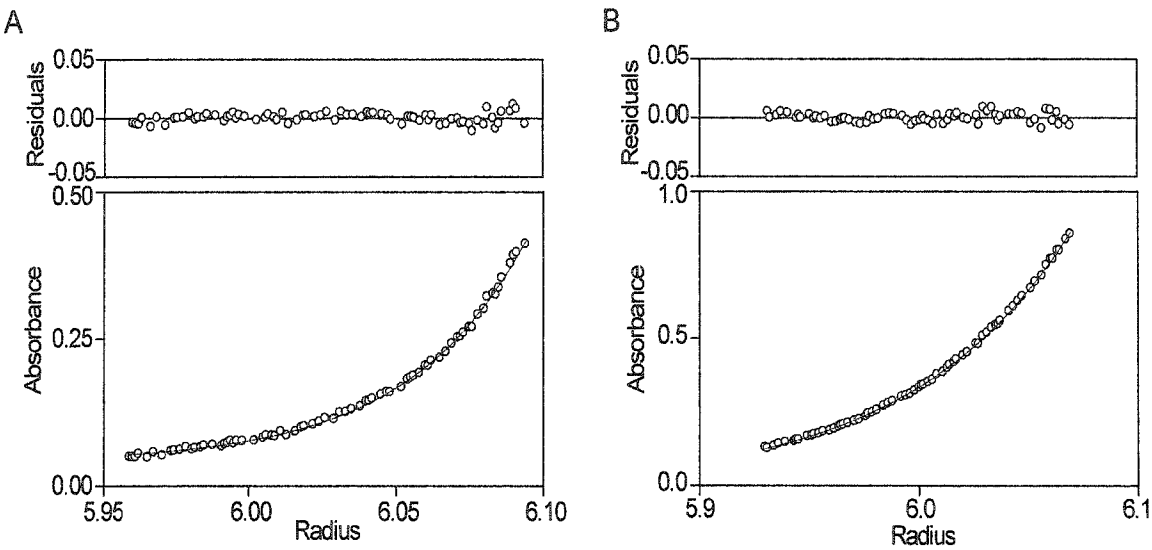

Figure 5. A) Sedimentation equilibrium of Tat in the presence of 1 mM $ZnCl_2$ fit to a single species model. The mass observed indicates Tat forms a dimer with zinc (Table 1). B) Absent of zinc, Tat fits to a single species with an observed mass close to that expected for a monomer. Both models fit to a single species with a random distribution of residuals.

Table 1: Sedimentation equilibrium analysis of Tat $^{+}$/- $ZnCl_2$.

Total concentration of Tat (μM)	Observed mass (kDa)	
Tat (expected mass for monomer: 10065 Da)		
	40 krpm	48 krpm
70	10.6	11.3
90	10.7	11.0
115	11.2	9.8
Tat + $ZnCl_2$ (expected mass for dimer: 20130 Da)		
	40 krpm	45 krpm
70	19.3	18.9
90	17.1	17.6
115	19.0	20.0

These results indicate that Tat is biologically active and largely unfolded at neutral pH both in the presence and absence of Zn^{2+}, although the results do not preclude the local formation of short elements of secondary structure. This result is in accord with a previous NMR study of the 86 amino acid Tat from the HIV-1 Zaire 2 isolate (Bayer *et al.*, 1995).

2.4b Tat Associates with KIX *in vitro*

Two different *in vitro* binding assays were used to screen for the binding of Tat to discrete CBP domains. Pull-down assays were used initially to screen GST-tagged C/H1, CR2 and KIX domains of CBP for Tat binding. In this assay format, Tat binds to the GST-KIX fusion protein, but not to GST, GST-C/H1 or GST-CR2 (Figure 6). In a reciprocal experiment, GST-Tat binds untagged KIX (Figure 6). These results suggest that Tat binds to KIX, and not to C/H1 or CR2.

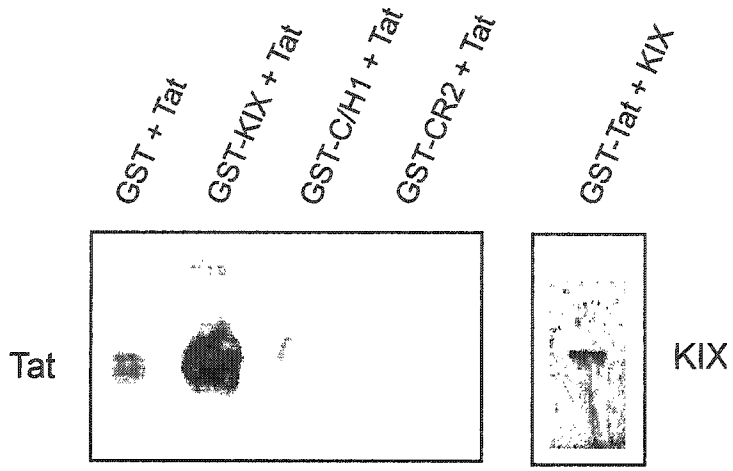

Figure 6. GST-pulldown screening of CBP domains for Tat binding. Tat interacts with GST-KIX, but not with GST, GST-C/H1, or GST-CR2. Tat was detected by Western blotting with a Tat-specific antibody. A reciprocal experiment shows that GST-Tat binds KIX.

CD spectroscopy was then used to test domains of CBP for direct Tat binding. The CD spectrum of free KIX is indicative of a helical protein (Figure 7A), in accord with the NMR structure of KIX (Radhakrishnan *et al.*, 1997) and previous CD results (Mestas and Lumb, 1999). Addition of Tat results in a significant increase in ellipticity over the calculated spectrum of non-interacting Tat and KIX (Figure 7A). This result suggests that Tat binds the KIX domain of CBP. In addition, the CD data suggest that complex formation is coupled with an increase in secondary structure (folding).

The CD spectrum of C/H1 is reminiscent of a partially helical protein (Figure 7B), in accord with previous results (Newton *et al.*, 2000). Addition of Tat to C/H1 results in a CD spectrum that is essentially identical to the calculated spectra of

non-interacting C/H1 and Tat (Figure 7B), suggesting that Tat does not bind the C/H1 domain. The CD spectrum of CR2 is reminiscent of a partially helical protein (Figure 7C). Addition of Tat to CR2 results in a CD spectrum that is essentially identical to the calculated spectra of non-interacting C/H1 and Tat (Figure 7C), suggesting that Tat does not bind the CR2 domain (Figure 7C).

Collectively, these results suggest that Tat binds the KIX domain of CBP, and that binding is accompanied by secondary structure formation.

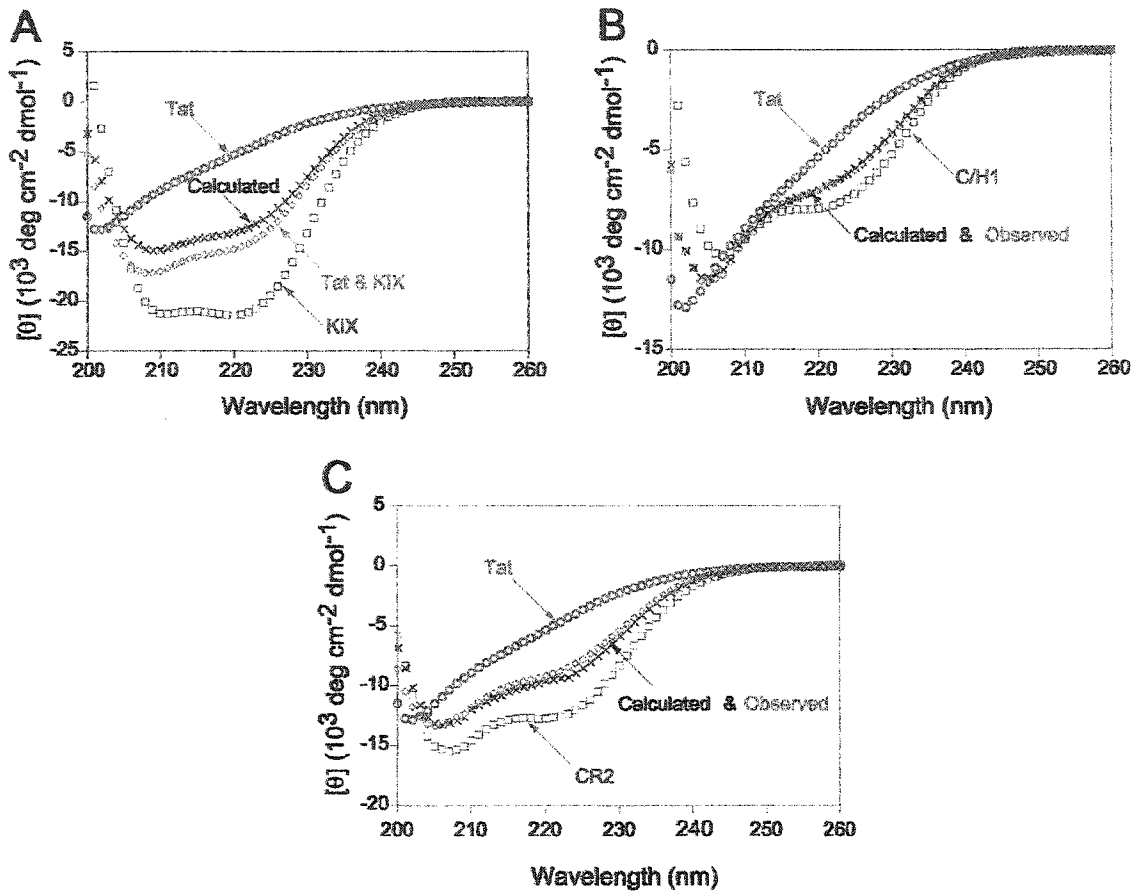

Figure 7. CD screening of CBP domains for Tat binding. Tat binds KIX, but not C/H1 or CR2. (A) Mixing of Tat (○) with KIX (□) results in a spectrum (◊) with greater helicity at 208 and 222 nm than expected from the sum of the spectra of the two isolated proteins (x), suggesting that KIX forms a complex with Tat in solution. (B) Mixing Tat (○) and C/H1 (□) results in a spectrum (◊) that is equal to the sum of the spectra of the two isolated proteins (x), suggesting that Tat and C/H1 do not interact. (C) Mixing Tat (○) and CR2 (□) results in a spectrum (◊) that is equal to the sum of the spectra of the two isolated proteins (x), suggesting that Tat and CR2 do not interact. Reproducible results were obtained from three independent experiments. Based on variations in CD spectra collected with independently prepared, ostensibly identical samples, the error in $[\theta]_{222}$ is less than 4%. The difference between the calculated and observed spectra of the Tat-KIX complex is 11% of the calculated spectrum.

2.5c KIX Mediates Tat-activated Transcription in Human T Cells

Since KIX interacts with Tat *in vitro*, KIX is expected to act as a dominant negative regulator of Tat activation *in vivo*. Therefore, Tat-dependent transcription in human T cells was analyzed in the presence and absence of KIX and CR2. Human T-cells (Jurkat) were transiently cotransfected with a luciferase reporter gene fused to the HIV-1 LTR promoter with plasmids encoding Tat, KIX or CR2. Tat efficiently activates transcription from the HIV-1 promoter, as expected (Figure 8A).

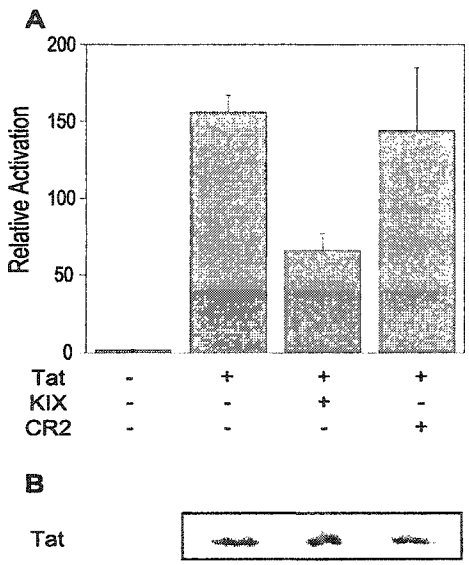

Figure 8. KIX and Tat interact in human T cells. (A) The relative fold activation of luciferase expression under the control of the HIV-1 LTR promoter was monitored to the extent of Tat activation. Plasmids encoding Tat and an LTR-luciferase reporter were co-transfected with plasmids encoding either KIX or CR2. KIX squelches Tat-dependent luciferase expression, suggesting that KIX acts as a dominant-negative for Tat mediated transcription *in vivo*. The effect is specific for KIX, since CR2 does not affect Tat-dependent expression. The finding that Tat interacts with KIX, but not CR2, in T cells is in accord with the *in vitro* binding assays. (B) Western blot analysis with Tat antiserum of whole-cell lysates suggests that the levels of Tat protein are unaffected by coexpression with KIX or CR2.

KIX expression squelches Tat-mediated transcription, suggesting that KIX can act as a dominant negative to CBP and disrupt normal Tat function. CR2, which does not bind Tat *in vitro* (Figure 7C), does not suppress Tat-mediated transcription in T cells, showing that the squelching was specific to KIX. Western blot analysis suggests that Tat expression is not reduced by coexpression with KIX or CR2 (Figure 8B), suggesting that the observed changes in Tat-mediated transcription do not reflect changes in the level of Tat protein. These *in vivo* functional results corroborate the *in vitro* finding that the KIX domain of CBP binds Tat.

2.4d The N-terminus of Tat binds KIX

CD spectroscopy was used to screen deletion mutants of Tat for binding to the KIX domain of CBP. The CD spectrum of Tat_{1-24} (residues 1-24 of Tat) is reminiscent of an unfolded protein with a minimum near 199 nm (Figure 9B). Addition of Tat_{1-24} to KIX results in a significant increase in ellipticity at the helical signature wavelengths of 208 and 222 nm over the calculated spectrum of non-interacting Tat_{1-24} and KIX (Figure 9B). This result suggests that the N-terminus of Tat binds KIX.

The CD spectrum of ARM (residues 48-86 of Tat) is reminiscent of an unfolded protein with a minimum near 199 nm (Figure 9A), as expected since full-length Tat is unfolded (Figure 2). Addition of ARM to KIX results in a CD spectrum that

is similar to the calculated spectra of non-interacting ARM and KIX, suggesting that ARM does not bind appreciably to KIX.

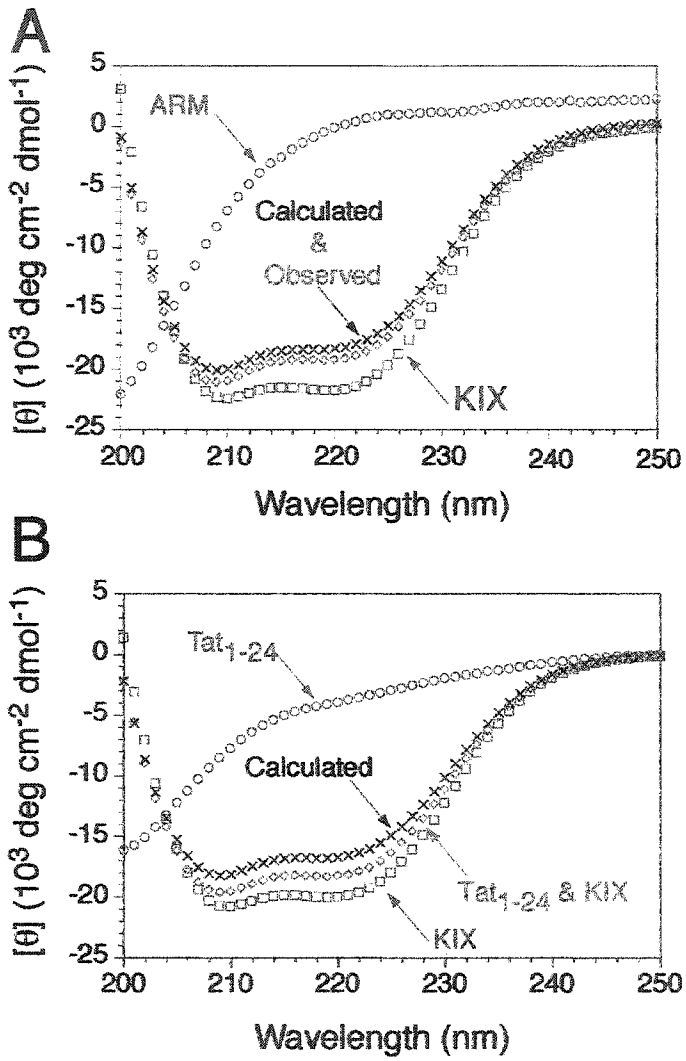

Figure 9. Association of KIX and the N-terminus of Tat monitored with CD spectroscopy. (A) Mixing of ARM (○) with KIX (□) results in a spectrum (◊) that is equal to the sum of the spectra of the two isolated proteins (x), suggesting that the C-terminus of Tat and KIX do not interact. (B) Mixing Tat_{1-24} (○) with KIX (□) results in a spectrum (◊) with greater helicity at 208 and 222 nm than expected from the sum of the spectra of the two isolated proteins (x), suggesting that Tat_{1-24} binds with KIX. Reproducible results were obtained from two independent experiments. Based on variations in CD spectra collected with independently prepared, ostensibly identical samples, the error in $[\theta]_{222}$ is approximately 3%. The difference between the calculated and observed spectra of the Tat_{1-24}-KIX complex is 9% of the calculated spectrum.

Studies of KIX binding to synthetic peptides corresponding to residues 1-48 and 21-48 of Tat, both of which contain seven Cys residues, are precluded by the limited solubility of the Tat peptide fragments.

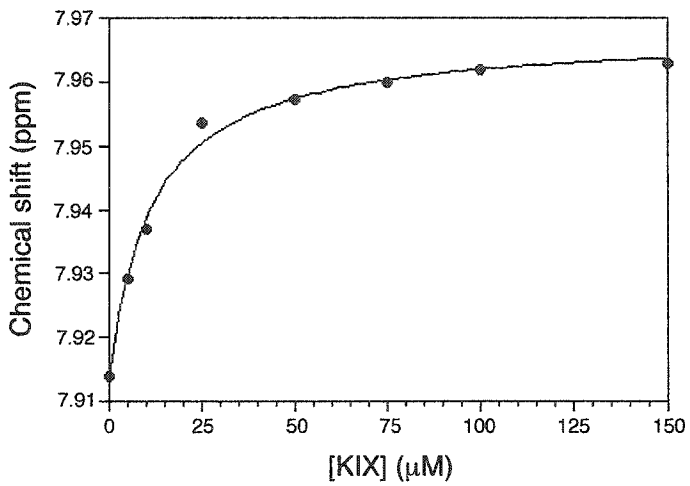

Figure 10. Association of KIX and Tat_{1-24} monitored with ^1H NMR spectroscopy. The change in the ^1H chemical shift of His 13 C2H of Tat_{1-24} with increasing KIX concentration is hyperbolic, as expected for a specific binding event. Fits for two independent experiments give K_d values of 10 and 12 μM, to yield a K_d of 11 ± 1 μM. The error in individual chemical-shift measurements was 0.005 ppm. Experiments were performed twice with reproducible results.

Formation of the Tat_{1-24}-KIX complex was also monitored with ^1H NMR spectroscopy. Resonances of the two aromatic side chains of Tat (Trp 11 and His 13) were assigned with a TOCSY spectrum, and the changes in chemical shift measured in 1D spectra as Tat_{1-24} was titrated with KIX. The experiment was performed in D_2O to allow exchange of the amide H^N protons and thus unambiguous observation of the His and Trp side chain resonances in 1D

spectra. Only the chemical shift of His 13 C2H changes appreciably upon binding KIX. The change in the His 13 C2H chemical shift upon titration with KIX is hyperbolic, as expected for a specific binding event, and yield a K_d for the Tat_{1-24}-KIX complex of 11 ± 1 μM (Figure 10). This affinity is comparable to the K_d of 9.7 μM for the complex of KIX with a 34-residue peptide derived from phosphorylated CREB (Mestas and Lumb, 1999) and 15 μM for a 25-residue peptide derived from c-Myb (Zor *et al.*, 2002).

2.5 DISCUSSION

CBP and the paralog p300 bind Tat and promote transcription from the HIV-1 promoter (Benkirane *et al.*, 1998; Marzio *et al.*, 1998). Both CBP and p300 exhibit acetyltransferase activity that may be required for nucleosomal modification during the early steps of HIV-1 transcription (Benkirane *et al.*, 1998; Marzio *et al.*, 1998), and Tat recruitment of CBP may be an essential step in nucleosome modification during HIV-1 transcription (He and Margolis, 2002). CBP contains several protein-protein interaction domains that bind transcription factors and regulators (Figure 1)

Using two *in vitro* assays and a dominant negative assay in human T-cells, we have localized the Tat-interacting region of CBP to the KIX domain. Since Tat binds to p300 (He and Margolis, 2002), and the KIX domains of CBP and p300 share 96% sequence identity, it is likely that Tat also binds the KIX domain of p300. Furthermore, we have shown that KIX interacts with the N-terminal region

of Tat from HIV-1 strain HXB2. The N-terminal 24 residues of strain HBX2 Tat share over 94% sequence identity with Tat proteins from HIV-1 strains such as LAI, pNL4-3, MN, NY-5 and SF2, suggesting that Tat proteins from different HIV-1 strains bind the KIX domain of CBP/p300.

KIX binds transcriptional activation domains via two discrete modes that employ structurally distinct surfaces. One mode is represented by the phosphorylation-induced binding of CREB (Radhakrishnan *et al.*, 1997). In contrast, MLL and c-Jun bind constitutively to a different surface of KIX than phosphorylated CREB (Campbell and Lumb, 2002; Goto *et al.*, 2002). Determination of the Tat binding surface of KIX is explored in detail in chapter 3.

Previously, only the ARM and Cys regions (Figure 1) of Tat have been shown to be molecular recognition domains involved in transcriptional regulation. ARM binds to the RNA stem-loop transcribed within the first 60 nucleotides of the HIV-1 genome (Huq *et al.*, 1999a), and the cyclin T_1 subunit of P-TEFb interacts with the Cys-rich domain of Tat (Bieniasz *et al.*, 1998). Our results identify another functional region of Tat, which is involved in the recruitment of the transcriptional coactivator CBP.

Our results show that Tat is devoid of significant α-helical or sheet secondary structure, in accord with a previous NMR study of 86-residue Tat (Bayer *et al.*, 1995). A number of proteins that are unfolded in isolation undergo coupled

folding upon binding events, including transcriptional activation domains that fold upon binding other transcription factors (Wright and Dyson, 1999). For example, phosphorylated CREB adopts a predominantly helical structure upon binding KIX (Radhakrishnan *et al.*, 1997). The increased negative ellipticity at the helical signature wavelengths of 208 and 222 nm observed for the Tat-KIX complex (Figure 5A) suggests that helix formation occurs upon formation of the complex. Other types of induced secondary structure that make a smaller contribution to the CD spectrum may also be present in the complex, and reliable determination of the secondary structure of the complex must await further study with high-resolution methods. Since KIX is a folded, globular protein (Radhakrishnan *et al.*, 1997), and Tat is largely unfolded in isolation, it is possible that Tat undergoes a folding transition upon binding KIX. Such behavior is seen for other activation domains (Wright and Dyson, 1999).

In conclusion, we have defined the interacting regions of Tat and CBP. Tat binds constitutively to the KIX domain of CBP, with complex formation mediated by the N-terminal region of Tat. Tat appears to fold upon binding KIX and possibly adopts a helical structure. Since Tat is a viable anti-viral drug target (Ptak, 2002), design of peptides that inhibit Tat folding, such as HIV-1 entry inhibitors that inhibit gp41 folding and association (Root *et al.*, 2001), may present an avenue for preventing HIV propagation.

Chapter 3

Identification of the HIV-1 Tat Interaction Surface of the KIX Domain of the Human Coactivator CBP

This chapter describes work submitted for publication in The Journal of Virology (Vendel & Lumb, 2003b). Experimental details and results have been expanded beyond those reported in the manuscript.

3.1 Abstract

Tat is required for the expression of the HIV-1 genome. HIV-1 Tat interacts with the human transcriptional coactivator and acetyltransferase CREB binding protein (CBP) via the KIX domain of CBP. Chemical-shift perturbation mapping with heteronuclear nuclear magnetic resonance spectroscopy was used to identify the surface of human KIX that interacts with Tat. It was found that that Tat binds to the c-Jun/MLL binding surface of KIX, as opposed to the CREB binding site. The results provide new insight into the molecular basis of the assembly of protein complexes involving p300/CBP and Tat during HIV gene expression.

3.2 Introduction

Expression of the HIV genome requires both viral and human proteins (Jones and Peterlin, 1994; Karn, 1999). Viral transcription initiation is mediated by endogenous human transcriptional activators such as NF-kB and SP-1, which presumably contribute to the recruitment of the general transcription machinery to the viral promoter (Jones and Peterlin, 1994; Karn, 1999). Efficient elongation, however, requires the essential HIV-1 transcriptional activator Tat (Jones and Peterlin, 1994; Karn, 1999). Tat binds the nascent transcribed viral RNA and interacts with a number of host transcription factors (Jones and Peterlin, 1994; Karn, 1999). For example, Tat recruits pTEFb (cyclin T_1-CDK9), which phosphorylates the C-terminal domain of RNA polymerase II to promote transcription elongation (Jones, 1997; Karn, 1999).

Tat also interacts with the transcriptional coactivator and acetyltransferase CBP and with the highly related but distinct p300 (Benkirane *et al.*, 1998; Hottiger and Nabel, 1998; Marzio *et al.*, 1998). In addition to a acetyltransferase domain, CBP and p300 contain several autonomously functional protein-protein interaction domains that bind transcription factors and contribute different functional properties (Chan and La Thangue, 2001; Goodman and Smolik, 2000). CBP and p300 contribute to the regulation of gene expression in normal cellular processes such as cell growth, differentiation, and tumor progression (Chan and La Thangue, 2001; Goodman and Smolik, 2000). Both CBP and p300 are believed to contribute to transcription during normal cellular processes via assembly of the

transcription machinery and through nucleosome remodeling (Chan and La Thangue, 2001; Goodman and Smolik, 2000).

A bevy of recent reports points to an important functional relationship between Tat and p300/CBP during HIV gene expression. Tat interacts with the acetyltransferase and KIX domains of p300/CBP and with the bromodomain of the p300/CBP-associated factor PCAF (Benkirane *et al.*, 1998; Deng *et al.*, 2000; Hottiger and Nabel, 1998; Mujtaba *et al.*, 2002; Vendel and Lumb, 2003a). Tat can also be acetylated by p300 and CBP (Deng *et al.*, 2000; Kiernan *et al.*, 1999; Ott *et al.*, 1999), and Tat is implicated in the p300/CBP-mediated acetylation of histone H4 and NF-κB (Col *et al.*, 2002; Deng *et al.*, 2001; Furia *et al.*, 2002). In addition, human transcription factors involved in HIV-1 gene expression also bind p300/CBP (Chan and La Thangue, 2001; Goodman and Smolik, 2000), and perhaps act in concert with Tat to recruit p300/CBP during assembly of the transcription enhanceosome.

The KIX domain of p300/CBP binds numerous cellular and viral transcription factors (Chan and La Thangue, 2001; Goodman and Smolik, 2000) via two discrete modes that employ structurally distinct surfaces of KIX. One mode is represented by the phosphorylation-induced binding of the KID region of CREB to KIX (Radhakrishnan *et al.*, 1997). c-Myb also binds constitutively to similar region of KIX as KID (Zor *et al.*, 2002). The second mode is exemplified by MLL

and c-Jun, which bind constitutively to a different surface of KIX than phosphorylated CREB (Campbell and Lumb, 2002; Goto *et al.*, 2002).

In Chapter Two, we demonstrated that Tat binds directly to the KIX domain of p300/CBP in vitro and interferes with KIX-mediated transcription in human T cells (Vendel and Lumb, 2003a). The interaction is localized to the N-terminal 24 residues of Tat, with Tat_{1-24}, corresponding to the N-terminal 24 residues of HXB2 isolate Tat, forming a specific complex with KIX (Vendel and Lumb, 2003a). Here we extend our previous studies of the Tat-KIX complex by identifying the Tat_{1-24}-binding site on KIX with heteronuclear nuclear magnetic resonance (NMR) spectroscopy. Our results show that Tat binds to the c-Jun/MLL binding surface of KIX, as opposed to the CREB binding site, and contribute to our understanding of the molecular basis of the Tat-p300/CBP interaction.

3.3 Methods

3.3a Protein Preparation and Purification

Tat was expressed and purified as described in Section 2.3a.

^{15}N-labeled Tat was prepared as described in Section 2.3a.

The KIX domain of human CBP (residues 589-679 with an additional N-terminal Met) was prepared as described in Section 2.3a.

^{15}N-labeled and ^{15}N, ^{13}C-labeled KIX were prepared as described in Section 2.3a except cells were grown in M9 minimal medium containing 0.8 g/L $^{15}NH_4Cl$ and ^{13}C-glucose (McIntosh and Dahlquist, 1990). Final yields of 15N-KIX was 2 mg/L.

Tat_{1-24} was prepared as described in Section 2.3b.

Proteins were stored as a lypholized powder and dialyzed against 10 mM sodium phosphate, 150 mM NaCl and 1 mM DTT, pH 7.0, overnight before use.

3.3b Protein Concentration Determination

Concentrations of protein stock solutions were determined by absorbance in 6 M GuHCl and 10 mM sodium phosphate and 150 mM sodium chloride, pH 6.5 at 25 °C using extinction coefficients for KIX and Tat_{1-24} at 280 nm of 12090 and 5690 M^{-1} cm^{-1}, respectively (Edelhoch, 1967).

3.3c NMR Spectroscopy

NMR spectra were acquired with a Varian Unity Inova operating at 500.1 MHz for ^1H and referenced to internal DSS at zero ppm. Data were processed with NMRPipe and analyzed with NMRView (Delaglio *et al.*, 1995; Johnson and Blevins, 1994). All spectra were acquired at 10 °C on samples prepared in 10 mM sodium phosphate and 150 mM NaCl, pH 7.0.

Assignments of KIX resonances in the Tat_{1-24}-KIX complex were obtained using gradient sensitivity-enhanced HNCA and HN(CO)CA spectra (Bax and Ikura, 1991; Ikura *et al.*, 1990; Kay *et al.*, 1994) collected with 16 transients per increment, respectively. Spectra comprised 1024, 64 and 32 complex points in the ^{1}H, ^{13}C and ^{15}N dimensions, respectively. Data were resolution enhanced and zero filled once prior to Fourier transformation. Samples contained 600 μM ^{15}N-^{13}C-KIX and 1 mM unlabeled Tat_{1-24} in 10 mM sodium phosphate, 150 mM NaCl, pH 7.0.

Changes in KIX chemical shifts upon binding Tat_{1-24} were measured from gradient ^{1}H-^{15}N heteronuclear single quantum coherence (HSQC) spectra (Kay *et al.*, 1992). Spectra consisted of 256 complex increments defined by 128 transients and 1024 complex points. Data were resolution enhanced and zero filled once prior to Fourier transformation to give a final digital resolution of 3 and 4 Hz/point in the ^{1}H and ^{15}N dimensions, respectively. Samples contained 225 μM ^{15}N KIX, or 225 μM ^{15}N KIX and 550 μM Tat_{1-24}.

Changes in chemical shift upon complex formation are reported as $\Delta\delta = \Delta H^{N} + \Delta N$, where ΔH^{N} and ΔN are the changes in amide H^{N} and ^{15}N chemical shifts, respectively (Radhakrishnan *et al.*, 1999).

110 μM full-length ^{15}N-Tat and 110 μM ^{15}N-Tat + 220 μM unlabeled KIX were prepared in 10 mM sodium phosphate, 50 mM NaCl, and 1 mM DTT, pH 6.0,

10% D_2O and DSS. Data was collected using spectral widths of 6000 and 1850 Hz in the ^1H and ^{15}N dimensions, respectively. Spectra consisted of 256 complex increments defined by 96 transients and 1024 complex points.

3.3d Analytical Ultracentrifugation

Sedimentation equilibrium was performed with a Beckman XL-I analytical ultracentrifuge. Data were collected at 280 nm at the rotor speeds and protein concentrations listed in Table 2. Samples were dialyzed against the reference buffer (20 mM sodium phosphate and 150 mM NaCl, pH 7.0). A calculated partial specific volume at 10 °C of 0.7157 ml g^{-1} was used for Tat_{1-24} (Laue *et al.*, 1992). The solvent density of 1.004 g ml^{-1} was measured directly. Data were fit to an ideal, single-species model with ORIGIN (Beckman).

3.4 Results

3.4a Monitoring KIX binding to HIV-1 Tat

^{15}N-edited HSQC NMR was used to monitor the binding of KIX to full-length ^{15}N-labeled Tat. In this experiment, only changes in chemical shifts of Tat that occur upon binding KIX are observed. Changes in Tat chemical shifts occur when two-fold excess of KIX was added (Figure 1). Characterization of complex formation of Tat with KIX was precluded by the limited solubility of full-length Tat of approximately 50 μM..

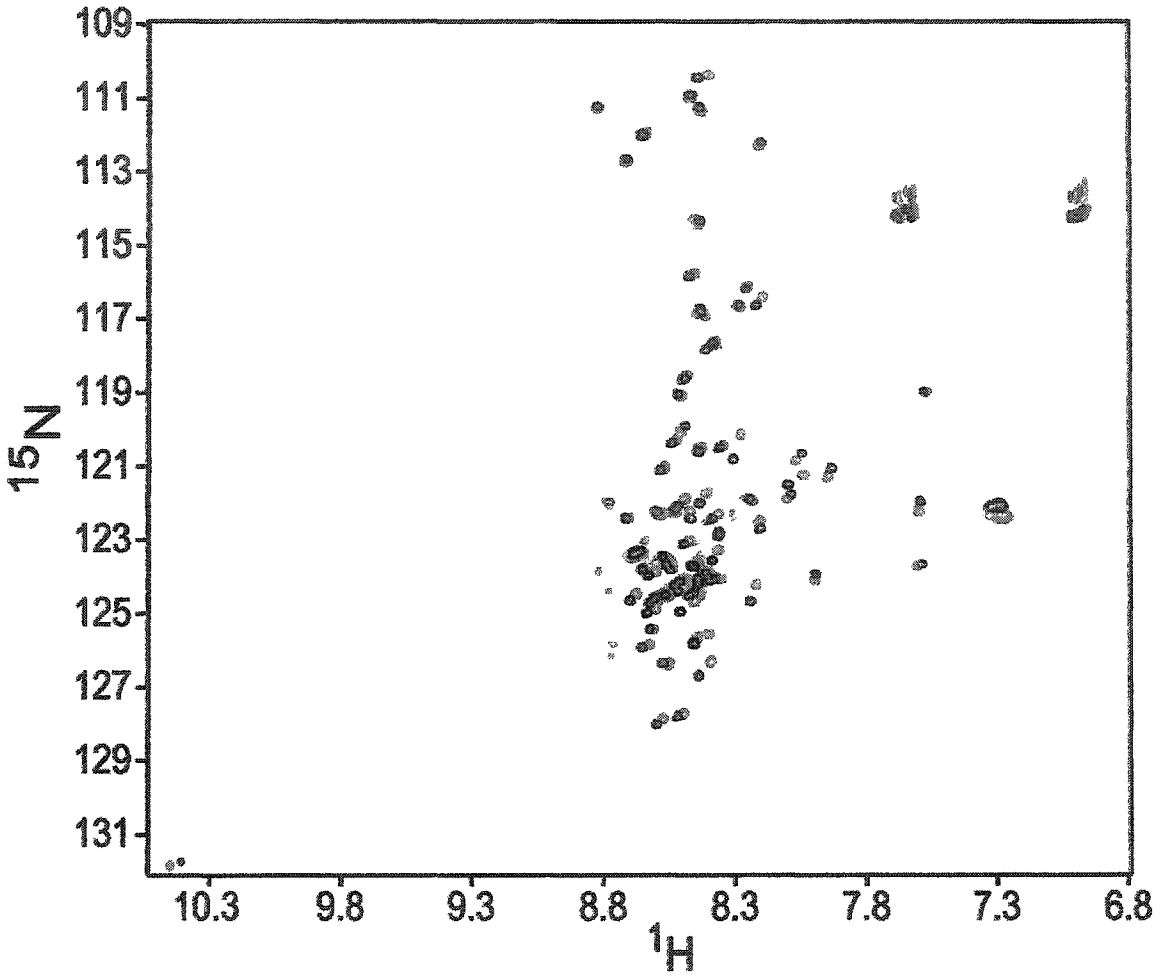

Figure 1. HSQC NMR spectra of ^{15}N-labeled Tat in the presence (◉) and absence (●) of ^{14}N-KIX (10°C, 10 mM sodium phophate, 50mM NaCl, 1mM DTT, 10%D_2O pH6.0). Some Tat resonances are shifted due to binding KIX indicating an environmental change of residues involved in complex formation.

3.4b Identification of the Tat Binding Surface of KIX

NMR spectroscopy provides an established method of mapping protein-protein interfaces (Zuiderweg, 2002). While it is generally not possible to ascribe changes in chemical shift to specific conformational changes due to the multifarious contributions to the chemical shift, residues that from a contiguous surface of a protein upon formation of a complex map the recognition interface of the protein-protein complex (Zuiderweg, 2002). For example, chemical shift mapping with NMR spectroscopy identified the known CREB binding site on KIX and mapped the interaction surfaces of c-Jun, MLL and c-Myb (Campbell and Lumb, 2002; Goto *et al.*, 2002; Radhakrishnan *et al.*, 1997; Zor *et al.*, 2002).

The NMR assignments of $^{13}C,^{15}N$-labeled KIX (600 μM) bound with Tat_{1-24} (2 mM) were obtained directly from gradient sensitivity-enhanced HNCA and HN(CO)CA spectra (Figure 2) (Campbell and Lumb, 2002). Assignments were obtained for 75 residues of KIX in the complex from an expected total of 90 (94 residues minus three Pro residues and Met 1) (Table 1). Changes in the ^{1}H and ^{15}N chemical shifts of KIX were then obtained with greater precision from gradient [^{1}H, ^{15}N] HSQC spectra (Kay *et al.*, 1992; Campbell and Lumb, 2002) of ^{15}N-labeled KIX (300 μM) bound with unlabeled Tat_{1-24} (3 mM) (Figure 2). The combination of HNCA, HN(CO)CA, and HSQC results allowed us to monitor changes in specific residues on KIX that are likely involved in complex formation with Tat (Figure 4, 5, & 6). ^{15}N and $^{13}C,^{15}N$-labeled KIX, corresponding to residues 589-679 of human CBP with an additional N-terminal Met, and Tat_{1-24}

were prepared as described previously (Campbell and Lumb, 2002; Vendel and Lumb, 2003a).

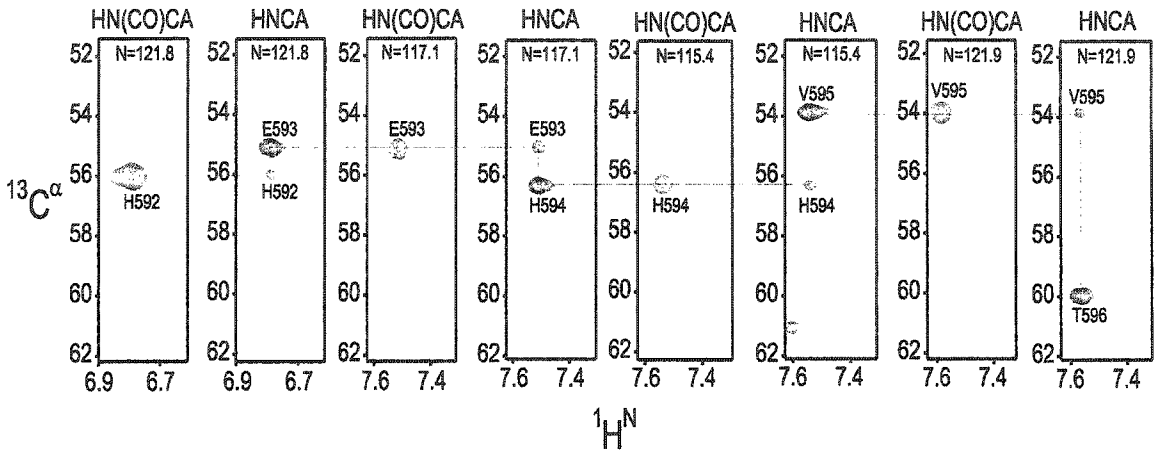

Figure 3. Example of sequential and intraresidue connectivity in HNCA and HN(CO)CA spectra used to assign the KIX-Tat_{1-24} complex at pH 7.00.

Table 1. Assignments of KIX at 10 °C, pH 7.0.

Residue	H^N	C^{α}	N	Residue	H^N	C^{α}	N
V587	7.99	53.9	125.11	**V595**	7.61	53.3	121.9
R588	8.72	60.2	127.74	**T596**	7.55	59.8	116.2
K589	8.26	54.9	123.00	**Q597**	9.05	57.6	121.4
G590	8.97	52.2	113.28	**D598**	8.57	56.6	118.9
W591	9.08	58.8	129.60	**L599**	7.67	55.1	123.8
H592	6.81	55.7	121.80	**R600**	7.91	56.0	119.6
E593	7.52	54.7	117.17	**S601**	8.55	58.1	113.9
H594	7.57	55.9	115.45	**H602**	7.96	59.6	123.8

Residue	H^N	C^α	N	Residue	H^N	C^α	N
L603	8.27	54.8	123.4	**M625**	6.93	61.7	113.4
V604	8.50	55.9	121.1	**E626**	8.37	56.0	120.5
H605	8.00	65.6	118.8	**N627**	8.38	57.7	119.1
K606	8.36	57.8	120.8	**L628**	8.01	53.7	124.8
L607	8.10	59.9	114.8	**V629**	8.61	55.7	121.0
V608	8.19	56.6	120.0	**A630**	7.90	64.7	121.5
Q609	8.18	65.3	116.9	**Y631**	7.93	55.4	121.4
A610	7.57	55.7	120.6	**A632**	8.63	58.7	123.6
I611	7.63	49.8	115.9	**K633**	8.76	53.0	117.1
F612	8.11	56.9	121.5	**K634**	7.80	57.5	124.6
P613				**V635**	8.05	57.0	120.3
T614	8.10	61.6	115.8	**E636**	8.58	63.7	121.3
P615				**G637**	8.23	59.1	108.3
D616				**D638**	8.26	54.8	123.4
P617				**M639**	8.02	54.9	122.5
A618	8.29	57.0	121.6	**Y640**	9.32	56.8	122.5
A619	7.83	51.3	122.3	**E641**	8.16	56.4	116.0
L620	7.77	51.0	119.0	**S642**	8.06	56.3	113.7
K621	8.15	55.5	122.2	**A643**	8.36	58.2	125.6
D622	7.95	54.3	121.6	**N644**	9.20	50.8	118.2
R623	8.34	62.4	121.8	**S645**	6.94	52.3	113.0
R624	7.91	56.7	118.8	**R646**	8.84	54.5	123.0

Residue	H^N	C^α	N	Residue	H^N	C^α	N
D647	8.32	56.8	118.2	**L664**	8.23	57.7	121.9
E648	7.83	51.4	122.3	**E665**	8.40	62.9	119.9
Y649	7.37	57.1	122.5	**E666**	8.41	56.0	121.0
Y650	8.22	58.8	116.8	**K667**	8.37	53.9	110.8
H651	8.24	56.8	119.8	**R668**	8.38	43.2	121.0
L652	9.05	57.6	121.6	**R669**	8.05	59.2	126.6
L653				**S670**	8.36	52.8	116.9
A654				**R671**			
E655	8.42	62.9	119.4	**L672**			
K656	7.90	56.9	122.1	**H673**			
I657	8.31	55.8	120.3	**K674**			
Y658	8.05	64.0	120.3	**Q675**			
K659	8.29	58.7	120.5	**G676**			
I660	8.46	57.7	122.2	**I677**			
Q661	8.32	55.9	119.8	**L678**			
K662	8.54	52.1	122.8	**G679**			
E663	8.23	53.8	117.8				

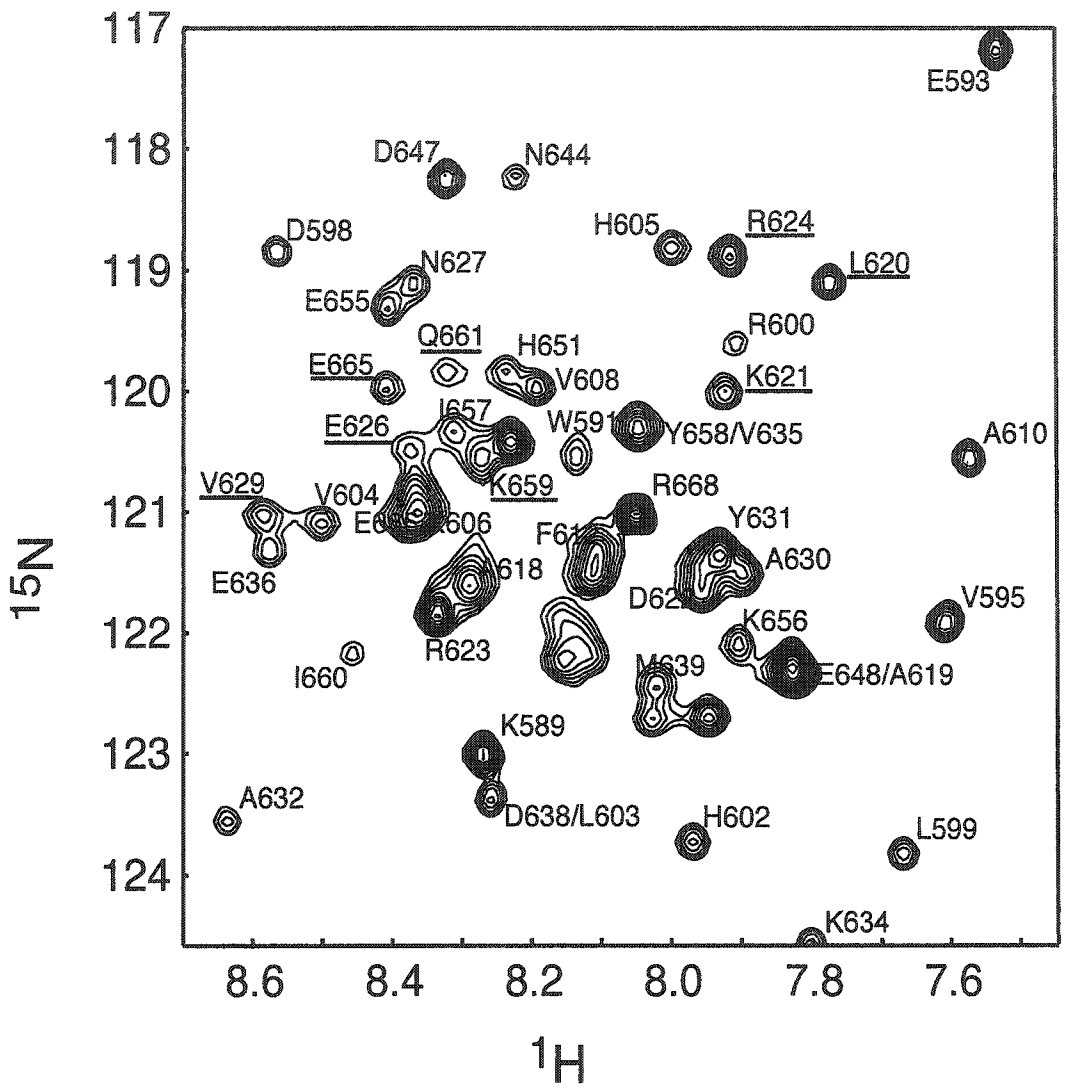

Figure 3. [^{1}H-^{15}N] HSQC spectrum of ^{15}N-labeled KIX bound to Tat_{1-24}. Only resonances from ^{15}N-labeled KIX are observed in this experiment. KIX resonances that have a significant chemical-shift change upon binding Tat_{1-24} are underlined.

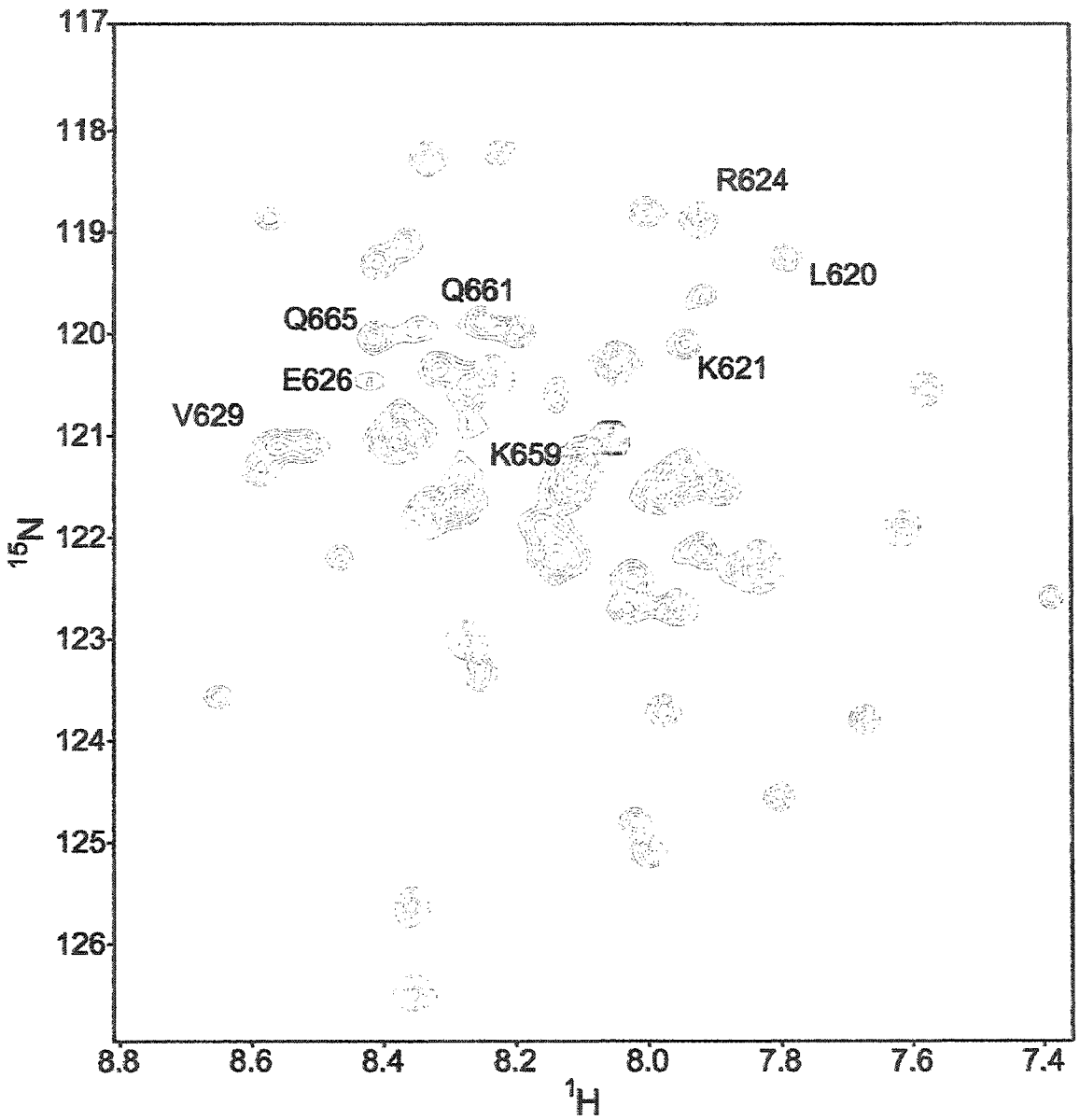

Figure 4. Detail of the HSQC spectra of ^{15}N-KIX and ^{15}N-KIX + Tat_{1-24} at pH 7.00. The ^{15}N-KIX spectrum is shown in black (•) and the ^{15}N-KIX +Tat_{1-24} spectrum is shown in green (◦). Residues with significant chemical shifts are labeled.

The largest chemical-shift perturbations induced in KIX upon binding Tat_{1-24} are seen for F612, T614, L620, D622, R624, E626, V629, K659, Q661, K662, and E665 (Figures 4 & 5). The change in ^{1}H and ^{15}N chemical shifts of these residues are at least two-fold greater than the average chemical-shift change of 0.01 for ^{1}H and 0.04 ppm for ^{15}N. The residues form a contiguous surface of KIX that contains both hydrophobic and polar residues that defines the Tat binding surface of KIX (Figure 7A). This surface corresponds to the c-Jun/MLL binding site of KIX.

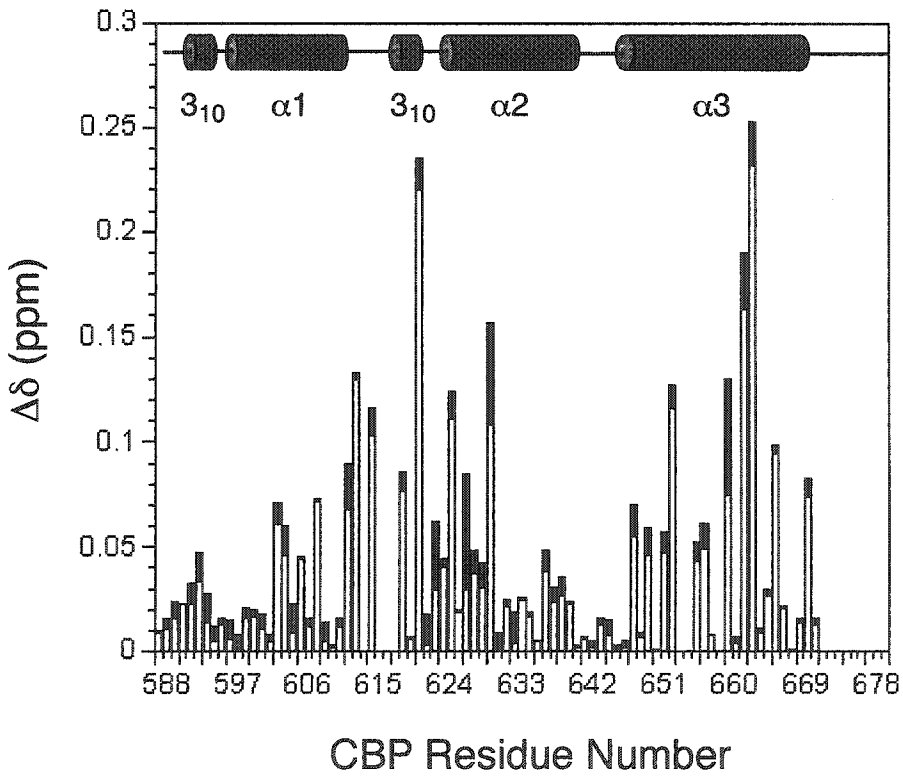

Figure 5. Chemical-shift changes induced in KIX by Tat_{1-24}. ^{15}N and ^{1}H changes are shown as open and filled bars, respectively. The secondary structure of KIX comprises three α and two 3_{10} helices (Radhakrishnan *et al.*, 1997) and is shown as a schematic.

The relatively small changes in chemical shifts may be due to incomplete complex formation. We used sedimentation equilibrium to examine the behavior of Tat_{1-24} in solution of concentrations near those used for NMR. Tat_{1-24} has an observed mass between that of a monomer and dimer at concentrations approaching those needed for NMR experiments with an average mass of 4023 Da (Table 2) (Figure 6).

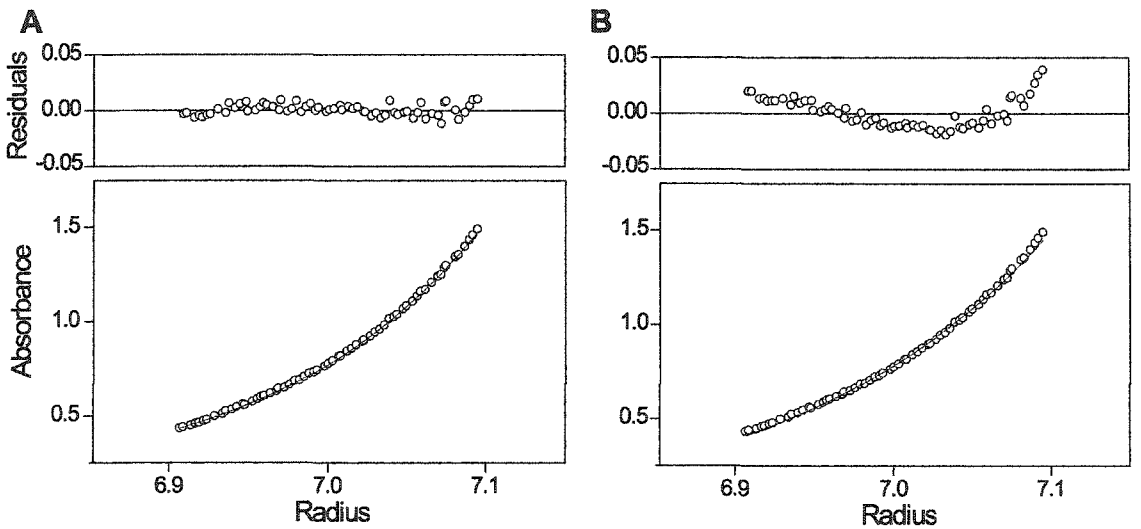

Figure 6. Sedimentation equilibrium of Tat_{1-24}. 100 mM Tat_{1-24} gives a mass of 3632 Da at 48 krpm when set to a single species model (A). At a set mass for a monomer (2719 Da) Tat_{1-24} displays residuals that imply a non-ideal aggregate (B).

Table 2. Sedimentation equilibrium analysis of Tat_{1-24} at pH 7.00.

Table 2: Sedimentation Equilibrium Analysis of Tat_{1-24}		
	Observed Mass (kDa)	
Total Concentration (μM)	45 krpm	48 krpm
Tat_{1-24} (Expected Mass for Monomer: 2719 Da)		
50	4.8	3.8
100	4.7	3.6
150	3.6	3.4

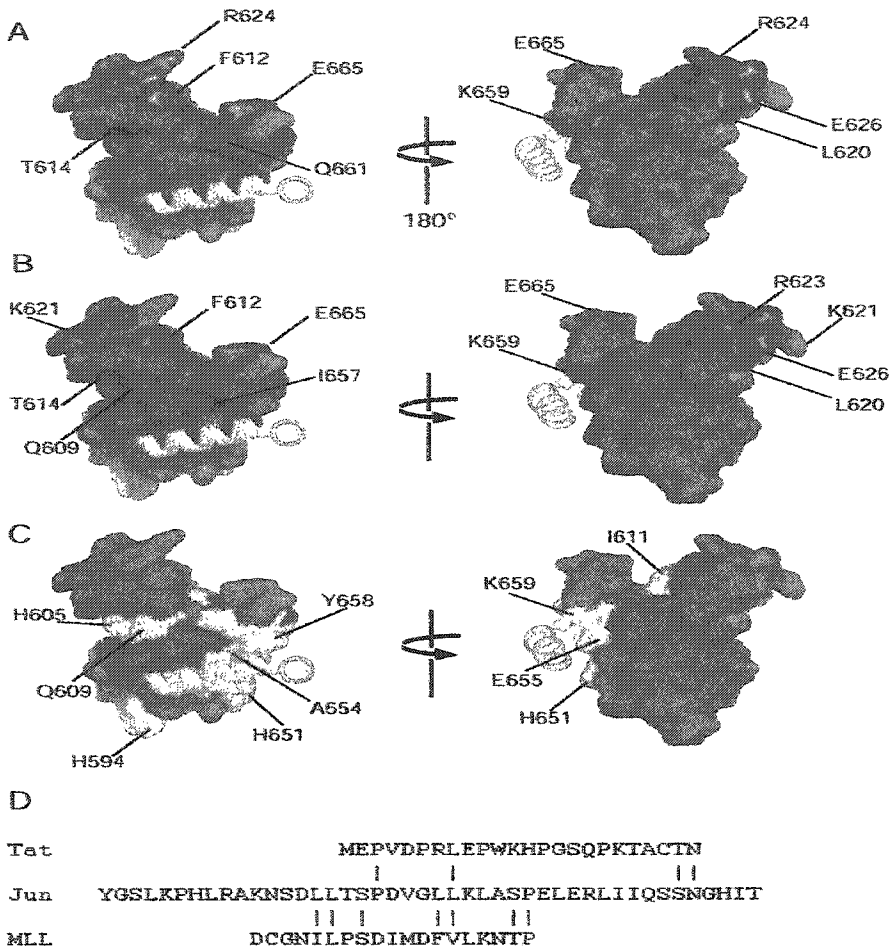

Figure 7. (A) Chemical-shift perturbation mapping of the Tat binding site. (B) Chemical-shift perturbation mapping of the Jun binding site, as reported previously (2). (C) Chemical-shift perturbation mapping of the CREB binding site, as reported previously (Campbell and Lumb, 2002; Radhakrishnan *et al.*, 1999). Regions of KIX that experience significant chemical shift changes upon binding Tat, c-Jun (Campbell and Lumb, 2002) and CREB (Campbell and Lumb, 2002; Radhakrishnan *et al.*, 1997) are shown in red, purple, and yellow, respectively. Regions of KIX that are unaffected by binding are shown in blue. The pKID region of CREB is shown as a yellow ribbon. Structures are drawn using the PDB file 1kdx (Radhakrishnan *et al.*, 1999) and PyMOL (DeLano, W. L.). (D) Sequence alignments of the KIX-interacting regions of HIV-1 Tat (Vendel and Lumb, 2003a), human c-Jun (Campbell and Lumb, 2002) and human MLL (Goto *et al.*, 2002). c-Jun and MLL share some sequence similarity. However, meaningful sequence similarity or a common sequence motif between Tat and the two human proteins is not apparent.

3.5 Discussion

CBP is involved in transcription of numerous cellular pathways and mediates its interactions through independently folded protein-protein interacting domains (Goodman and Smolik, 2000). The protein binding regions on CBP interact with a wealth of transcriptional activators and coactivators (Goodman and Smolik, 2000). The HIV-1 transcriptional activator Tat utilizes the promiscuous binding features of CBP to aid in replication of its viral genome (Benkirane *et al.*, 1998; Marzio *et al.*, 1998; Vendel and Lumb, 2003a).

The interaction between HIV-1 Tat and CBP has been well established (Benkirane *et al.*, 1998; Marzio *et al.*, 1998; Vendel and Lumb, 2003a). We have previously shown that Tat interacts with the KIX domain of CBP *in vitro* and *in vivo* and this interaction is involved in transcription from the HIV-1 promoter (Vendel and Lumb, 2003a). Here we further define the interaction between Tat and CBP by using structural techniques to map the Tat binding surface on KIX.

The Tat binding site of KIX is distinct from the CREB binding site and instead corresponds to the Jun binding mode. The chemical-shift changes seen upon binding Tat_{1-24} occur in the same region of KIX as observed upon the c-Jun activation domain (Figure 7B), and not at the $\alpha1$-$\alpha3$ surface recognized by CREB and c-Myb (Figure 7C). MLL also binds to KIX at a similar surface to that occupied by c-Jun (Goto *et al.*, 2002). The chemical-shift perturbations of KIX induced by Tat_{1-24} are somewhat smaller than the changes caused by the c-Jun

and MLL activation domains (Campbell and Lumb, 2002; Goto *et al.*, 2002), but map to the same surface of KIX as those induced by c-Jun (Figure 7). We conclude that HIV-1 Tat, human c-Jun and human MLL recognize a common binding surface of KIX.

Although HIV-1 Tat, human c-Jun and human MLL bind the same surface of KIX, the sequence similarity between the KIX-interacting regions of Tat and c-Jun or Tat and MLL is insignificant (Figure 7D). The KIX-interacting regions of c-Jun and MLL share a higher degree of sequence similarity (Figure 7D), but do not share an obvious common sequence motif with Tat (Figure 7D). The sequences of all three peptides can be arranged as amphipathic helices, and quaternary interactions with KIX may impart a common structural motif that defines the binding mode to the Tat/Jun/MLL site. Alternatively, the lack of sequence identity between Tat and Jun or MLL may reflect a divergent binding mode for Tat. Further investigation with high-resolution structural methods is needed to distinguish between these possibilities.

HIV infection can lead to associated pathogenesis such as Kaposi's sarcoma and non-Hodgkin's lymphoma that depend in part on the deregulation of normal gene expression. Our results imply that the normal functions of transcription factors that use the c-Jun or MLL binding site of KIX binding site may be disrupted directly by the competitive sequestration of p300/CBP by Tat. Since p300/CBP is believed to be present at limiting quantities in the cell (Horvai *et al.*, 1997;

Hottiger *et al.*, 1998; Kamei *et al.*, 1996), sequestration of CBP by Tat may have significant consequences for deregulating cellular processes that depend in part on interactions mediated by the KIX domain during gene expression.

In conclusion, we have used NMR spectroscopy to identify the Tat-interacting surface of the KIX domain of CBP. We find that Tat binds the same site of KIX that recognizes c-Jun and MLL, which is distinct from the site used by CREB and c-Myb. The results provide new insight into the molecular basis of the assembly of protein complexes involving p300/CBP and Tat during HIV gene expression and provide a rational framework for future structure-function studies of the Tat-p300/CBP interaction.

Chapter 4

KIX-mediated Assembly of the CREB-CBP-HTLV-1 Tax Complex

This chapter describes a collaboration with Steven J. McBryant. Steve synthesized a peptide that was used in preliminary work and performed sedimentation equilibrium (Figures 2 and 7). This work has been submitted for publication (Vendel *et al.*, 2003). Experimental details and results have been expanded beyond those reported in the manuscript.

4.1 ABSTRACT

The HTLV-1 transcription activator Tax is required for viral replication and pathogenesis. In concert with human CREB, Tax recruits the human transcriptional coactivator and histone acetyltransferase p300/CBP to the HTLV-1 promoter. Here we investigate the structural features of the interaction between Tax and the KIX domain of p300/CBP. Circular dichroism spectroscopy, nuclear magnetic resonance chemical-shift perturbation mapping and sedimentation equilibrium show that a subdomain of Tax (residues 59-98) binds KIX. Chemical-shift perturbation mapping reveals that the Tax-binding surface of KIX is distinct from that utilized by CREB, and corresponds to the site of KIX that interacts with MLL, c-Jun, and HIV-1 Tat. Sedimentation equilibrium shows that Tax and the phosphorylated KID domain of CREB can simultaneously bind KIX to form a ternary 1:1:1 complex. The results provide a molecular description of the concerted recruitment of p300/CBP via the KIX domain by Tax and phosphorylated CREB during Tax-mediated gene expression.

4.2 Introduction

HTLV-1 predominantly infects CD4+ T-cells and is the etiological agent of adult T-cell leukemia and of the neurological disorder tropical spastic paraparesis/HTLV-1-associated myelopathy (Barmak *et al.*, 2003). HTLV-1 replication and pathogenesis is dependant on the virally encoded transcriptional activator Tax (Bex and Gaynor, 1998; Jeang, 2001; Yoshida, 2001). In addition to activating viral gene expression, Tax alters the expression of numerous cellular genes involved in cell cycle regulation and apoptosis (Bex and Gaynor, 1998; Jeang, 2001; Yoshida, 2001). The interference of Tax with normal cellular processes likely contributes to the extensive modulation of the transcriptional profile of HTLV-1 infected lymphocytes (Pise-Masison *et al.*, 2002) and to HTLV-1-associated pathogenesis (Bex and Gaynor, 1998; Jeang, 2001; Yoshida, 2001).

Tax contributes to the activation of HTLV-1 genes by promoting the binding of human CREB at atypical CRE sites of the viral promoter (Bex and Gaynor, 1998; Jeang, 2001; Yoshida, 2001). Tax and CREB then cooperate to recruit the related but distinct human transcriptional coactivators p300 and CBP (Bex and Gaynor, 1998; Jeang, 2001; Yoshida, 2001). The interaction between CREB and p300/CBP normally depends on CREB phosphorylation in a region of CREB called KID (Chrivia *et al.*, 1993; Parker *et al.*, 1996). In contrast, during Tax-mediated expression at both viral and host CRE-containing promoters, the requirement for CREB phosphorylation is circumvented by Tax forming a

molecular bridge between the bZIP region of CREB and the KIX region of p300/CBP (Giebler *et al.*, 1997; Kwok *et al.*, 1996).

The interaction between p300/CBP and Tax is mediated by the KIX domain of p300/CBP and residues 81-95 of Tax (Harrod *et al.*, 1998). Several studies have demonstrated the existence of the Tax-KIX interaction *in vitro* and *in vivo* (Garcia *et al.*, 1988; Georges *et al.*, 2003; Harrod *et al.*, 1998; Kwok *et al.*, 1996; Lu *et al.*, 2002; Yan *et al.*, 1998). Tax-mediated gene expression likely relies in part on the ability of p300 and CBP to interact with a range of host transcription factors (Kashanchi *et al.*, 1998) and the acetyltransferase chromatin remodeling activity of p300/CBP or the p300/CBP-associated factor (PCAF) (Georges *et al.*, 2003; Lu *et al.*, 2002). In addition to a role in HTLV-1 gene expression, p300 and CBP contribute to normal cellular processes such as cell growth, differentiation and tumor progression (Chan and La Thangue, 2001; Goodman and Smolik, 2000).

KIX interacts with numerous human transcription factors such as p53, MLL, c-Myb, SREBP and c-Jun (Chan and La Thangue, 2001; Goodman and Smolik, 2000). KIX binds transcription factors via one of two modes that employ structurally distinct surfaces of KIX (Campbell and Lumb, 2002; Goto *et al.*, 2002). One surface of KIX is recognized by the KID region of phosphorylated CREB (Radhakrishnan *et al.*, 1997), whereas a different surface is utilized by human MLL, human c-Jun, and HIV-1 Tat (Campbell and Lumb, 2002; Goto *et al.*, 2002; Vendel and Lumb, 2003b). The existence of two discrete binding sites

on KIX allows KIX to form ternary complexes with two activation domains (Campbell and Lumb, 2002; Goto *et al.*, 2002). For example, KIX forms ternary complexes with the activation domains of CREB and MLL (Ernst *et al.*, 2001), of c-Myc and MLL (Goto *et al.*, 2002), and of c-Jun and CREB (Campbell and Lumb, 2002).

Here we present an investigation of the Tax-KIX interaction and the formation of a ternary complex involving Tax, the KIX domain of CBP, and the phosphorylated KID region of CREB. With NMR chemical-shift perturbation mapping (Zuiderweg, 2002), we show that a subdomain of Tax (residues 59-98) binds to a contiguous site on KIX that corresponds to the site recognized by c-Jun, MLL, and HIV-1 Tat and is distinct from the binding site for CREB and c-Myb. In accord with the presence of two distinct binding sites for CREB and Tax, we show that KIX forms a ternary complex with Tax_{59-98} and phosphorylated KID. These results suggest a modified view of the assembly of the Tax-CREB-CBP complex during Tax-mediated gene expression in which ternary complex formation is facilitated by direct interactions between KIX and the phosphorylated KID region of CREB during p300/CBP recruitment.

4.3 Methods

4.3a Protein Preparation and Purification

Tax_{59-98}, corresponding to residues 59-98 of HTLV-1 Tax plus an N-terminal Tyr for concentration determination, was synthesized on MBHA (4-methylbenzhydrylamine hydrochloride salt) resin (100-200 mesh) using manual Boc chemistry (Schnölzer *et al.*, 1992). The side chains of Arg, Asp, Gln, His, Lys, Ser, Thr and Tyr were protected with Tos, Bzl, Xan, DNP, ClZ, Bzl, Bzl, and BrZ respectively. Tax_{59-98} was purified by reversed phase C_{18} HPLC using a linear water/acetonitrile gradient containing 0.1% TFA. The identity of Tax_{59-98} was confirmed with electrospray mass spectrometry, and the observed and expected masses agreed to within 1 Da.

KIX (residues 589-679 of human CBP with an additional N-terminal Met) and ^{15}N-KIX were expressed in Escherichia coli strain BL21 (DE3) pLysS and purified as described previously in sections 2.3a and 3.3a. Final purification was by reversed phase C_{18} HPLC using a linear water/acetonitrile gradient containing 0.1% TFA. The identity of KIX was confirmed with electrospray mass spectrometry, and the observed and expected masses agreed to within 1 Da.

pKID corresponds to residues 87-143 of human CREB phosphorylated at Ser 118 (which is identical to residues 102-158 of mouse CREB phosphorylated at Ser 133) with an additional N-terminal Met. Purified pKID was the generous gift of Y. Wei. KID was expressed in *E. coli* strain BL21 (DE3) as a His-tag fusion

protein with a pET15b plasmid harboring a PCR product encoding KID amplified from a plasmid carrying human CREB-A (Berkowitz and Gilman, 1990) (S. P. Mestas and K. J. Lumb, unpublished results). KID was purified from the soluble cell lysate fraction with Ni-affinity chromatography and the His tag was cleaved with thrombin. KID was phosphorylated with protein kinase A (Sigma) (Parker *et al.*, 1996). Final purification was by reversed phase C_{18} HPLC using a linear water/acetonitrile gradient containing 0.1% TFA. The identity of KIX was confirmed with MALDI mass spectrometry, and the observed and expected masses agreed to within 1 Da.

Proteins were stored lypholized and dialyzed against 20 mM sodium phosphate, 50 mM NaCl, pH 7.0, before use.

4.3b Protein Concentration Determination

Concentrations of protein stock solutions were determined by absorbance in 6 M GuHCl, 10 mM sodium phosphate, and 150 mM sodium chloride, pH 6.5 at 25 °C. using an extinction coefficient of 1450 M^{-1} cm^{-1} at 276 nm for Tax_{59-98} and pKID, and of 12090 M^{-1} cm^{-1} at 280 nm for KIX (Edelhoch, 1967).

4.3c CD spectroscopy

CD spectra were acquired with a Jasco J720 spectrometer. Samples were prepared in 20 mM sodium phosphate and 50 mM sodium chloride, pH 7.0, and contained either 20 μM, 30 μM, or 40 μM of each protein. Spectra comprised 20 scans recorded at 10 °C. Binding was detected by differences between observed spectra and the spectra expected if the two proteins do not interact, calculated as the normalized sum of the spectra of the individual proteins (Campbell and Lumb, 2002; Vendel and Lumb, 2003a).

4.3d Analytical Ultracentrifugation

Sedimentation equilibrium was performed with a Beckman XL-I analytical ultracentrifuge. Data were collected at 280 nm at the rotor speeds and protein concentrations listed in Tables 1 & 2. Samples were dialyzed against the reference buffer (20 mM sodium phosphate and 150 mM NaCl, pH 7.0). Calculated partial specific volumes at 10 °C of 0.75, 0.71, 0.73, 0.72, 0.74, and 0.73 ml g^{-1} were used for Tax_{59-98}, pKID, KIX, pKID-KIX, Tax_{59-98}-KIX, Tax_{59-98}-pKID-KIX, respectively (Laue *et al.*, 1992). The solvent density of 1.004 g ml^{-1} was measured directly. Data were fit to an ideal, single-species model with ORIGIN (Beckman).

4.3e NMR Spectroscopy

NMR spectra were acquired with a Varian Unity Inova operating at 500.1 MHz for ^{1}H. All spectra were acquired at 10 °C. Samples were prepared in 20 mM sodium phosphate and 50 mM NaCl, pH 7.0 and referenced to internal DSS at zero ppm. Gradient [^{1}H-^{15}N] HSQC spectra (Kay *et al.*, 1992) consisted of 256 complex increments defined by 192 transients and 1024 complex points. Data were processed with NMRPipe and analyzed with NMRView (Delaglio *et al.*, 1995; Johnson and Blevins, 1994). Chemical shift assignments for the Tax_{59-98}-KIX complex were obtained by following changes in HSQC spectra of ^{15}N-labeled KIX (550 μM) upon addition of increasing amounts of unlabeled Tax_{59-98} (up to 1.1 mM). ^{1}H and ^{15}N assignments of unbound KIX have been previously reported (17, 20). Changes in chemical shift upon complex formation are reported as $\Delta\delta = \sqrt{[(\Delta H^N)^2 + (\Delta N/5)^2]}$, where ΔH^N and ΔN are the changes in amide H^N and ^{15}N chemical shifts, respectively.

180 μM full-length ^{15}N-KIX and 180 μM ^{15}N-KIX + 360 μM unlabeled Tax_{59-98} mutant L68P were prepared in 20 mM sodium phosphate and 50 mM NaCl, pH7.0 with 10 % D_2O and DSS. Data was collected using spectral widths of 6000 and 1850 Hz in the ^{1}H and ^{15}N dimensions. Spectra consisted of 128 complex increments defined by 128 transients and 1024 complex points.

4.4 RESULTS

4.4a Tax_{59-98} Binds the KIX Domain of CBP

The CD spectrum of Tax_{59-98} is reminiscent of an unfolded protein, with a minimum at 200 nm and a lack of spectral characteristics above 210 nm that are reflective of helix or sheet structure (Figure 1). The CD spectrum of free KIX is indicative of a helical protein (Figure 1), in accord with previous CD results (Campbell and Lumb, 2002; Mestas and Lumb, 1999; Parker *et al.*, 1996; Vendel and Lumb, 2003a) and the solution structure of KIX (Radhakrishnan *et al.*, 1997).

Addition of Tax_{59-98} to KIX results in a significant increase in ellipticity over the calculated spectrum of non-interacting Tax_{59-98} and KIX (Figure 1). This result suggests that Tax_{59-98} binds the KIX domain of CBP, in accord with previous studies of a shorter Tax peptide (Harrod *et al.*, 1998). In addition, the increase in ellipicity at the helical signature wavelengths of 208 and 222 nm suggests an increase in helix content upon binding.

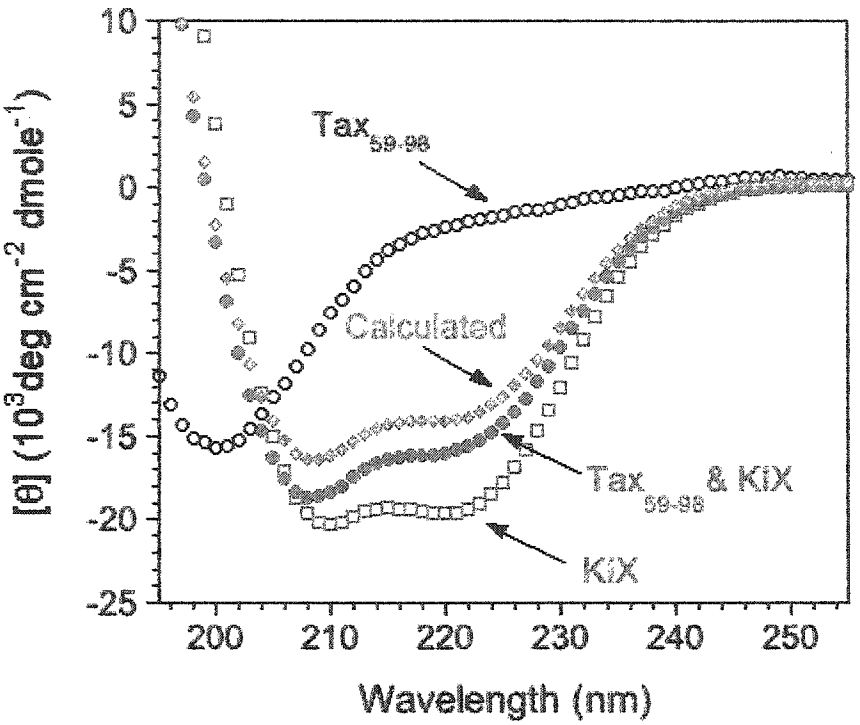

Figure 1. CD analysis of Tax_{59-98} binding to KIX. Mixing of Tax_{59-98} with KIX results in a CD spectrum of greater negative ellipicity at 208 and 222 nm than expected from the sum of the spectra of the two isolated proteins, suggesting that Tax_{59-98} binds KIX. Experiments were performed at three equimolar protein concentrations (20, 30 and 40 μM) in duplicate with reproducible results. From these six data sets, the error in the CD signal is estimated at 2%. This error is significantly less than the difference of 20% at 222 nm between the calculated and observed spectra.

Analytical ultracentrifugation also indicates that Tax_{59-98} and KIX interact to form a 1:1 complex (Figure 2). The apparent mass of equimolar Tax_{59-98} and KIX is 13.4 ± 2.3 kDa, which is within 15% of the mass expected for a 1:1 complex (Table 1). If the complex did not form, then the apparent mass would reflect the weighted mass average of the individual proteins of 7.8 kDa. The lower than observed mass may reflect experimental error, peptides that are not 100% active

(yet must be over 85% active to give the observed mass), or incomplete formation of the complex, since 99% complex formation requires that the free ligand concentration be in a 100-fold excess over the K_d (Creighton, 1993).

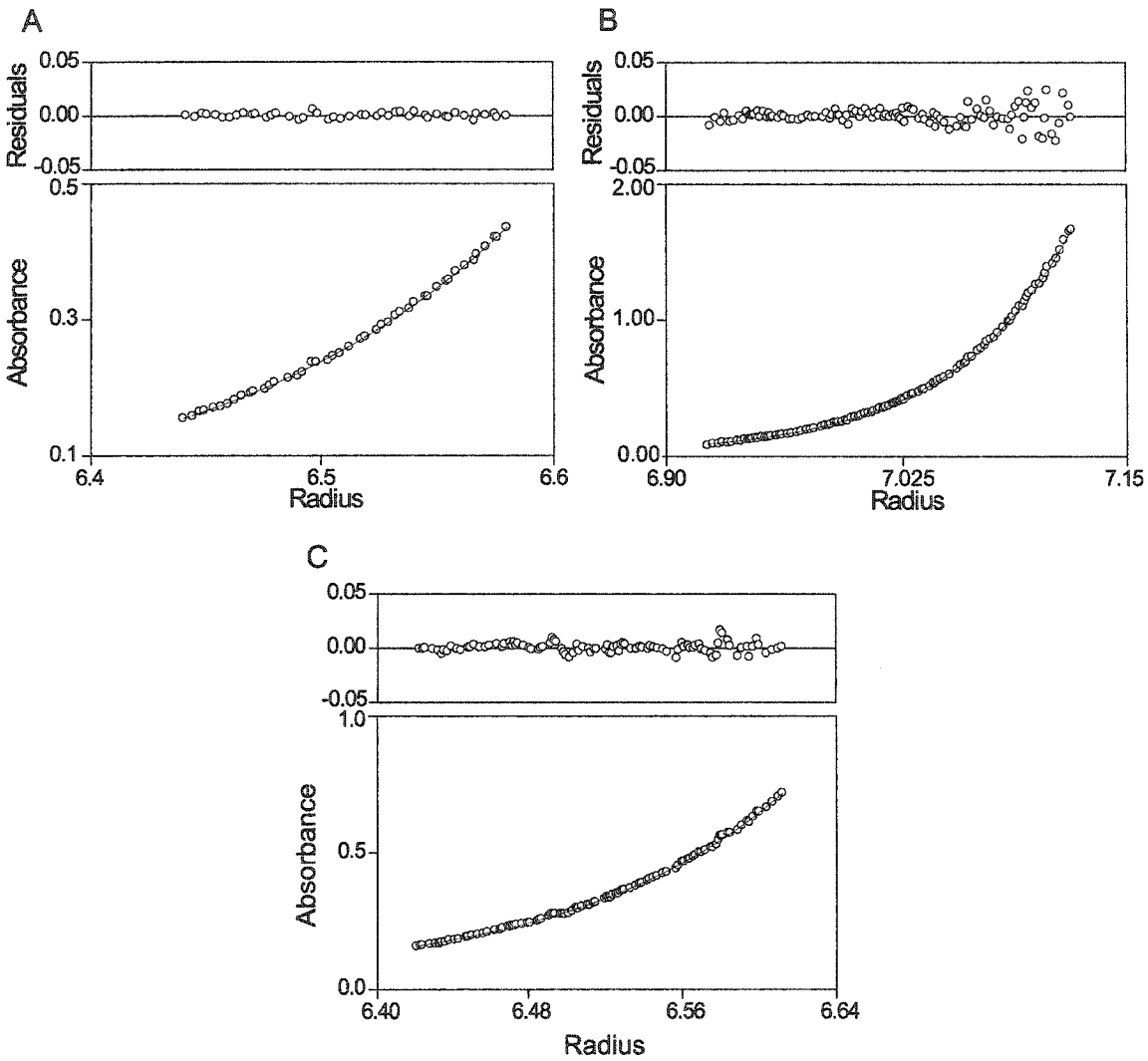

Figure 2. Sedimentation equilibrium analysis of A) Tax_{59-98}, B) KIX, and C) Tax_{59-98} binding to KIX. The data are accounted for by ideal, single species models with the mass expected for a monomer for both Tax_{59-98} and KIX and a 1:1 Tax_{59-98}-KIX complex, as shown by the random distribution of residues.

Table 1. Sedimentation equilibrium analysis of binary complex formation of Tax_{59-98} and KIX.

Total concentration of each peptide (μM)	Observed mass (kDa)	
Tax_{59-98} (expected mass for monomer: 4607 Da)		
	45 krpm	48 krpm
250	4.0	4.7
400	5.4	4.6
500	4.7	4.6
KIX (expected mass for monomer: 11139.8 Da)		
	40 krpm	45 krpm
40	11.7	11.4
50	11.7	11.5
60	11.8	12.1
Tax_{59-98} + KIX (expected mass for 1:1 complex: 15 747 Da)		
	25 krpm	30 krpm
37	14.2	13.1
50	14.2	12.6
62	13.0	13.3

The observed mass of Tax_{59-98} does not vary systematically with concentration, as expected for an ideal single species, and is within 1% of the mass expected for a monomer (Table 1). KIX is also monomeric (Table 1), in accord with previous results (Campbell and Lumb, 2002; Wei *et al.*, 2003). Thus the observed mass of the equimolar solution of Tax_{59-98} and KIX is not the result of self-association of Tax_{59-98} or KIX as opposed to formation of the Tax_{59-98}-KIX complex.

4.4b A Single-Point Variant of Tax Disrupts KIX Binding.

The CD results suggest an increase in helix content upon Tax_{59-98} binding to KIX. Two regions of Tax_{59-98} are predicted with AGADIR (Muñoz *et al.*, 1996) to have a propensity for helical formation (residues 60-71 and 83-89). If one of these two helices are important for binding, then replacement of a potential hydrophobic interface residue with the secondary structure breaker Pro (Serrano, 2000) might be expected to disrupt binding. The L68P variant of Tax_{59-98} did not bind KIX as monitored with CD spectroscopy (Figure 3) or with NMR spectroscopy by changes in the [^{1}H-^{15}N] HSQC spectrum of ^{15}N-labeled KIX upon the addition of a two fold excess of the L86P variant (Figure 4). This result provides evidence for a specific interaction between Tax_{59-98} and KIX.

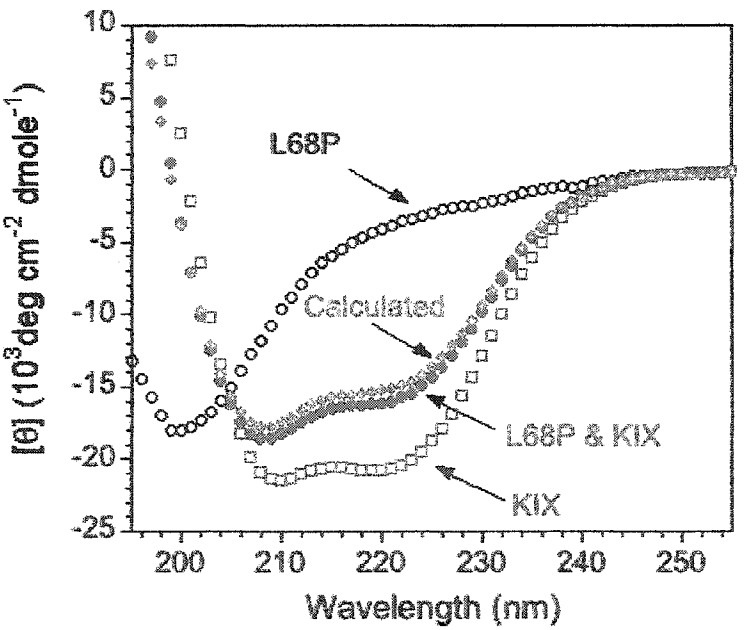

Figure 3. CD analysis of the L68P variant of Tax_{59-98}. Mixing of the L68P variant of Tax_{59-98} and KIX results in a CD spectrum that is very similar to the sum of the spectra of the two isolated proteins, suggesting that the L68P variant of Tax_{59-98} does not bind KIX.

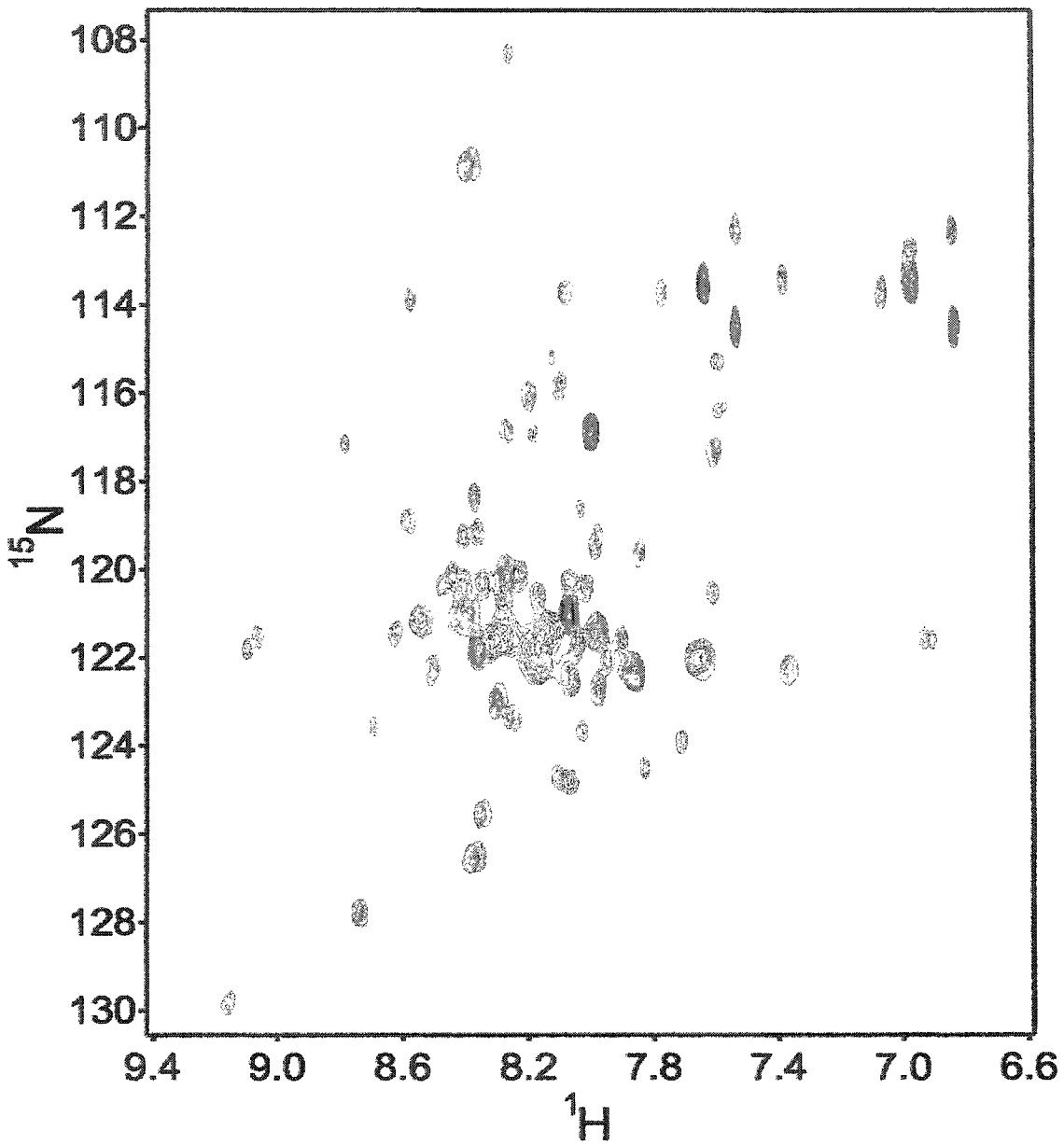

Figure 4. HSQC spectra of ^{15}N-KIX and unlabeled mutant Tax_{59-98} L68P. The 15N-KIX spectrum is shown in black (•) and the 15N-KIX spectrum is shown in red (•). Two-fold excess of the L68P mutant failed to induce significant chemical shift changes in KIX indicating that the Pro mutant engineered to disrupt a predicted helix in Tax does not bind KIX.

4.4c NMR Mapping of the Tax_{59-98} Binding Surface of KIX.

The Tax_{59-98} binding surface of KIX was identified by monitoring chemical-shift changes in HSQC spectra of ^{15}N-labeled KIX upon the addition of increasing amounts of unlabeled Tax_{59-98} at neutral pH (Figure 5).

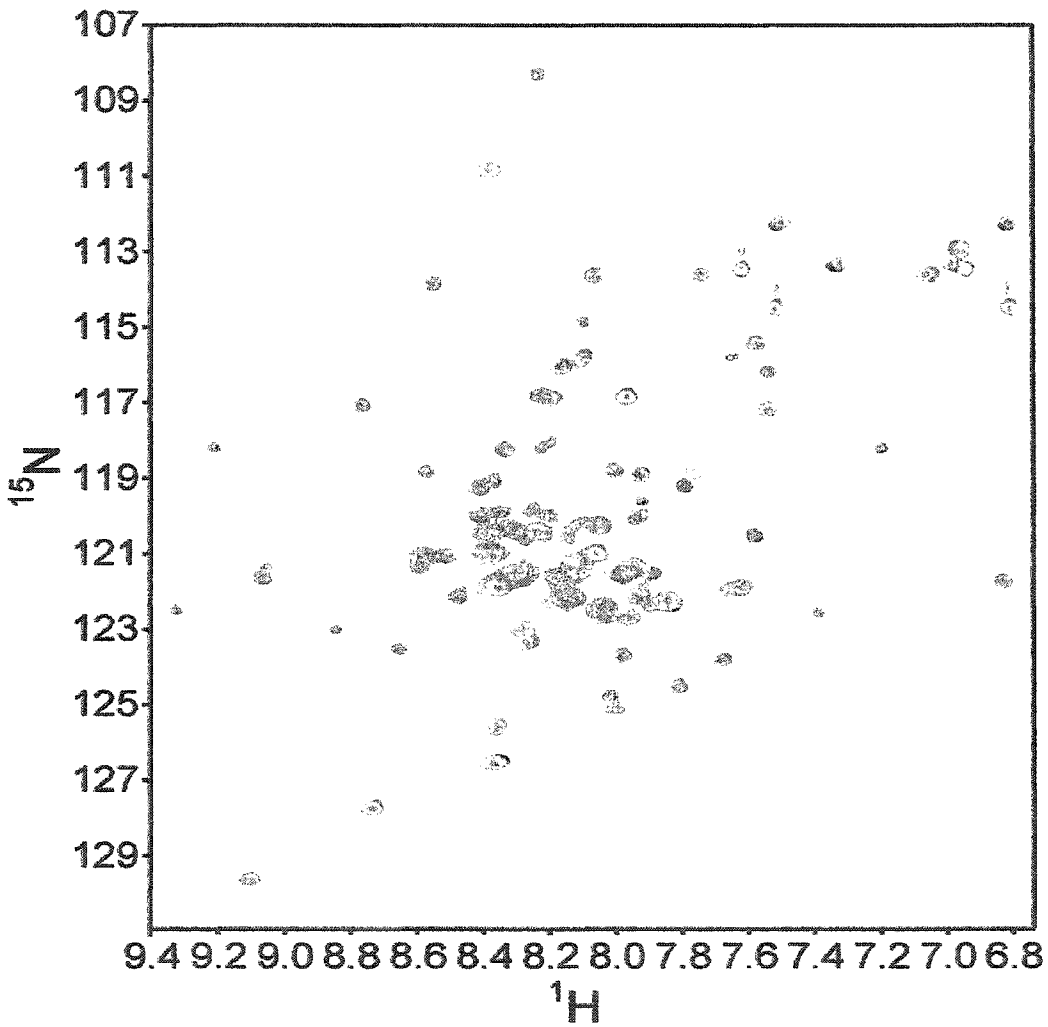

Figure 5. Titration HSQC NMR of Tax binding to ^{15}N-KIX. Chemical shift assignments for KIX at neutral pH have been previously been reported. Sequential changes in chemical shift upon titration of Tax indicate specific residues on KIX that are involved in complex formation. Spectrum in black represent ^{15}N-KIX, spectrum in Red represent a 1:1 complex of Tax and ^{15}N-KIX, and spectrum in Green represent 2:1 complex of Tax and ^{15}N-KIX.

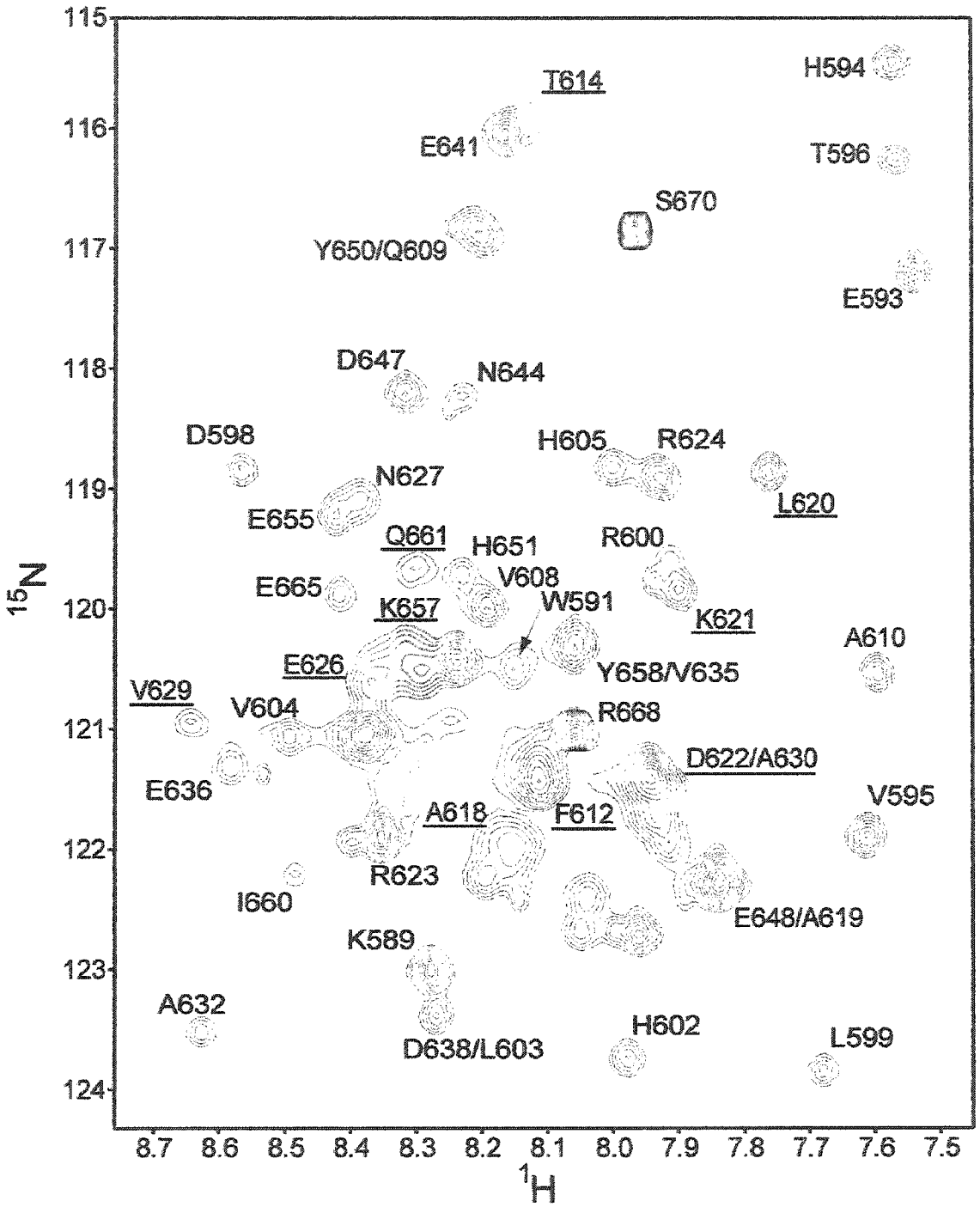

Figure 6. ^{15}N-edited HSQC spectrum of ^{15}N-labeled KIX bound to Tax_{59-98}. KIX resonances that have a significant chemical-shift perturbation upon binding Tax_{59-98} are underlined and colored orange ($\Delta\delta$ > 0.05 ppm) or red ($\Delta\delta$ > 0.08 ppm).

Although absolute changes in chemical shift cannot usually be interpreted in detailed structural terms, residues that from a contiguous surface of a protein upon formation of a complex map the recognition interface of the protein-protein complex (Zuiderweg, 2002). Tax_{59-98} induces progressive changes in the ^{1}H and ^{15}N chemical shifts of KIX, indicating that complex formation is in the fast exchange regime on the chemical-shift time-scale. The average change in chemical shift upon formation of the Tax_{59-98}-KIX complex is 0.02 ppm (Figure 7). Significant changes in chemical shift (>0.05 ppm) are seen for Thr 614, Ala 618, Lys 621, Asp 622, Glu 626, Ala 630, and Gln 661, with the largest shifts (>0.08 ppm) observed for Phe 612, Leu 620, Val, 629, and Lys 659 (Figure 6).

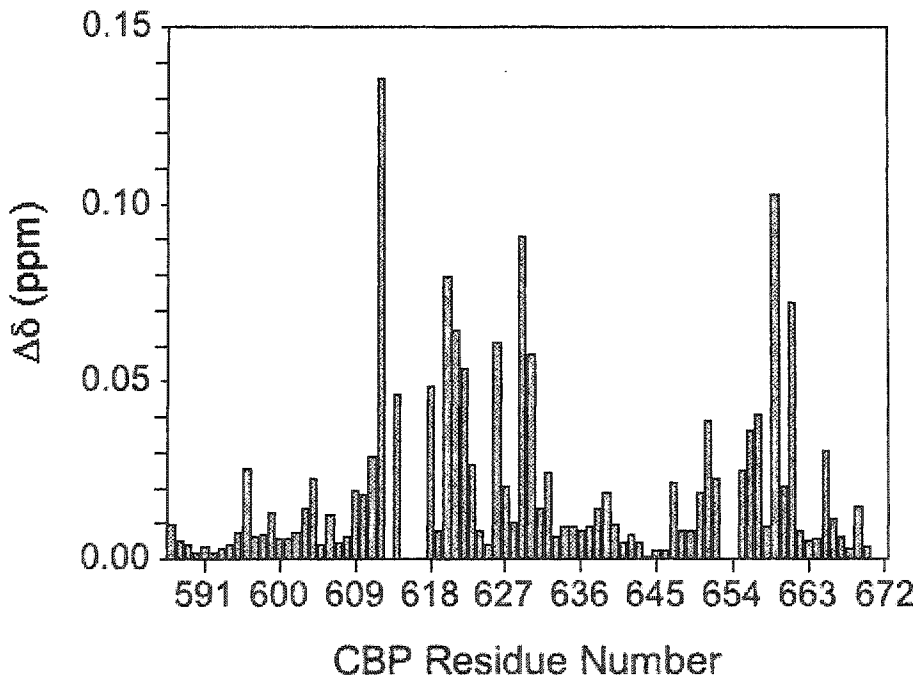

Figure 7. Chemical-shift perturbations ($\Delta\delta$) induced in KIX by Tax_{59-98}. Changes are normalized averages of the amide H^N and N chemical-shift perturbations (Radhakrishnan *et al.*, 1999).

These residues form a contiguous surface on KIX containing both hydrophobic and polar residues that define the Tax_{59-98} binding surface (Figure 8). The binding site of Tax_{59-98} on KIX corresponds to the site recognized by MLL, c-Jun, and HIV-1 Tat (Campbell and Lumb, 2002; Goto *et al.*, 2002; Vendel and Lumb, 2003b) and is distinct from the surface utilized by phosphorylated KID (Radhakrishnan *et al.*, 1997) (Figure 8).

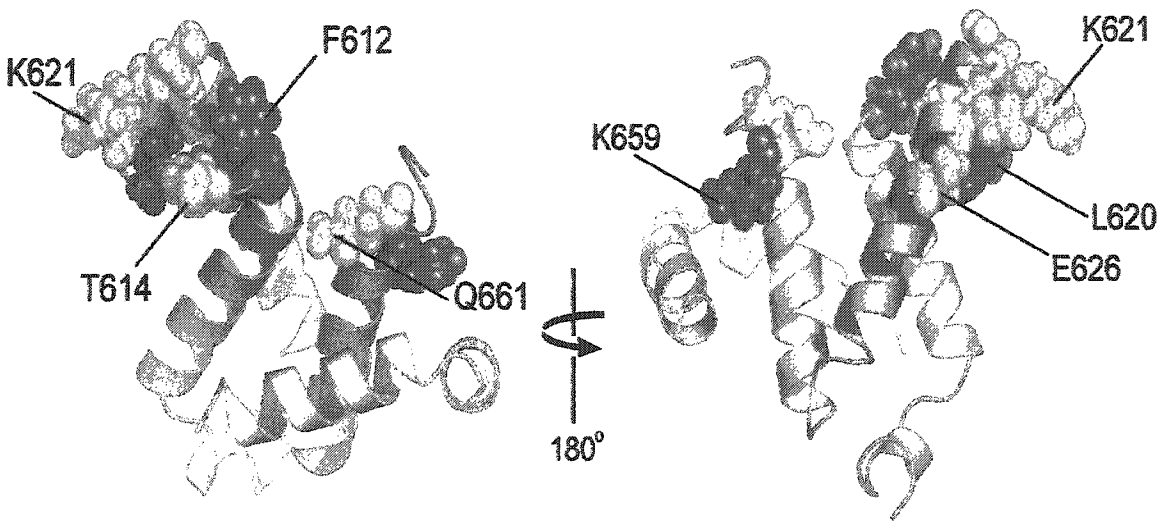

Figure 8. Chemical-shift perturbation mapping of the Tax_{59-98} binding site of KIX. Residues of KIX with the largest chemical-shift changes form a contiguous surface of KIX that is distinct from the site occupied by pKID and corresponds to the site bound by human c-Jun and HIV-1 Tat (Campbell and Lumb, 2002; Vendel and Lumb, 2003b). KIX residues with normalized chemical-shift changes of 0.05-0.79 and >0.08 ppm are orange and red, respectively. The helical ribbons of KIX and pKID are blue and wheat yellow, respectively. Drawn using PyMol (DeLano,) and the Protein Data Bank file 1kdx (Radhakrishnan *et al.*, 1997).

4.4d Formation of the Ternary Tax_{59-98}-pKID-KIX Complex.

Sedimentation equilibrium indicates that Tax_{59-98}, pKID, and KIX form a ternary complex (Figure 9). The observed mass of 21.5 ± 1.2 kDa is within 5% of the expected mass of a 1:1:1 ternary complex of 22.6 kDa (Table 2). If the ternary complex did not form, then the apparent mass would be significantly lower to reflect the weight average of the Tax_{59-98}-KIX and pKID-KIX binary complexes and the unbound proteins.

Table 2. Sedimentation equilibrium analysis of binary and ternary complex formation of pKID and KIX, and Tax_{59-98}-KIX-pKID.

Total concentration of each peptide (μM)	Observed mass (kDa)	
pKID (expected mass for monomer: 6856 Da)		
	45 krpm	48 krpm
200	7.1	7.6
300	6.9	6.8
400	7.0	7.0
pKID + KIX (expected mass for 1:1 complex: 17 996 Da)		
	25 krpm	30 krpm
30	19.4	16.5
45	19.1	17.8
55	17.9	17.0
Tax59-98 +pKID + KIX (expected mass for 1:1:1 complex: 22 603 Da)		
	25 krpm	30 krpm
35	23.0	21.3
45	21.0	21.5
55	20.2	21.8

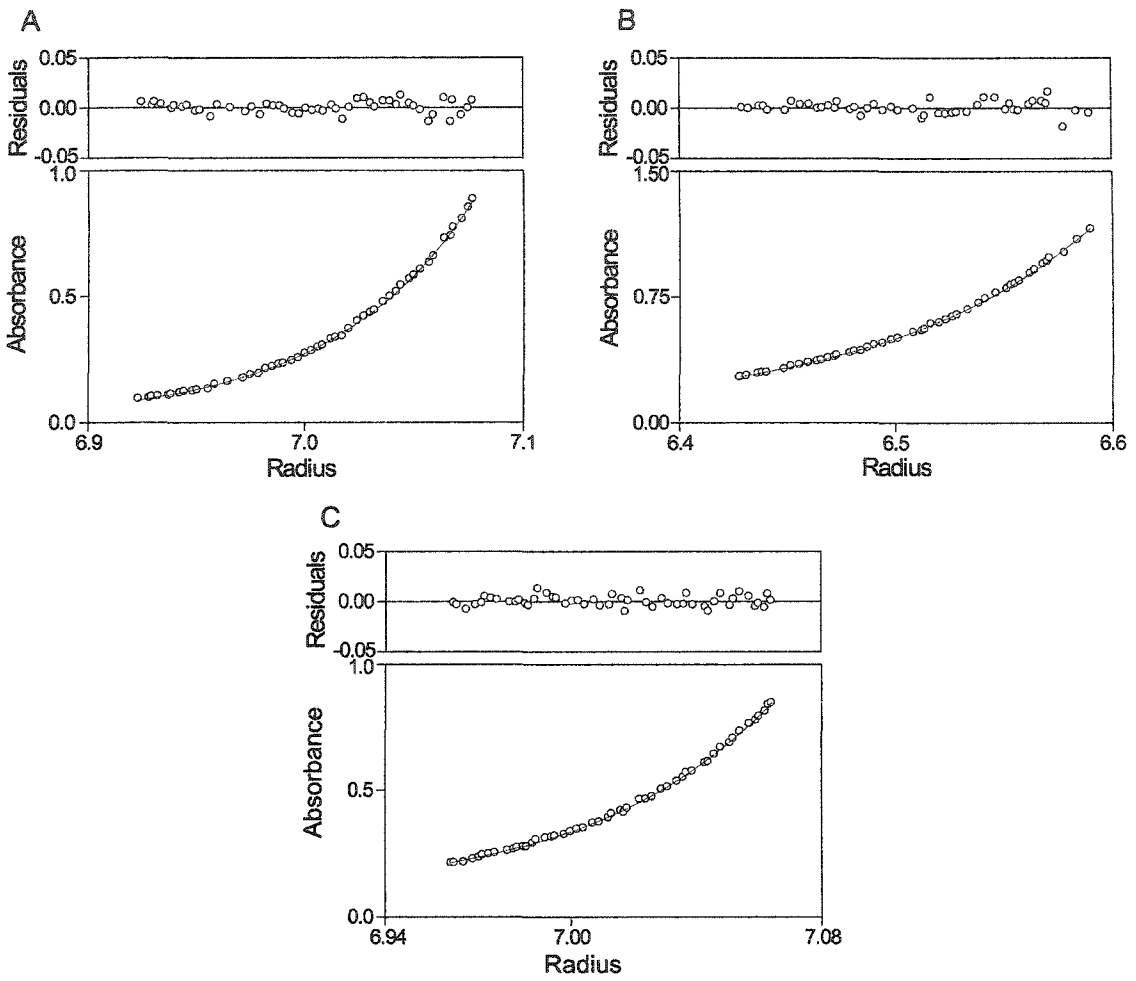

Figure 9. Sedimentation equilibrium analysis of A) pKID, B) pKID-KIX complex, and C) ternary complex of Tax_{59-98}, pKID and KIX. The data are accounted for by an ideal, single species model with masses expected of a monomer for pKID, a 1:1 pKID-KIX complex, and a 1:1:1 Tax_{59-98}-pKID-KIX complex, as shown by the random distribution of residues.

Sedimentation equilibrium shows that pKID and KIX associate to form a binary 1:1 complex, in accord with previous results (Mestas and Lumb, 1999; Radhakrishnan *et al.*, 1997). The observed mass of 17.9 ± 0.8 kDa is essentially identical to the expected mass of the binary complex (Table 2). pKID is a

monomer in solution with an observed mass of 7.1 ± 0.2 kDa, which is within 3% of the expected mass of 6.8 kDa (Table 2). These results indicate that the observed mass of the Tax_{59-98}-pKID-KIX complex is not due to self-association of the individual proteins or binary complexes.

4.5 DISCUSSION

Transcriptional activation requires the formation of numerous protein-DNA and protein-protein interactions (Orphanides and Reinberg, 2002). During CREB-mediated gene expression, the human coactivators CBP and p300 are recruited by the phosphorylated KID region of CREB, which binds the KIX domain of p300/CBP (Chrivia *et al.*, 1993; Parker *et al.*, 1996). During HTLV-1 gene expression, CBP and p300 are recruited jointly by HTLV-1 Tax and human CREB (Kwok *et al.*, 1996). CBP and p300 may then contribute to transcription activation by making contacts with the general transcription machinery and by modifying the nucleosome architecture surrounding the promoter (Chan and La Thangue, 2001; Goodman and Smolik, 2000; Vo and Goodman, 2001). The KIX domain of CBP/p300 also binds several human transcriptional activators in addition to CREB, such as c-Jun, SREBP, MLL, c-Myb and p53, and the viral activator HIV-1 Tat (Chan and La Thangue, 2001; Goodman and Smolik, 2000; Vo and Goodman, 2001). CBP and p300 are believed to be present at limiting quantities in the cell and so, as noted previously (Ariumi *et al.*, 2000; Suzuki *et al.*, 1999; Van Orden *et al.*, 1999b), competition for KIX between human transcription factors and HTLV-1 Tax may have significant consequences for

deregulating cellular processes that depend in part on interactions mediated by the KIX domain during gene expression.

Previous molecular biology studies have shown that a Tax peptide corresponding to residues 76-95 binds specifically to the KIX domain of CBP (Harrod *et al.*, 1998). Here we used a peptide corresponding to residues 59-98 of HTLV-1 Tax to study the Tax-KIX interaction. This peptide incorporates the region of Tax previously shown to bind KIX (Harrod *et al.*, 1998) plus additional flanking residues that may stabilize the formation of the complex with KIX. A combination of CD spectroscopy, NMR spectroscopy and sedimentation equilibrium results show that KIX and Tax_{59-98} associate to form a 1:1 complex. Complex formation is disrupted by a single-site variation of Tax_{59-98}, in which Leu 68, a candidate residue for participation in a hydrophobic Tax-KIX interface, is replaced with the secondary structure breaker Pro. Using NMR spectroscopy, we find that Tax recognizes the surface of KIX utilized by the human transcriptional activators MLL and c-Jun (and HIV-1 Tat), and not that utilized by CREB.

The CD results suggest an increase in helix content upon binding. Since KIX is an ordered, globular protein (Radhakrishnan *et al.*, 1997) and unbound Tax_{59-98} is devoid of significant regular helical or strand structure, it is possible that Tax_{59-98} folds to a helical structure upon binding KIX. Coupled folding upon binding of KIX has been observed directly with NMR for the KID region of CREB (Radhakrishnan *et al.*, 1997), and has been inferred from CD studies for the

activation domains from human c-Jun and HIV-1 Tat upon binding KIX (Campbell and Lumb, 2002; Vendel and Lumb, 2003b).

Although HTLV-1 Tax, HIV-1 Tat, human c-Jun and human MLL bind the same surface of KIX, the four transcriptional activators lack significant sequence similarity (less than 10%) within the KIX-interacting regions. Quaternary interactions with KIX may impart a common motif that characterizes the binding mode to the Tax/Tat/c-Jun/MLL site. Alternatively, the lack of sequence similarity may reflect different induced structures of Tax, Tat, MLL and c-Jun when bound to KIX.

The identification of the Tax-binding site on KIX provides a straightforward structural mechanism for Tax antagonism of human transcriptional activators that occupy the same site as Tax, and not the CREB binding site of KIX. For example, Tax and human c-Jun compete for binding KIX (Van Orden *et al.*, 1999b) and the structural insights presented here and previously (Campbell and Lumb, 2002) show that this likely arises from direct competition for the same surface of KIX. Likewise, Tax interference with p300/CBP binding to p53 (Ariumi *et al.*, 2000; Pise-Masison *et al.*, 2001; Van Orden *et al.*, 1999a) and MyoD (Riou *et al.*, 2000) may also occur through direct competition for the Tax-binding site of KIX [and not through the CREB-binding site, as originally presumed for p53 (Van Orden *et al.*, 1999b)].

In contrast to the direct antagonism described above, Tax interference with transcription factors that bind the CREB site of KIX likely occurs through indirect mechanisms, rather than by direct competition for KIX. For example, Tax interferes with Myb-mediated transcription (Nicot *et al.*, 2000). NMR chemical-shift mapping clearly shows that c-Myb occupies the region of KIX that is bound by CREB (Zor *et al.*, 2002), and not the site shown here to be occupied by Tax. On structural grounds, therefore, it appears unlikely that Tax and c-Myb compete directly for KIX as previously supposed (Colgin and Nyborg, 1998). Instead, our structural results are consistent with the notion that c-Myb responsive genes are suppressed by Tax indirectly through activation of NF-κB, which in turn activates expression of proteins that repress c-Myb (Nicot *et al.*, 2000; Nicot *et al.*, 2001).

The structurally distinct CREB and Tax sites suggest that KIX can bind simultaneously to Tax and CREB, which is seen here directly with sedimentation equilibrium. This observation provides an additional perspective on Tax mediated gene expression. Tax has previously been considered to act as a bridge between the bZIP domain of the HTLV-1 promoter-bound CREB and KIX to evade the cellular requirement for CREB phosphorylation during p300/CBP recruitment (Giebler *et al.*, 1997; Kwok *et al.*, 1996). However, our results show that Tax and the phosphorylated KID region of CREB can together directly bind KIX. Indeed, CREB phosphorylation markedly stabilizes p300/CBP assembly with CREB and Tax at both cellular and viral CRE-containing promoters (Giebler

et al., 1997), supporting the notion that both Tax and phosphorylated CREB bind KIX during p300/CBP recruitment.

In conclusion, Tax and phosphorylated KID employ structurally distinct modes of KIX that allows Tax and phosphorylated CREB to jointly interact with the KIX domain of p300/CBP. Phosphorylated CREB may therefore contribute more directly to p300/CBP recruitment during Tax-mediated expression of both viral and host genes than previously recognized. Although Tax has can circumvent the need for CREB phosphorylation (Giebler *et al.*, 1997; Kwok *et al.*, 1996), it is an intriguing notion that, though Tax, HTLV-1 may be also take advantage of CREB phosphorylation during coactivator recruitment.

References

Ariumi, Y., Kaida, A., Lin, J.-Y., Hirota, M., Masui, O., Yamaoka, S., Taya, Y. and Shimotohno, K. (2000) HTLV-I Tax oncoprotein represses the p53-mediated trans-activation function through coactivator CBP sequestration. *Oncogene*, **19**, 1491-1499.

Barmak, K., Harhaj, E., Grant, C., Alefantis, T. and Wigdahl, B. (2003) Human T cell leukemia virus type I-induced disease: pathways to cancer and neurodegeneration. *Virology*, **308**, 1-12.

Bax, A. and Ikura, M. (1991) An efficient 3D NMR technique for correlating the proton and 15N backbone amide resonances with the alpha-carbon of the preceding residue in uniformly $^{15}N/^{13}C$ enriched proteins. *J. Biomol. NMR*, **1**, 99-104.

Bayer, P., Kraft, M., Ejchart, A., Westendorp, M., Frank, R. and Rösch, P. (1995) Structural studies of HIV-1 Tat protein. *J. Mol. Biol.*, **247**, 529-535.

Benkirane, M., Chun, R.F., Xiao, H., Ogryzko, V.V., Howard, B.H., Nakatani, Y. and Jeang, K.T. (1998) Activation of integrated provirus requires histone acetyltransferase. p300 and P/CAF are coactivators for HIV-1 Tat. *J. Biol. Chem.*, **273**, 24898-905.

Berkowitz, L.A. and Gilman, M.Z. (1990) Two distinct forms of active transcription factor CREB (cAMP response element binding protein). *Proc. Natl. Acad. Sci. USA*, **87**, 5258-5262.

Bex, F. and Gaynor, R.B. (1998) Regulation of gene expression by HTLV-1 Tax protein. *Methods*, **16**, 83-94.

Bieniasz, P.D., Grdina, T.A., Bogerd, H.P. and Cullen, B.R. (1998) Recruitment of a protein complex containing Tat and cyclin T1 to TAR governs the species specificity of HIV-1 Tat. *EMBO J.*, **17**, 7056-65.

Brockmann, D., Lehmkuhler, O., Schmucker, U. and Esche, H. (2001) The histone acetyltransferase activity of PCAF cooperates with the brahma/SWI2-related protein BRG-1 in the activation of the enhancer A of the MHC class I promoter. *Gene*, **277**, 111-20.

Campbell, K.M. and Lumb, K.J. (2002) Structurally distinct modes of recognition of the KIX domain of CBP by Jun and CREB. *Biochemistry*, **41**, 13956-13964.

Campbell, K.M., Terrell, A.R., Laybourn, P.J. and Lumb, K.J. (2000) Intrinsic structural disorder of the C-terminal activation domain from the bZIP transcription factor Fos. *Biochemistry*, **39**, 2708-13.

Chan, H.M. and La Thangue, N.B. (2001) p300/CBP proteins: HATs for transcriptional bridges and scaffolds. *J. Cell Sci.*, **114**, 2363-73.

Chen, I.S., McLaughlin, J., Gasson, J.C., Clark, S.C. and Golde, D.W. (1983) Molecular characterization of the genome of a novel human T-cell leukaemia virus. *Nature*, **305**, 502-5.

Chen, X., Ko, L.J., Jayaraman, L. and Prives, C. (1996) p53 levels, functional domains, and DNA damage determine the extent of the apoptotic response of tumor cells. *Genes Dev.*, **10**, 2438-51.

Christensen, T. (1979) *Peptides: Structure and Biological Function*. Pierce Chemical Co., Rockford, IL.

Chrivia, J.C., Kwok, R.P., Lamb, N., Hagiwara, M., Montminy, M.R. and Goodman, R.H. (1993) Phosphorylated CREB binds specifically to the nuclear protein CBP. *Nature*, **365**, 855-9.

Col, E., Gilquin, B., Caron, C. and Khochbin, S. (2002) Tat-controlled protein acetylation. *J. Biol. Chem.*, **277**, 37955-37960.

Colgin, M.A. and Nyborg, J.K. (1998) The human T-cell leukemia virus type 1 oncoprotein Tax inhibits the transcriptional activity of c-Myb through competition for the CREB binding protein. *J. Virol.*, **72**, 9396-9399.

Cox, E.H. and McLendon, G.L. (2000) Zinc-dependent protein folding. *Curr. Opin. Chem. Biol.*, **4**, 162-5.

Creighton, T.E. (1993) *Proteins: Structures and Molecular Properties*. W. H. Freeman and Company, New York, NY.

Dames, S.A., Martinez-Yamout, M., De Guzman, R.N., Dyson, H.J. and Wright, P.E. (2002) Structural basis for HIF-1alpha/CBP recognition in the cellular hypoxic response. *Proc. Natl. Acad. Sci. U S A*, **99**, 5271-6.

De La Fuente, C., Santiago, F., Deng, L., Eadie, C., Zilberman, I., Kehn, K., Maddukuri, A., Baylor, S., Wu, K., Lee, C.G., Pumfery, A. and Kashanchi, F. (2002) Gene expression profile of HIV-1 Tat expressing cells: a close interplay between proliferative and differentiation signals. *BMC Biochem*, **3**, 14.

Delaglio, F., Grzesiek, S., Vuister, G.W., Zhu, G., Pfeifer, J. and Bax, A. (1995) NMRPipe: A multidimensional spectral processing system based on UNIX pipes. *J. Biomol. NMR*, **6**, 277-293.

DeLano, W.L. The PyMOL Molecular Graphics System. *http://www.pymol.org.*

DeLano, W.L., Ultsch, M.H., de Vos, A.M. and Wells, J.A. (2000) Convergent solutions to binding at a protein-protein interface. *Science*, **287**, 1279-83.

Demarest, S.J., Martinez-Yamout, M., Chung, J., Chen, H., Xu, W., Dyson, H.J., Evans, R.M. and Wright, P.E. (2002) Mutual synergistic folding in recruitment of CBP/p300 by p160 nuclear receptor coactivators. *Nature*, **415**, 549-53.

Deng, L., de la Fuente, C., Fu, P., Wang, L., Donnelly, R., Wade, J.D., Lambert, P., Li, H., Lee, C. and Kashanchi, F. (2000) Acetylation of HIV-1 Tat by CBP/p300 increases transcription of integrated HIV-1 genome and enhances binding to core histones. *Virology*, **277**, 278-295.

Deng, L., Wang, D., de la Fuente, C., Wang, L., Li, H., Lee, C.G., Donnelly, R., Wade, J.D., Lambert, P. and Kashanchi, F. (2001) Enhancement of the p300 HAT activity by HIV-1 Tat on chromatin DNA. *Virology*, **289**, 312-326.

Edelhoch, H. (1967) Spectroscopic determination of tryptophan and tyrosine in proteins. *Biochemistry*, **6**, 1948-54.

Ernst, P., Wang, J., Huang, M., Goodman, R.H. and Korsmeyer, S.J. (2001) MLL and CREB bind cooperatively to the nuclear coactivator CREB-binding protein. *Mol. Cell. Biol.*, **21**, 2249-58.

Frankel, A.D., Biancalana, S. and Hudson, D. (1989) Activity of synthetic peptides from the Tat protein of human immunodeficiency virus type 1. *Proc. Natl. Acad. Sci. U S A*, **86**, 7397-401.

Frankel, A.D. and Pabo, C.O. (1988) Cellular uptake of the Tat protein from human immunodeficiency virus. *Cell*, **55**, 1189-93.

Frankel, A.D. and Smith, C.A. (1998) Induced folding in RNA-protein recognition: more than a simple molecular handshake. *Cell*, **92**, 149-51.

Frankel, A.D. and Young, J.A.T. (1998) HIV-1: Fifteen proteins and an RNA. *Annual Review of Biochemistry*, **67**, 1-25.

Freedman, S.J., Sun, Z.Y., Poy, F., Kung, A.L., Livingston, D.M., Wagner, G. and Eck, M.J. (2002) Structural basis for recruitment of CBP/p300 by hypoxia-inducible factor-1 alpha. *Proc. Natl. Acad. Sci. U S A*, **99**, 5367-72.

Furia, B., Deng, L., Wu, K., Baylor, S., Kehn, K., Li, H., Donnelly, R., Coleman, T. and Kashanchi, F. (2002) Enhancement of nuclear factor κB acetylation by coactivator p300 and HIV-1 Tat proteins. *J. Biol. Chem.*, **277**, 4973-4980.

Garcia, J.A., Harrich, D., Pearson, L., Mitsuyasu, R. and Gaynor, R.B. (1988) Functional domains required for Tat-induced transcriptional activation of the HIV-1 long terminal repeat. *EMBO J.*, **7**, 3143-7.

Georges, S.A., Giebler, H.A., Cole, P.A., Luger, K., Laybourn, P.J. and Nyborg, J.K. (2003) Tax recruitment of CBP/p300, via the KIX domain, reveals a potent requirement for acetyltransferase activity that is chromatin dependent and histone tail independent. *Mol. Cell. Biol.*, **23**, 3392-404.

Giebler, H.A., Loring, J.E., van Orden, K., Colgin, M.A., Garrus, J.E., Escudero, K.W., Brauweiler, A. and Nyborg, J.K. (1997) Anchoring of CREB binding protein to the human T-cell leukemia virus type 1 promoter: a molecular mechanism of Tax transactivation. *Mol. Cell. Biol.*, **17**, 5156-64.

Glover, J.N. and Harrison, S.C. (1995) Crystal structure of the heterodimeric bZIP transcription factor c-Fos-c-Jun bound to DNA. *Nature*, **373**, 257-61.

Goodman, R.H. and Smolik, S. (2000) CBP/p300 in cell growth, transformation, and development. *Genes Dev.*, **14**, 1553-77.

Goto, N.K., Zor, T., Martinez-Yamout, M., Dyson, H.J. and Wright, P.E. (2002) Cooperativity in transcription factor binding to the coactivator CREB-binding protein (CBP). *J. Biol. Chem.*, **277**, 43168-43174.

Harrod, R., Tang, Y., Nicot, C., Lu, H.S., Vassilev, A., Nakatani, Y. and Giam, C.-Z. (1998) An exposed KID-like domain in human T-cell lymphotropic virus type 1 tax is responsible for the recruitment of coactivators CBP/p300. *Mol. Cell. Biol.*, **18**, 5052-5061.

Hauber, J., Perkins, A., Heimer, E.P. and Cullen, B.R. (1987) Trans-activation of human immunodeficiency virus gene expression is mediated by nuclear events. *Proc. Natl. Acad. Sci. U S A*, **84**, 6364-8.

He, G. and Margolis, D.M. (2002) Counterregulation of chromatin deacetylation and histone deacetylase occupancy at the integrated promoter of human immunodeficiency virus type 1 (HIV-1) by the HIV-1 repressor YY1 and HIV-1 activator Tat. *Mol. Cell. Biol.*, **22**, 2965-73.

Horvai, A.E., Xu, L., Korzus, E., Brard, G., Kalafus, D., Mullen, T.M., Rose, D.W., Rosenfeld, M.G. and Glass, C.K. (1997) Nuclear integration of JAK/STAT and Ras/AP-1 signaling by CBP and p300. *Proc. Natl. Acad. Sci. USA*, **94**, 1074-1079.

Hottiger, M.O., Felzien, L.K. and Nabel, G.J. (1998) Modulation of cytokine-induced HIV gene expression by competitive binding of transcription factors to the coactivator p300. *EMBO J.*, **17**, 3124-3134.

Hottiger, M.O. and Nabel, G.J. (1998) Interaction of human immunodeficency virus type 1 Tat with the transcriptonal coactivators p300 and CREB binding protein. *J. Virol.*, **72**, 8252-8256.

Huq, I., Ping, Y.H., Tamilarasu, N. and Rana, T.M. (1999a) Controlling human immunodeficiency virus type 1 gene expression by unnatural peptides. *Biochemistry*, **38**, 5172-7.

Huq, I., Tamilarasu, N. and Rana, T.M. (1999b) Visualizing tertiary folding of RNA and RNA-protein interactions by a tethered iron chelate: analysis of HIV-1 Tat-TAR complex. *Nucleic Acids Res.*, **27**, 1084-93.

Ikura, M., Kay, L.E. and Bax, A. (1990) A novel approach for sequential assignment of ^{1}H, ^{13}C, and ^{15}N spectra of proteins: heteronuclear triple-resonance three-dimensional NMR spectroscopy. Application to calmodulin. *Biochemistry*, **29**, 4659-67.

Isel, C. and Karn, J. (1999) Direct evidence that HIV-1 Tat stimulates RNA polymerase II carboxyl-terminal domain hyperphosphorylation during transcriptional elongation. *J. Mol. Biol.*, **290**, 929-41.

Jeang, K.-T. (2001) Functional activities of the human T-cell leukemia virus type 1 Tax oncoprotein: cellular signalling through NF-κB. *Cytokine & Growth Factor Reviews*, **12**, 207-217.

Jeeninga, R.E., Hoogenkamp, M., Armand-Ugon, M., de Baar, M., Verhoef, K. and Berkhout, B. (2000) Functional differences between the long terminal repeat transcriptional promoters of human immunodeficiency virus type 1 subtypes A through G. *J. Virol.*, **74**, 3740-51.

Johnson, B.A. and Blevins, R.A. (1994) NMRView: A computer program for the visualization and analysis of NMR data. *J. Biomol. NMR*, **4**, 603-614.

Jones, K.A. (1997) Taking a new TAK on Tat transactivation. *Genes Dev.*, **11**, 2593-2599.

Jones, K.A. and Peterlin, B.M. (1994) Control of RNA initiation and elongation at the HIV-1 promoter. *Annu. Rev. Biochem.*, **63**, 717-43.

Kaiser, E., Colescott, R.L., Bossinger, C.D. and Cook, P.I. (1970) Color test for detection of free terminal amino groups in the solid-phase synthesis of peptides. *Anal. Biochem.*, **34**, 595-8.

Kamei, Y., Xu, L., Heinzel, T., Torchia, J., Kurokawa, R., Gloss, B., Lin, S.C., Heyman, R.A., Rose, D.W., Glass, C.K. and Rosenfeld, M.G. (1996) A CBP integrator complex mediates transcriptional activation and AP-1 inhibition by nuclear receptors. *Cell*, **85**, 403-14.

Karn, J. (1999) Tackling Tat. *J. Mol. Biol.*, **293**, 235-254.

Kashanchi, F., Duvall, J.F., Kwok, R.P.S., Lundblad, J.R., Goodman, R.H. and Brady, J.N. (1998) The coactivator CBP stimulates human T-cell lymphotrophic virus type I tax transactivation in vitro. *J. Biol. Chem.*, **273**, 34646-34652.

Kay, L., Keifer, P. and Saarinen, T. (1992) Pure absorption gradient enhanced heteronuclear single quantum correlation spectroscopy with improved sensitivity. *J.A.C.S.*, **114**, 10663-10665.

Kay, L., Xu, G. and Yamazaki, T. (1994) Enhanced-sensitivity triple-resonance spectroscopy with minimal H_2O saturation. *J. Mag. Res.*, **109**, 129-133.

Kiernan, R.E., Vanhulle, C., Schiltz, L., Adam, E., Xiao, H., Maudoux, F., Calomme, C., Burny, A., Nakatani, Y., Jeang, K.T., Benkirane, M. and Van Lint, C. (1999) HIV-1 Tat transcriptional activity is regulated by acetylation. *EMBO J.*, **18**, 6106-18.

Kimzey, A.L. and Dynan, W.S. (1998) Specific regions of contact between human T-cell leukemia virus type I Tax protein and DNA identified by photocross-linking. *J. Biol. Chem.*, **273**, 13768-75.

Klaver, B. and Berkhout, B. (1994) Comparison of 5' and 3' long terminal repeat promoter function in human immunodeficiency virus. *J. Virol.*, **68**, 3830-40.

Ko, L.J. and Prives, C. (1996) p53: puzzle and paradigm. *Genes Dev.*, **10**, 1054-72.

Kwok, R.P.S., Laurance, M.E., Lundblad, J.R., Goldman, P.S., Shih, H., Conner, L.M., Marriot, S.J. and Goodman, R.H. (1996) Control of cAMP-regulated enhancers by the viral transactivator Tax through CREB and the co-activator CBP. *Nature*, **380**, 642-646.

Laue, T.M., Shah, B.D., Ridgeway, T.M. and Pelletier, S.L. (1992) Computer-aided interpretation of analytical sedimentation data for proteins. In Harding, S.E., Rowe, A.J. and Horton, J.C. (eds.), *Analytical Ultracentrifugation in*

Biochemistry and Polymer Science. The Royal Society of Chemistry, Cambridge, pp. 90-125.

Lemon, B. and Tjian, R. (2000) Orchestrated response: a symphony of transcription factors for gene control. *Genes Dev.*, **14**, 2551-69.

Lenzmeier, B.A., Giebler, H.A. and Nyborg, J.K. (1998) Human T-cell leukemia virus type 1 Tax requires direct access to DNA for recruitment of CREB binding protein to the viral promoter. *Mol. Cell. Biol.*, **18**, 721-31.

Lin, C.H., Hare, B.J., Wagner, G., Harrison, S.C., Maniatis, T. and Fraenkel, E. (2001) A small domain of CBP/p300 binds diverse proteins: solution structure and functional studies. *Mol. Cell*, **8**, 581-90.

Lu, H., Pise-Masison, C.A., Fletcher, T.M., Schiltz, R.L., Nagaich, A.K., Radonovich, M., Hager, G., Cole, P.A. and Brady, J.N. (2002) Acetylation of nucleosomal histones by p300 facilitates transcription from Tax-responsive human T-cell leukemia virus type I chromatin template. *Mol. Cell. Biol.*, **22**, 4450-4462.

Lydyard, P.M., Whelan, A. and Fanger, M.W. (2000) *IMMUNOLOGY*. BIOS Scientific Publishers Ltd., Oxford.

Martinez-Balbas, M.A., Bannister, A.J., Martin, K., Haus-Seuffert, P., Meisterernst, M. and Kouzarides, T. (1998) The acetyltransferase activity of CBP stimulates transcription. *EMBO J.*, **17**, 2886-93.

Marzio, G. and Giacca, M. (1999) Chromatin control of HIV-1 gene expression. *Genetica*, **106**, 125-30.

Marzio, G., Tyagi, M., Gutierrez, M.I. and Giacca, M. (1998) HIV-1 tat transactivator recruits p300 and CREB-binding protein histone acetyltransferases to the viral promoter. *Proc. Natl. Acad. Sci. USA*, **95**, 13519-24.

McEwan, I.J., Dahlman-Wright, K., Ford, J. and Wright, A.P. (1996) Functional interaction of the c-Myc transactivation domain with the TATA binding protein: evidence for an induced fit model of transactivation domain folding. *Biochemistry*, **35**, 9584-93.

McIntosh, L.P. and Dahlquist, F.W. (1990) Biosynthetic incorporation of ^{15}N and ^{13}C for assignment and interpretation of nuclear magnetic resonance spectra of proteins. *Q. Rev. Biophys.*, **23**, 1-38.

Mestas, S.P. and Lumb, K.J. (1999) Electrostatic contribution of phosphorylation to the stability of the CREB-CBP activator-coactivator complex. *Nature Struct. Biol.*, **6**, 613-4.

Mujtaba, S., He, Y., Zeng, L., Farooq, A., Carlson, J.E., Ott, M., Verdin, E. and Zhou, M.M. (2002) Structural basis of lysine-acetylated HIV-1 Tat recognition by PCAF bromodomain. *Mol. Cell*, **9**, 575-86.

Muñoz, V., Cronet, P., López-Hernández, E. and Serrano, L. (1996) Analysis of the effect of local interactions in protein stability. *Folding and Design*, **1**, 167-178.

Naar, A.M., Lemon, B.D. and Tjian, R. (2001) Transcriptional coactivator complexes. *Annu. Rev. Biochem.*, **70**, 475-501.

Newton, A.L., Sharpe, B.K., Kwan, A., Mackay, J.P. and Crossley, M. (2000) The transactivation domain within cysteine/histidine-rich region 1 of CBP comprises two novel zinc-binding modules. *J. Biol. Chem.*, **275**, 15128-34.

Nicot, C., Mahieux, R., Opavsky, R., Cereseto, A., Wolff, L., Brady, J.N. and Franchini, G. (2000) HTLV-I Tax transrepresses the human c-Myb promoter independently of its interaction with CBP or p300. *Oncogene*, **19**, 2155-2164.

Nicot, C., Mahieux, R., Pise-Masison, C.A., Brady, J.N., Gessain, A., Yamaoka, S. and Franchini, G. (2001) Human T-cell lymphotropic virus type I Tax represses c-Myb-dependent transcription through activation of the NF-κB pathway and modulation of coactivator usage. *Mol. Cell. Biol.*, **21**, 7391-7402.

O'Hare, P. and Williams, G. (1992) Structural studies of the acidic transactivation domain of the Vmw65 protein of herpes simplex virus using ^{1}H NMR. *Biochemistry*, **31**, 4150-6.

Orphanides, G. and Reinberg, D. (2002) A unified theory of gene expression. *Cell*, **108**, 439-451.

O'Shea, E.K., Rutkowski, R., Stafford, W.F., and Kim, P.S. (1989) Preferential heterodimer formation by isolated leucine zippers from Fos and Jun. *Science*, **245**, 646-8.

Ott, M., Schnolzer, M., Garnica, J., Fischle, W., Emiliani, S., Rackwitz, H.R. and Verdin, E. (1999) Acetylation of the HIV-1 Tat protein by p300 is important for its transcriptional activity. *Curr. Biol.*, **9**, 1489-92.

Parker, D., Ferreri, K., Nakajima, T., LaMorte, V.J., Evans, R., Koerber, S.C., Hoeger, C. and Montminy, M.R. (1996) Phosphorylation of CREB at Ser-133 induces complex formation with CREB-binding protein via a direct mechanism. *Mol. Cell. Biol.*, **16**, 694-703.

Pise-Masison, C.A., Mahieux, R., Radonovich, M., Jiang, H. and Brady, J.N. (2001) Human T-lymphotropic virus type I Tax protein utilizes distinct pathways for p53 inhibition that are cell type dependent. *J. Biol. Chem.*, **276**, 200-205.

Pise-Masison, C.A., Radonovich, M., Mahieux, R., Chatterjee, P., Whiteford, C., Duvall, J., Guillerm, C., Gessain, A. and Brady, J.N. (2002) Transcription profile of cells infected with human T-cell leukemia virus type I comapred with activated lymphocytes. *Cancer Research*, **62**, 3562-3571.

Plaxco, K.W. and Gross, M. (1997) Cell biology. The importance of being unfolded. *Nature*, **386**, 657, 659.

Poiesz, B.J., Ruscetti, F.W., Gazdar, A.F., Bunn, P.A., Minna, J.D. and Gallo, R.C. (1980) Detection and isolation of type C retrovirus particles from fresh and cultured lymphocytes of a patient with cutaneous T-cell lymphoma. *Proc. Natl. Acad. Sci. U S A*, **77**, 7415-9.

Ptak, R.G. (2002) HIV-1 regulatory proteins: targets for novel drug development. *Expert Opin. Investig. Drugs*, **11**, 1099-1115.

Ptashne, M. (1988) How eukaryotic transcriptional activators work. *Nature*, **335**, 683-9.

Ptashne, M. and Gann, A. (1997) Transcriptional activation by recruitment. *Nature*, **386**, 569-77.

Radhakrishnan, I., Pérez-Alvarado, G.C., Parker, D., Dyson, H.J., Montminy, M. and Wright, P.E. (1999) Structural analysis of CREB-CBP transcriptional activator-coactivator complexes by NMR spectroscopy: Implications for mapping the boundaries of structural domains. *J. Mol. Biol.*, **287**, 859-865.

Radhakrishnan, I., Pérez-Alvarado, G.C., Parker, D., Dyson, H.J., Montminy, M.R. and Wright, P.E. (1997) Solution structure of the KIX domain of CBP bound to the transactivation domain of CREB: a model for activator:coactivator interactions. *Cell*, **91**, 741-52.

Rhim, H., Echetebu, C.O., Herrmann, C.H. and Rice, A.P. (1994) Wild-type and mutant HIV-1 and HIV-2 Tat proteins expressed in Escherichia coli as fusions with glutathione S-transferase. *J. Acquir. Immune Defic. Syndr.*, **7**, 1116-21.

Riou, P., Bex, F. and Gazzolo, L. (2000) The human T cell leukemia/lymphotropic virus type 1 Tax protein represses MyoD-dependent transcription by inhibiting MyoD-binding to the KIX domain of p300. A potential mechanism for Tax-mediated repression of the transcriptional activity of basic helix-loop-helix factors. *J. Biol. Chem.*, **275**, 10551-60.

Roebuck, K.A. and Saifuddin, M. (1999) Regulation of HIV-1 transcription. *Gene Expr.*, **8**, 67-84.

Roeder, R.G. (1996) The role of general initiation factors in transcription by RNA polymerase II. *Trends Biochem. Sci.*, **21**, 327-35.

Root, M.J., Kay, M.S. and Kim, P.S. (2001) Protein design of an HIV-1 entry inhibitor. *Science*, **291**, 884-8.

Sadaie, M.R., Rappaport, J., Benter, T., Josephs, S.F., Willis, R. and Wong-Staal, F. (1988) Missense mutations in an infectious human immunodeficiency viral genome: functional mapping of Tat and identification of the rev splice acceptor. *Proc. Natl. Acad. Sci. U S A*, **85**, 9224-8.

Schmitz, M.L., dos Santos Silva, M.A., Altmann, H., Czisch, M., Holak, T.A. and Baeuerle, P.A. (1994) Structural and functional analysis of the NF-kappa B p65 C terminus. An acidic and modular transactivation domain with the potential to adopt an alpha-helical conformation. *J Biol Chem*, **269**, 25613-20.

Schnölzer, M., Alewood, P., Jones, A., Alewood, D. and Kent, S.B.H. (1992) *In situ* neutralization in Boc-chemistry solid phase peptide synthesis. *Int. J. Pept. Prot. Res.*, **40**, 180-193.

Scoggin, K.E., Ulloa, A. and Nyborg, J.K. (2001) The oncoprotein Tax binds the SRC-1-interacting domain of CBP/p300 to mediate transcriptional activation. *Mol. Cell. Biol.*, **21**, 5520-30.

Serrano, L. (2000) The relationship between sequence and structure in elementary folding units. *Adv. Prot. Chem.*, **53**, 49-85.

Shaulian, E. and Karin, M. (2001) AP-1 in cell proliferation and survival. *Oncogene*, **20**, 2390-400.

Slice, L.W., Codner, E., Antelman, D., Holly, M., Wegrzynski, B., Wang, J., Toome, V., Hsu, M.C. and Nalin, C.M. (1992) Characterization of recombinant HIV-1 Tat and its interaction with TAR RNA. *Biochemistry*, **31**, 12062-8.

Struhl, K. (1988) The JUN oncoprotein, a vertebrate transcription factor, activates transcription in yeast. *Nature*, **332**, 649-50.

Suzuki, T., Uchida-Toita, M. and Yoshida, M. (1999) Tax protein of HTLV-I inhibits CBP/p300-mediated transcription by interfering with recruitment of CBP/p300 onto DNA element of E-box or p53 binding site. *Oncogene*, **18**, 4137-4143.

Swope, D.L., Mueller, C.L. and Chrivia, J.C. (1996) CREB-binding protein activates transcription through multiple domains. *J. Biol. Chem.*, **271**, 28138-45.

Tjian, R. and Maniatis, T. (1994) Transcriptional activation: a complex puzzle with few easy pieces. *Cell*, **77**, 5-8.

Toth, F.D., Mosborg-Petersen, P., Kiss, J., Aboagye-Mathiesen, G., Hager, H., Juhl, C.B., Gergely, L., Zdravkovic, M., Aranyosi, J., Lampe, L. and Ebbesen, P. (1995) Interactions between human immunodeficiency virus type 1 and human cytomegalovirus in human term syncytiotrophoblast cells coinfected with both viruses. *J. Virol.*, **69**, 2223-32.

Triezenberg, S.J. (1995) Structure and function of transcriptional activation domains. *Curr. Opin. Genet. Dev.*, **5**, 190-6.

Turner, B.G. and Summers, M.F. (1999) Structural biology of HIV. *J. Mol. Biol.*, **285**, 1-32.

Van Lint, C., Emiliani, S., Ott, M. and Verdin, E. (1996) Transcriptional activation and chromatin remodeling of the HIV-1 promoter in response to histone acetylation. *EMBO J.*, **15**, 1112-20.

Van Orden, K., Giebler, H.A., Lemasson, I., Gonzales, M. and Nyborg, J.K. (1999a) Binding of p53 to the KIX domain of CREB binding protein. A potential link to human T-cell leukemia virus, type I-associated leukemogenesis. *J. Biol. Chem.*, **274**, 26321-8.

Van Orden, K., Yan, J.P., Ulloa, A. and Nyborg, J.K. (1999b) Binding of the human T-cell leukemia virus Tax protein to the coactivator CBP interferes with CBP-mediated transcriptional control. *Oncogene*, **18**, 3766-72.

Vendel, A., C. and Lumb, K.J. (2003a) Molecular recognition of the human coactivator CBP by the HIV-1 transcriptional activator Tat. *Biochemistry*, **42**, 910-916.

Vendel, A.C. and Lumb, K.J. (2003b) Identification of the HIV-1 Tat Interaction Surface of the KIX Domain of the Human Coactivator CBP. *Submitted for publication.*

Vendel, A.C., McBryant, S.J., and Lumb, K.J. (2003) KIX-mediated assembly of the CREB-CBP-HTLV-1 Tax complex. *Biochemistry*, in press.

Vo, N. and Goodman, R.H. (2001) CREB-binding protein and p300 in transcriptional regulation. *J. Biol. Chem.*, **276**, 13505-13508.

Wei, Y., Horng, J.C., Vendel, A.C., Raleigh, D.P. and Lumb, K.J. (2003) Contribution to stability and folding of a buried polar residue at the CARM1 methylation site of the KIX domain of CBP. *Biochemistry*, **42**, 7044-9.

WHO (2002) AIDS Epidemic Update (2002). World Health Organization, http://www.unaids.org/worldaidsday/2002/press/Epiupdate.html.

Wright, P.E. and Dyson, H.J. (1999) Intrinsically unstructured proteins: Re-assessing the protein structure-function paradigm. *J. Mol. Biol.,* **293**, 321-331.

Yan, J., Garrus, J., Giebler, H.A., Stargell, L.A. and Nyborg, J.K. (1998) Molecular interactions between the coactivator CBP and the human T-cell leukemia virus Tax protein. *J. Mol. Biol.*, **281**, 395-400.

Yang, X.J., Ogryzko, V.V., Nishikawa, J., Howard, B.H. and Nakatani, Y. (1996) A p300/CBP-associated factor that competes with the adenoviral oncoprotein E1A. *Nature*, **382**, 319-24.

Yoshida, M. (2001) Multiple viral strategies of HTLV-1 for dysregulation of cell growth control. *Annual Rev. Immun.*, **19**, 475-496.

Zor, T., Mayr, B.M., Dyson, H.J., Montminy, M.R. and Wright, P.E. (2002) Roles of phosphorylation and helix propensity in the binding of the KIX domain of CBP

by constitutive (c-Myb) and inducible (CREB) activators. *J. Biol. Chem.*, **277**, 42241-42248.

Zuiderweg, E.R.P. (2002) Mapping protein-protein interactions in solution by NMR spectroscopy. *Biochemistry*, **41**, 1-7.